MIT-D15

DEUTERIUM CONCENTRATION BY CHEMICALLY-REFLUXED AMMONIA-HYDROGEN EXCHANGE

SUPPLEMENTARY REPORTS

by

M. Benedict, E.A. Mason, E.R. Chow, J.S. Baron

June 1969

FOR
E.I. DUPONT DE NEMOURS & COMPANY
UNDER
U.S. ATOMIC ENERGY COMMISSION SUBCONTRACT AX-210280

Department of Nuclear Engineering
Massachusetts Institute of Technology
Cambridge, Massachusetts 02139

(MITNE-103)

AECL PROPRIETARY DOCUMENT

Notice: This document contains information obtained from Atomic Energy of Canada Limited, designated AECL PROPRIETARY. Documents so designated are made available to the USAEC pursuant to the Memorandum of Understanding executed June 7, 1960, for distribution restricted to the USAEC or its contractors. No other distribution is to be made without permission of AECL which may be secured by requesting specific clearance from the Scientific Representative, USAEC, Chalk River Liaison Office, Chalk River, Ontario.

DEUTERIUM CONCENTRATION BY CHEMICALLY-REFLUXED AMMONIA-HYDROGEN EXCHANGE

SUPPLEMENTARY REPORTS

by

M. Benedict, E.A. Mason, E.R. Chow, J.S. Baron

June 1969

for
E.I. duPont de Nemours & Company
under
U.S. Atomic Energy Commission Subcontract AX-210280
(MIT DSR-70672)

Department of Nuclear Engineering
Massachusetts Institute of Technology
Cambridge, Massachusetts 02139

(MITNE-103)

Table of Contents

Page

Supplement D

Prediction of Plate Efficiency in the Hydrogen Deuterium--Ammonia Exchange Reaction

List of Tables

List of Figures

INTRODUCTORY NOTE

The six topical reports contained in this volume supplement the final report (1) of a research project whose objective was to evaluate the use of chemical reflux in processes for deuterium extraction. The studies were carried out by the Department of Nuclear Engineering at the Massachusetts Institute of Technology for the U. S. Atomic Energy Commission under a subcontract from the E. I. duPont de Nemours & Company.

Major emphasis during the two years of study was given to the design and evaluation of a process employing chemical reflux in the ammonia-hydrogen exchange system. Basic thermodynamic information relating to the system NH_3 - H_2 - N_2 was developed for this purpose and is presented in Supplements A, B, and C. Methods were developed for estimating the transfer efficiency of plate-type and stirred-type contactors for the exchange of hydrogen and deuterium in the gas-liquid system of synthesis gas and liquid ammonia; these methods are presented in Supplements D and E. The information in these five supplements was used in developing the process design for the overall deuterium extraction plant discussed in the final report.

The results of a brief survey of chemical reflux in the water-hydrogen sulfide process for deuterium extraction are presented in Supplement F.

---

(1) M. Benedict, E.A. Mason, E.R. Chow, and J.S. Baron, "Deuterium Concentration by Chemically-Refluxed Ammonia Hydrogen Exchange," Department of Nuclear Engineering, M.I.T., Cambridge, Mass., (June 1969) MIT-D14.

SUPPLEMENT A
LIQUID-VAPOR EQUILIBRIUM IN SYSTEM NH_3 - H_2 - N_2

1. Introduction

Under subcontract No. AX 210280 with E. I. du Pont de Nemours and Company, MIT has started study of the ammonia-hydrogen exchange process for concentrating deuterium for du Pont and the U. S. Atomic Energy Commission. Exchange tower design calculations for this process require accurate phase equilibrium data for a system whose gas phase consists of hydrogen and nitrogen in 3 to 1 molar ratio plus ammonia vapor and whose liquid phase consists of hydrogen and nitrogen dissolved in liquid ammonia. This memorandum correlates experimental data on liquid-vapor equilibria for this system and presents it in a form convenient for use in tower calculations. The principal experimental investigators whose measurements were correlated are

Larson and Black, 1925 (References 5 and 6)

Michels, et al., 1950, 1959 (References 3 and 4)

and Lefrancois and Vaniscotti, 1960 (References 1 and 2)

2. Results

2.1 Liquid Phase. - Liquid phase compositions have been reported as Henry's law constants for hydrogen H_{H_2} and nitrogen H_{N_2}. The Henry's law constant is defined as

$$H_i = \frac{y_i \pi}{x_i}$$

where y_i = mole fraction of hydrogen or nitrogen in vapor

x_i = mole fraction of corresponding component in liquid

π = total pressure

graphical correlations of these constants are presented in the following figures:

Variable	Range	at Constant	Figure - Number H_2	Figure - Number N_2
Temp.	-40 to +50°C	Pressure	1	3
Pressure	0 to 500 atm	Temp.	2	4

original data points and their sources are indicated by the different symbols on the figures. Curves correlating the data have been drawn through the points in such a way as to provide a regular family. By providing plots against both pressures and temperatures, interpolation to intermediate values of these variables has been facilitated.

2.2 Vapor Phase. - Vapor phase compositions have been reported in terms of $y_{NH_3}\pi$, where y_{NH_3} is the equilibrium mole fraction of ammonia in the vapor phase and π is the total pressure. Figure 5 is a plot of $y_{NH_3}\pi$ vs $1/T$ at constant pressure, on semilog paper. Experimental points fall on essentially straight lines as would be expected from the Clapeyron equation. The range of pressures is from 50 to 600 atm, and the range of temperature is from -50 to +50°C. Figure 6

is a plot of $y_{NH_3}\pi$ vs pressure at constant temperature on semilog paper. This was used primarily to interpolate experimental data taken at irregular pressures to the even pressures plotted in Figure 5.

3. Sources of Data

Lefrancois and Vaniscotti reported gas solubilities in liquid ammonia from -50 to +50°C at three pressures - 100, 300, and 500 kg/cm^2, giving at the same time empirical equations of gas solubilities as functions of temperature.[1] In another report,[2] these two men reported on ammonia vaporization into a mixture of synthesis gas from -70 to +60°C at 300 and 500 kg/cm^2, also giving an empirical equation based on their data.

Earlier, Michels, Skelton and Dumoulin[3,4] gave data on gas solubilities and ammonia vaporization at pressures ranging from 25 to 800 atmospheres and temperatures from -30.0 to 121.8°C, although not at regular increments of either parameter. They summarized their data in the form of pressure-NH_3 mole fraction and temperature-NH_3 mole fraction diagrams.

Much earlier yet, Larson and Black experimentally obtained ammonia concentrations in the vapor phase at 50, 100, 300, 600, 1000 atmospheres total pressure at various temperatures from -22.0 to 18.7°C.[5] At about the same time, they reported on synthesis gas solubility in liquid ammonia at 50, 100, and 150 atmospheres total pressure for the same temperature range.[6]

4. Procedure for Correlating Data

4.1 Henry's Law Constants. - By virtue of being the most regular and exhaustive, the data of Lefrancois and Vaniscotti have been invariably admitted as the most reliable of the three. At 300 and 500 kg/cm^2, Henry's law constants for both hydrogen and nitrogen have been calculated based entirely on either their data points or their empirical equations. At 100 kg/cm^2, concentrations in the liquid phase were obtained directly from Lefrancois' data, but the corrections in the vapor phase due to ammonia vaporization had to be obtained from the vapor phase correlation of all three sets of data. Table 1 lists the values of Henry's law constants at these three pressures for temperatures from 50 to -50°C.

For purposes of comparison and of extending the results into the lower pressure region, calculations were made at 100 and 50 atmospheres based on Larson and Black's liquid phase concentrations. Results are listed in Table 2. Vapor phase corrections again were taken from an over-all correlation. Then, by plotting the Henry's law constants at 50 atm, 290.3 atm (300 kg/cm^2), and 483.9 atm (500 kg/cm^2) with temperature as parameter on the H vs π graphs, straight lines were obtained that gave values at intermediate pressures. (Figures 2 and 4).

Now, on the H vs t graphs (Figures 1 and 3) isobars at 290.3, and 483.9 atm gave smooth curves for both hydrogen and nitrogen. In the case of nitrogen, extra isobars at 50 atm and 96.78 atm (100 kg/cm^2) were drawn; and for hydrogen, an extra isobar at 100 atm was included. By using the H vs π lines, values at 0.200, and 400 atm at various temperatures were read off and plotted on the H vs t curves. These cross-plotted values are connected by dotted lines on the H vs t$^\circ$C graph.

Henry's law constants at other temperatures and pressures within the range covered may be obtained by the same technique of interpolation and cross-plotting. A brief examination of the H vs π straight lines shows that the ultimate guide in fitting the lines was that the slope should gradually decrease for increasing temperatures. The regularity of the lines had to be upheld. In fact, straight lines were drawn only because the scarcity of the data could justify no other curve.

Table 3 illustrates how Henry's law constants are calculated, showing at the same time the sources from which the necessary information has been obtained.

4.2 Ammonia Content of Vapor. - Figure 5 is a semilog plot of $y_{NH_3}\pi$ vs $\frac{1}{T}$ K^{-1}. Here again, Lefrancois and Vaniscotti's data[2] at 290.3 atm (300 kg/cm^2) and 483.9 atm (500 kg/cm^2) served as guides. At these two pressures, data points listed under Table 4 yielded straight lines when plotted on Figure 5.

Larson and Black[5] provided a few points at 50, 100, and 600 atm, listed in Table 5. Their data points, however, did not cover a considerable temperature range. So to extend the 50, 100, and 600 atm isobars on Figure 5 throughout the temperature range, more points were obtained by means of a cross-plot of $y_{NH_3}\pi$ vs π atmospheres (Figure 6).

On Figure 6, Michel's data points[3,4] were plotted along with a few points from other sources available at the same temperatures as Michel's data. Best curves were drawn on Figure 6 at the five temperatures of Michel's data: 49.73, 24.5, 0, -14.90, and -30.96°C. Points were picked off from these curves at 50, 100, and 600 atm and reploted on Figure 5 to complete the isobars. Best lines were drawn through the points.

The 40.0 and 10.0°C curveson Figure 6 were obtained by cross-plotting points from Figure 5 at 50, 100, 290.3, 483.9 and 600 atm, the five pressures at which isobars had been completed on Figure 5. Finally, points for the 150, 200 and 400 atm isobars in Figure 5 were picked off the seven isotherms of Figure 6 and cross-plotted vs 1/t in Figure 5.

TABLE I. VALUES OF HENRY'S LAW CONSTANTS: LIQUID PHASE

DATA FROM LEFRANCOIS AND VANISCOTTI (REFERENCE 1)

HENRY'S LAW CONSTANT, ATM.

Pressure:	483.9 atm ($500 kg/cm^2$)		290.3 atm ($300 kg/cm^2$)		96.78 atm ($100 kg/cm^2$)	
Temp.	H_2	N_2	H_2	N_2	H_2	N_2
50°C	8,530	8,920	8,360	7,990	8,270	6,130
40°C	10,270	10,840	9,870	9,510	8,680	6,940
30°C	12,640	13,490	11,860	11,550	9,980	8,140
20°C	15,200	16,400	14,070	13,850	11,780	9,800
10°C	19,560	22.590	16,436	16,880	14,110	11,740
0°C	21,350	25,830	19,250	20,320	16,710	13,830
-10°C	24,610	31,040	22,690	24,480	20,270	16,700
-20°C	30,660	39,880	27,020	30,150	24,830	20,450
-30°C	34,170	46,660	32,780	37,840	31,140	25,680
-40°C	41,150	60,450	40,760	49,010	39,080	32,040
-50°C	53,720	85,490	52,360	65,720	49,730	40,820

TABLE 2. VALUES OF HENRY'S LAW CONSTANTS: LIQUID PHASE

DATA FROM LARSON AND BLACK (REFERENCE 6)

AT 50 ATM. TOTAL PRESSURE

Temp.	H_2	N_2
-25.2°C	28,872	21,320
-18.5°C	24,517	18,533
-10.0°C	22,272	16,370
-3.0°C	19,264	14,029
0.0°C	17,225	12,960
2.5°C	16,529	12,497
19.0°C	12,990	9,459

AT 100 ATM. TOTAL PRESSURE

-25.0°C	29,087	23,739
-20.0°C	26,106	21,937
-16.5°C	24,819	19,489
-10.0°C	21,454	17,257
-5.2°C	19,451	15,569
0.0°C	17,681	13,688
22.0°C	11,625	9,085

TABLE 3. SAMPLE COMPUTATIONS FOR HENRY'S LAW CONSTANTS AT 0.0°C FOR THREE PRESSURES

TEMPERATURE 0.0°C

	Item	Source			
(1)	Total Pressure π		483.9	290.3	100.0
(2)	Moles Synthesis gas/mole NH_3	[a]Lef and Van. data point [b]Lef and Van. empirical equation [c]Larson and Black data point	0.02158[a]	0.01465[b]	0.005749[c]
(3)	$x_{N_2} + x_{H_2}$	$\frac{(2)}{1 + (2)}$	0.02112	0.01444	0.005716
(4)	$\frac{x_{N_2}}{x_{N_2} + x_{H_2}}$	[d]Interpolation from Lef and Van [e]Larson and Black data	0.216[d]	0.240[d]	0.301[e]
(5)	x_{N_2}	(3) · (4)	0.004562	0.003466	0.001721
(6)	x_{H_2}	(3) - (4)	0.016558	0.010974	0.003995
(7)	y_{NH_3}	[f]Lef and Van. data [g]Larson and Black interpolation	0.0260[f]	0.02979[f]	0.0581[g]
(8)	y_{N_2}	$0.25\ [1-(7)]$	0.2435	0.2426	0.2355
(9)	y_{H_2}	$0.75\ [1-(7)]$	0.7305	0.7277	0.7064
(10)	H_{N_2}	$\frac{y_{N_2}\pi}{x_{N_2}}$	25,830	20,320	13,688
(11)	H_{H_2}	$\frac{y_{H_2}\pi}{x_{H_2}}$	21,350	19,250	17,681

TABLE 4. AMMONIA CONTENT OF VAPOR EXPRESSED AS $y_{NH_3}\pi$.

DATA FROM LEFRANCOIS AND VANISCOTTI (Ref. 2)

AT 483.9 ATM. (500 kg/cm^2), DATA POINTS

Temp., °C	$\frac{1}{T}$ °K^{-1} x 10^3	y_{NH_3}	$y\pi$ atm.
62.5	2.98	0.1451	70.70
52.5	3.07	0.1134	54.87
40.0	3.194	0.08173	39.55
30.0	3.299	0.06384	30.89
20.0	3.412	0.04789	23.17
10.0	3.532	0.03615	17.49
0.0	3.662	0.02600	12.58
-10.0	3.801	0.01826	8.836
-20.0	3.951	0.01283	6.208
-32.0	4.151	0.00815	3.944
-40.0	4.292	0.00567	2.744
-50.0	4.482	0.003587	1.736
-69+1.5	4.903	0.001198	0.580

AT 290.3 ATM. (300 kg/cm^2), DATA POINTS

t °C	$\frac{1}{T}$ °K^{-1} x 10^3	y_{NH_3}	$y\pi$ atm.
50.0	3.094	0.1292	55.74
40.0	3.194	0.09902	28.75
20.0	3.412	0.05758	16.72
0.0	3.662	0.02979	8.648
-25.0	4.030	0.01163	3.376
-50.0	4.482	0.003984	1.157
-69+1.5	4.903	0.001498	0.435

AT 290.3 ATM., EMPIRICAL EQUATION

t °C	$\frac{1}{T}$ °K^{-1} x 10^3	y_{NH_3}	$y\pi$ atm.
+30.0	3.299	0.07707	22.37
+10.0	3.532	0.04206	12.21
-10.0	3.801	0.02086	6.056
-20.0	3.951	0.01417	4.114
-30.0	4.113	0.009394	2.727
-40.0	4.292	0.006078	1.764

TABLE 5. AMMONIA CONTENT OF VAPOR EXPRESSED AS $y_{NH_3}\pi$.

DATA FROM LARSON AND BLACK (REFERENCE 5)

AT 600 ATM. DATA POINTS

Temp., °C	$\frac{1}{T}$ °K^{-1} x 10^3	y_{NH_3}	$y\pi$ atm.
15.5	3.464	0.0432	25.92
0.0	3.662	0.0246	14.76
-8.6	3.780	0.0183	10.98
-14.0	3.859	0.0145	8.700
-22.0	3.982	0.0118	7.080

AT 100 ATM. DATA POINTS

18.0	3.435	0.1050	10.50
9.9	3.533	0.0817	8.17
0.0	3.662	0.0581	5.81
-7.6	3.766	0.0452	4.52
-19.8	3.947	0.0337	3.37

AT 50 ATM. DATA POINTS

18.7	3.427	0.1926	9.63
10.0	3.532	0.1397	6.98
0.0	3.662	0.1000	5.00
-6.8	3.754	0.0808	4.04
-20.0	3.951	0.0570	2.85

TABLE 6. AMMONIA CONTENT OF VAPOR EXPRESSED AS $y_{NH_3}\pi$.

DATA FROM MICHELS, ET AL (REFERENCE 3 AND 4)

π atm.	y_{NH_3}	$y\pi$ atm.
	AT CONSTANT TEMPERATURE 49.73°C	
49.1	0.4659	22.88
102.0	0.2590	26.42
196.6	0.1645	32.34
292.7	0.1325	38.78
585.1	0.0993	58.10
782.5	0.0902	70.58
	AT 24.5°C	
25.2	0.4183	10.54
49.7	0.2290	11.38
102.1	0.1306	13.33
196.6	0.0810	15.92
294.6	0.0642	18.91
395.0	0.0564	22.28
487.4	0.0512	24.95
585.1	0.0490	28.70
782.5	0.0454	35.53
	AT 0°C	
26.0	0.1790	4.654
48.9	0.1026	5.017
102.0	0.0557	5.681
292.8	0.0299	8.755
487.4	0.0242	11.80
782.5	0.0218	17.06
	AT -14.90°C	
9.22	0.2375	2.190
24.30	0.0964	2.343
49.37	0.0505	2.493
74.34	0.0359	2.669
99.36	0.0300	2.981
200.60	0.0192	3.852
300.06	0.0158	4.741
498.68	0.0130	6.483
800.95	0.0116	9.791
	AT -30.96°C	
9.25	0.1092	1.010
24.17	0.0479	1.158
49.33	0.0242	1.194
74.27	0.0185	1.374
99.32	0.0150	1.490
300.00	0.0076	2.280
398.78	0.0071	2.831
598.82	0.0063	3.773
799.43	0.0058	4.637

Fig. 1 HENRY'S LAW CONSTANT OF H_2 IN LIQUID NH_3 VS. TEMPERATURE t°C

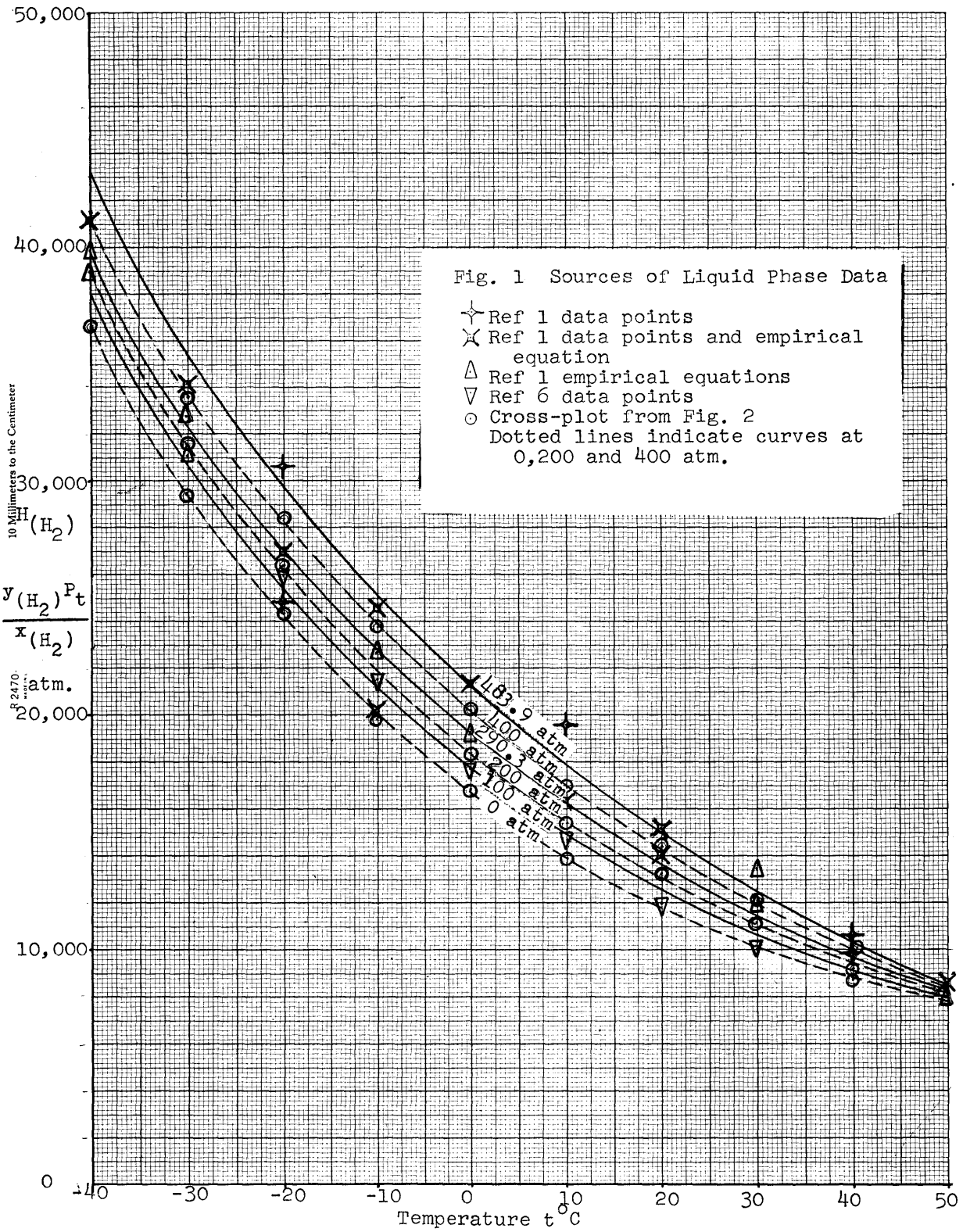

Fig. 2 CROSS-PLOT OF HENRY'S CONSTANTS OF H_2 IN LIQUID NH_3 VS. π ATM.

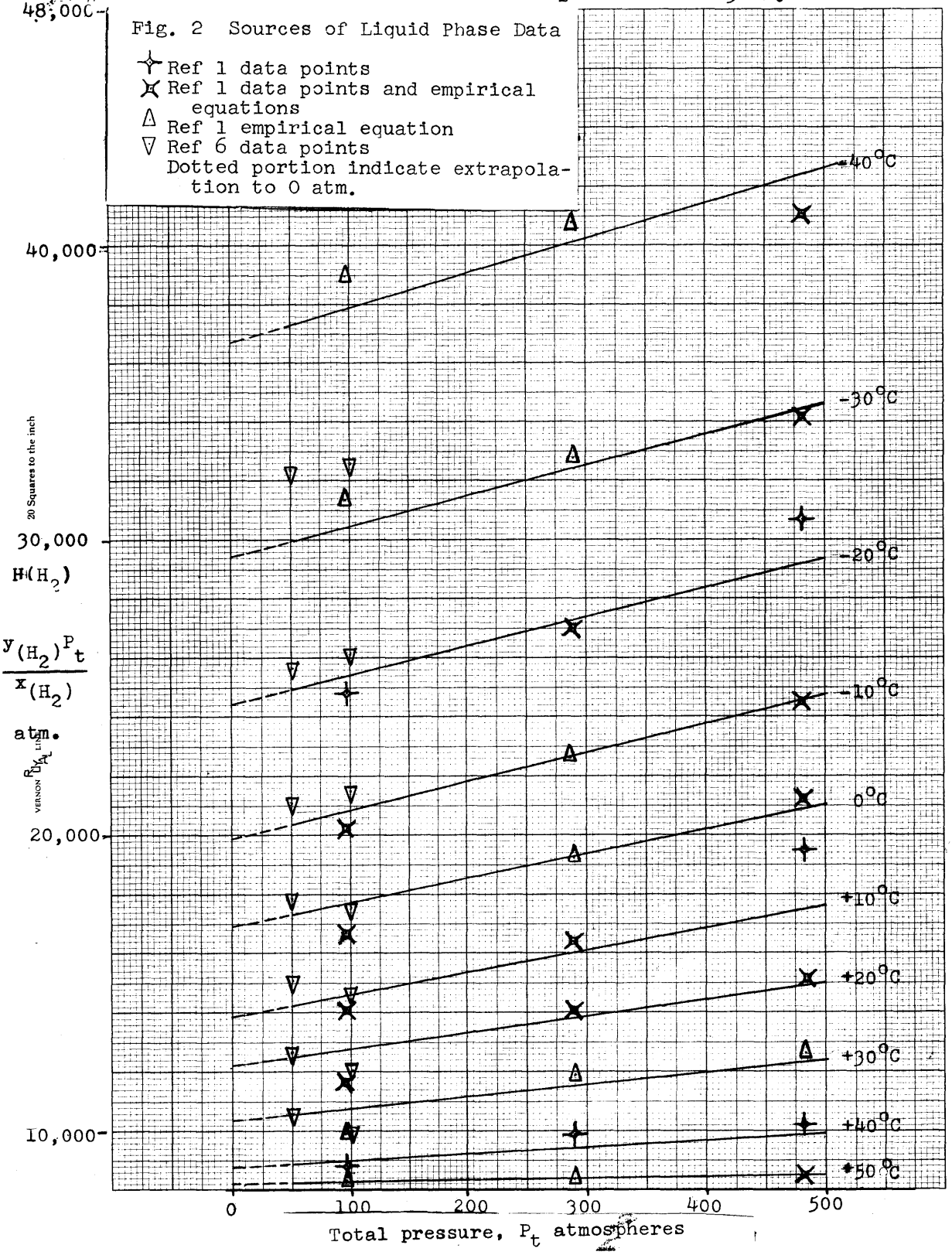

FIG. 3 HENRY'S LAW CONSTANT OF N_2 IN LIQUID NH_3 VS. TEMPERATURE $t^{\circ}C$

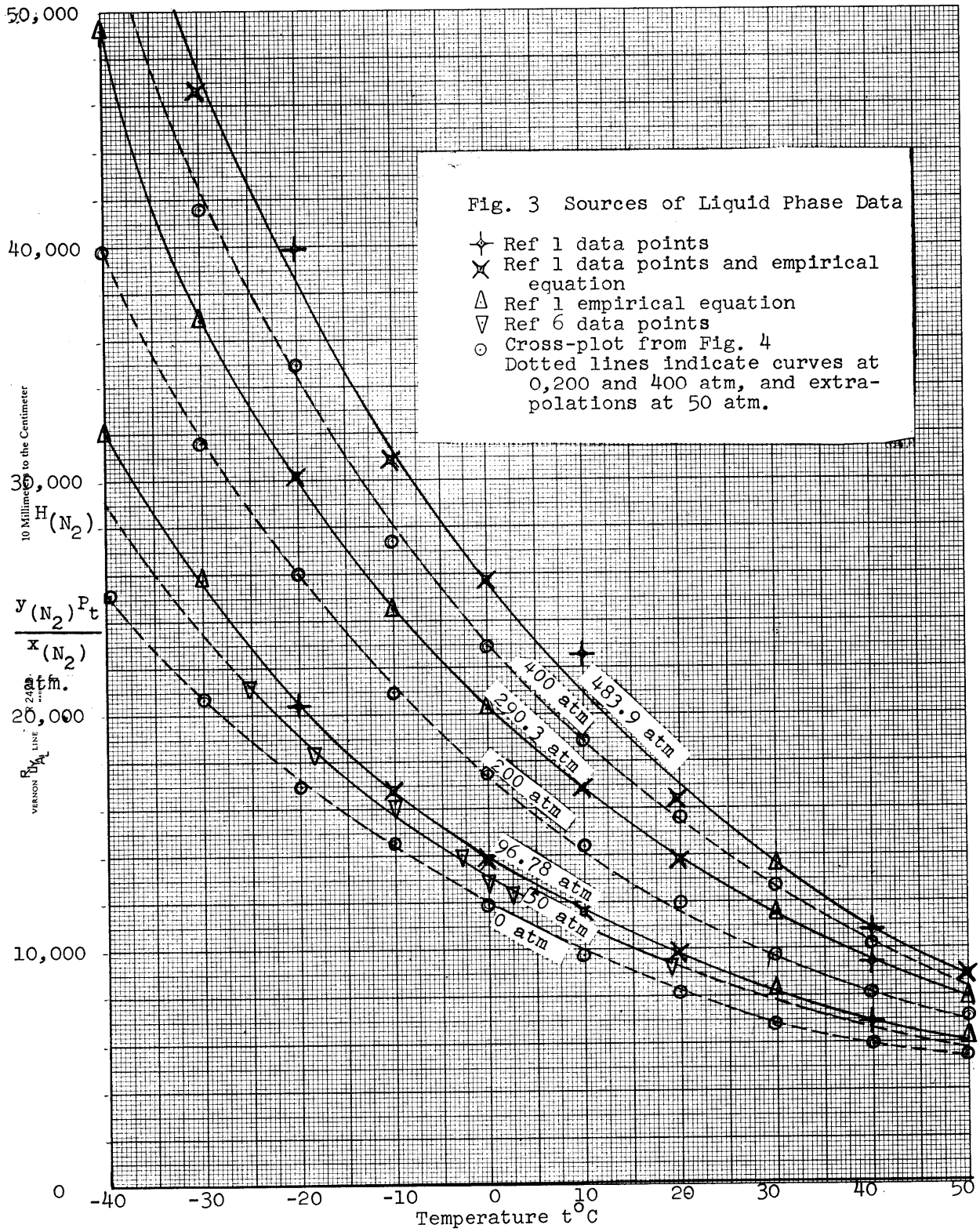

FIG. 4 CROSS PLOT OF HENRY'S CONSTANTS OF N_2 IN LIQUID NH_3 VS. π ATM.

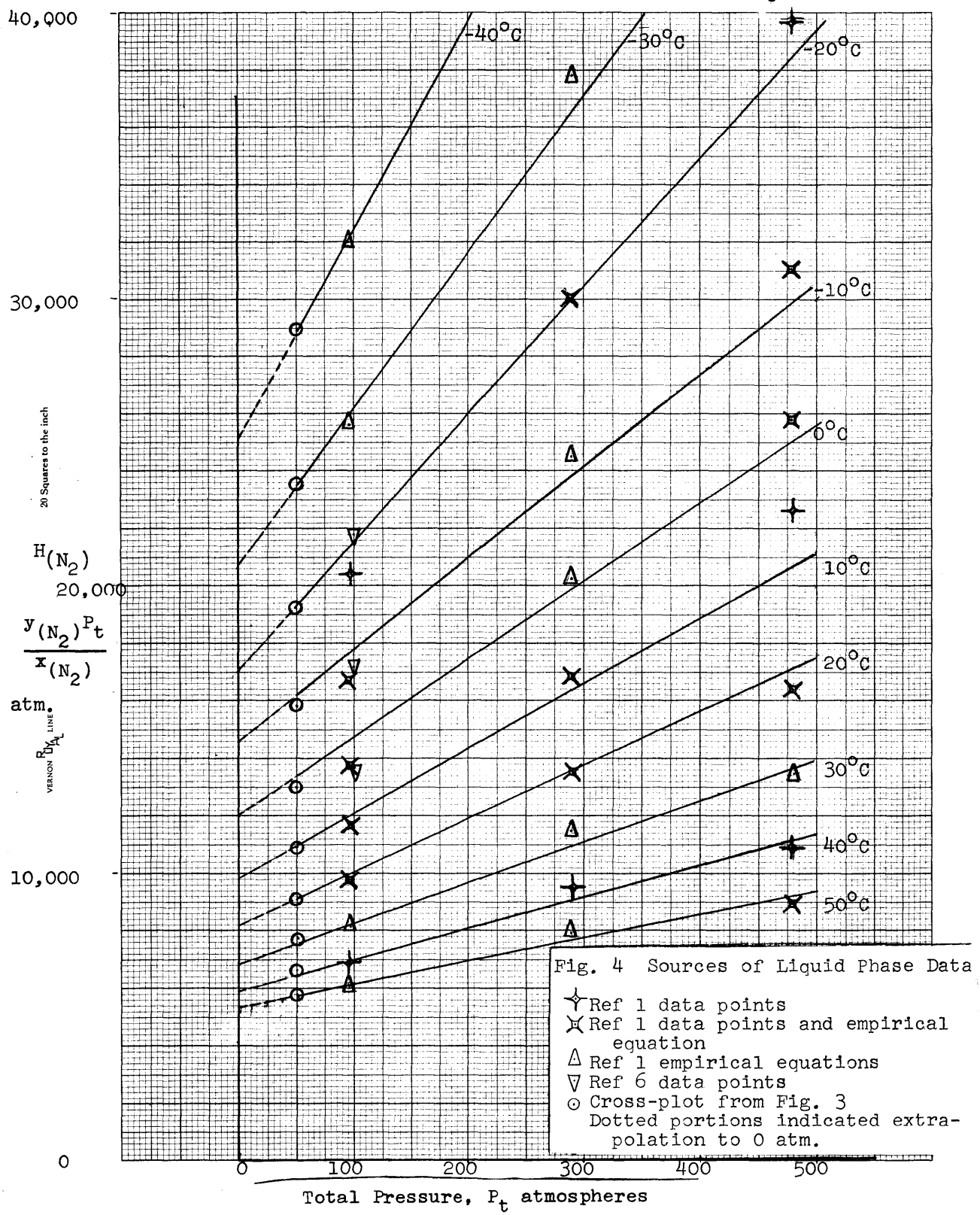

Fig. 4 Sources of Liquid Phase Data

- Ref 1 data points
- Ref 1 data points and empirical equation
- Ref 1 empirical equations
- Ref 6 data points
- Cross-plot from Fig. 3
  Dotted portions indicated extrapolation to 0 atm.

FIG. 5 AMMONIA CONTENT OF VAPOR $y_{NH_3}\pi$ VS. $\frac{1}{T}$ $^{o}K^{-1}$ A-17

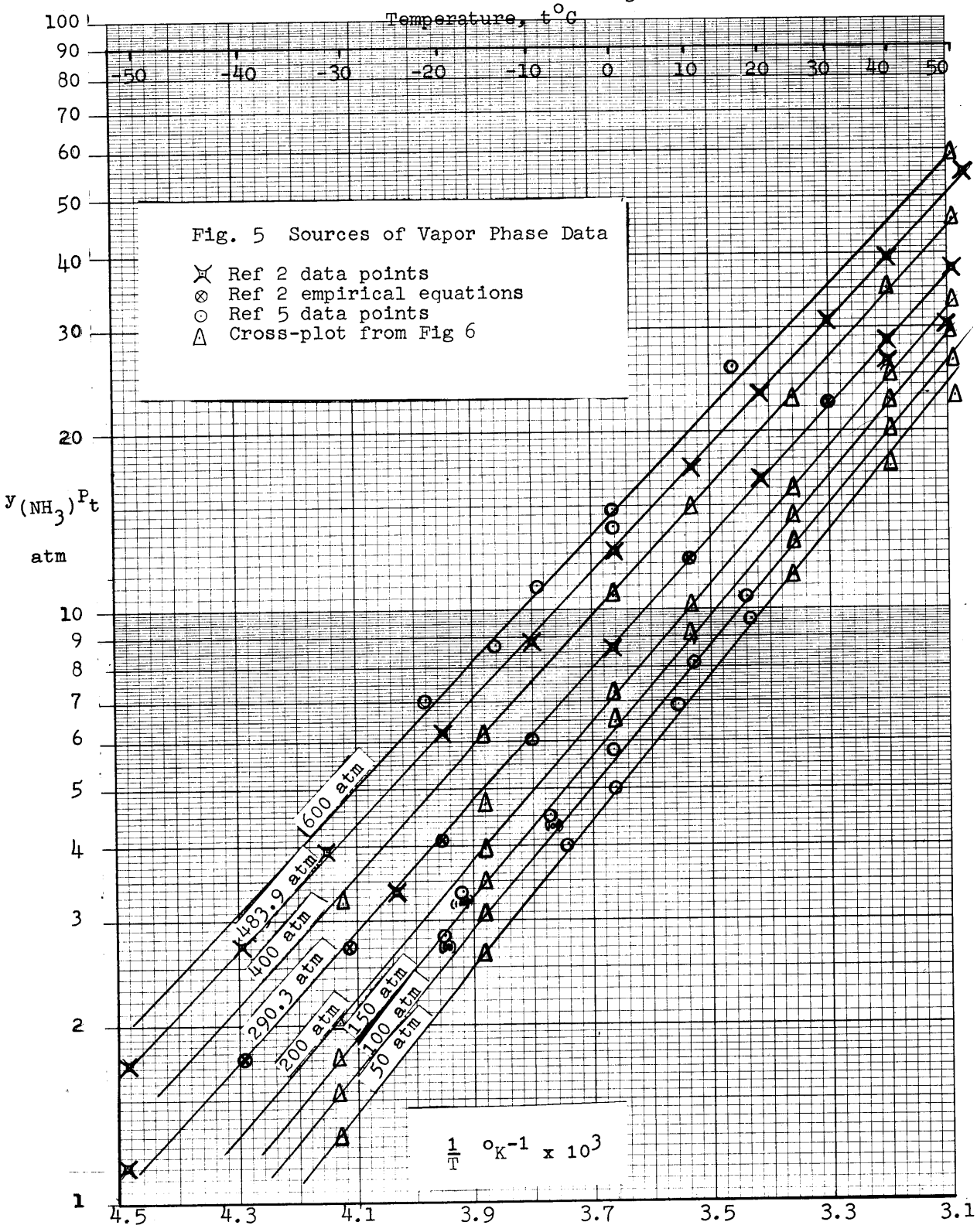

FIG. 6 CROSS-PLOT OF AMMONIA CONTENT OF VAPOR $y_{NH_3}\pi$ VS. π ATM.

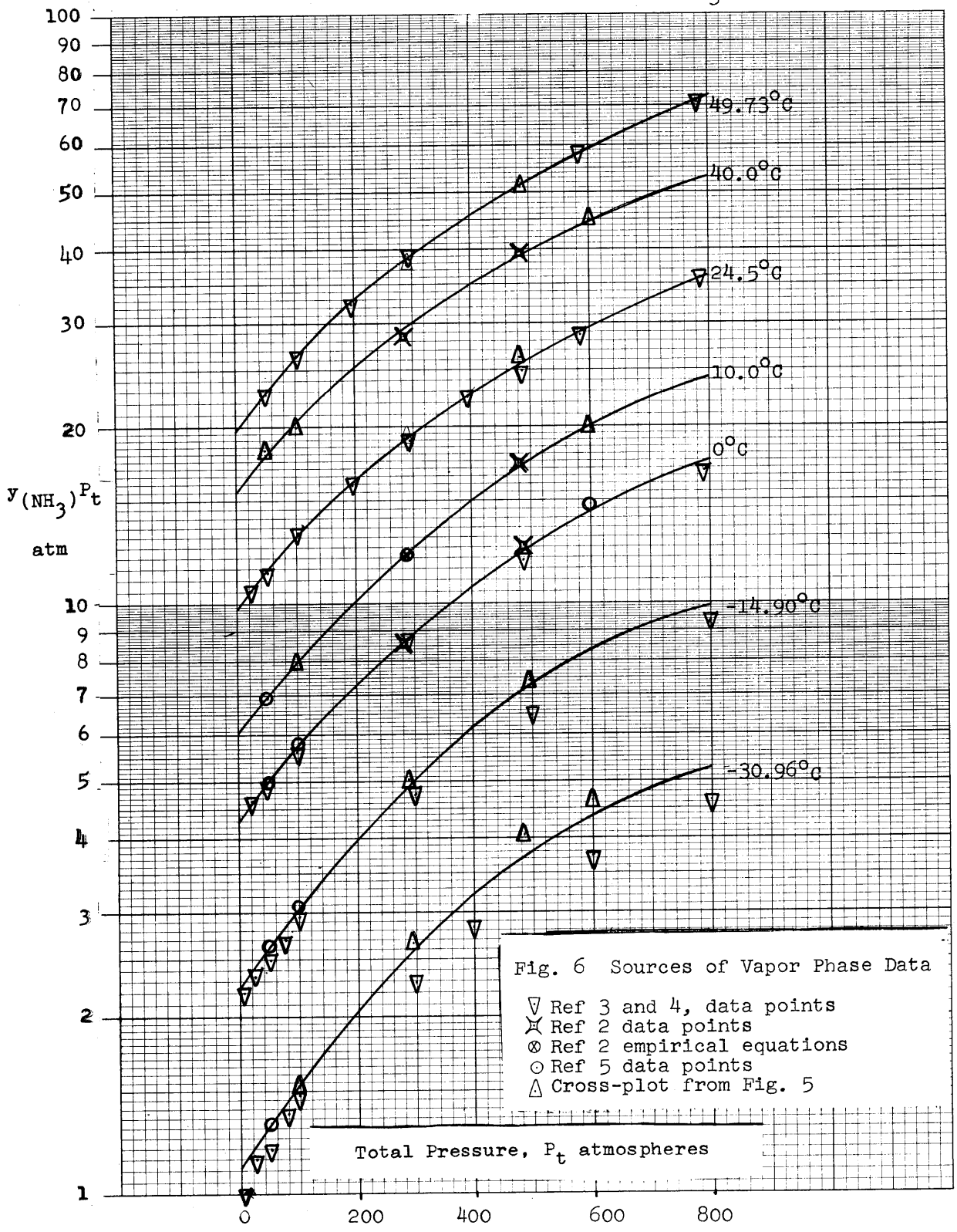

BIBLIOGRAPHY

1. Lefrancois, B. et Vaniscotti, C., "Solubilité du mélange gazeux (N_2 + H_2) dans l'ammoniac liquide." Genie Chimique, 83, 139-144, Mai 1960.

2. Lefrancois, B. et Vaniscotti, C., "Saturation en ammoniaque du mélange gazeux (N_2 + H_2) en présence d'ammoniaque liquide à 300 et 500 kg/cm^2 entre -70° et + 60°C." Chaleur et Industrie, 419, 183-186, Juin 1960.

3. Michels, A., Skelton, G.F., and Dumoulin, E., "Gas-Liquid Phase Equilibrium in the System Ammonia-Hydrogen-Nitrogen." Physica, XVI, 831-838, December 1950.

4. Michels, A., and others, "Gas Liquid Phase Equilibrium Below 0°C in the System NH_3 -H_2-N_2 and in the System NH_3-Kr." Physica, 25, 840-848, 1959.

5. Larson, Alfred T. and Black, Charles A., "The Concentration of Ammonia in a Compressed Mixture of Hydrogen and Nitrogen over Liquid Ammonia." Journal of American Chemical Society, 47, 1015-1020, April 1925.

6. Larson, Alfred T. and Black, Charles A., "Solubility of a Mixture of Hydrogen and Nitrogen in Liquid Ammonia." Industrial and Engineering Chemistry, 17, 715-716, July 1925.

SUPPLEMENT B
ENTHALPIES OF HYDROGEN, NITROGEN, AND AMMONIA TO 1400°F AND FROM 0 TO 200 ATMOSPHERES

I GENERAL INFORMATION

A. Introduction

The design of the ammonia cracking section as the source of chemical reflux constitutes a major step in the study of the monothermal ammonia-hydrogen chemical exchange process for the production of heavy water. The deuterium-enriched ammonia stream from the exchange towers is thermally cracked into nitrogen and enriched hydrogen. Part of the resulting mixture from the cracking reactor is cooled to recover uncracked ammonia, which is recycled to the cracking reactor, and the nitrogen and enriched hydrogen is refluxed into the exchange towers. The accurate design of the cracking reactor and its associated heat exchangers requires enthalpy values for hydrogen, nitrogen, and ammonia throughout the temperature and pressure ranges involved. This report presents enthalpy values for the three substances, within the ranges indicated:

	Temperature	Pressure
Hydrogen	-260 to 1400°F	14.7 to 6000 psia
Nitrogen	-60 to 1540°F	0 to 220 atm
Ammonia	-100 to 1400°F	0 to 3000 psia

B. Manner of Reporting

The graphs are plots of enthalpy versus temperature with pressure as the parameter. Units of enthalpy are Btu/lb-mole of substance.

The non-uniformity of pressure units is due to the manner in which the original data are reported. Hydrogen

and ammonia enthalpies were available mostly in psia, while nitrogen enthalpies were in atmospheres. Since interpolating between pressures is not so difficult, no attempt was made to cross-plot enthalpy versus pressure. And likewise, no attempt was made to report all three stbstances in uniform pressure units.

To facilitate the use of the graphs, enthalpies of all three substances are reported using the same basis: zero for free elements at $0^{\circ}K$ and 0 pressure. For hydrogen and nitrogen this poses no problem. But for ammonia, enthalpy at $0^{\circ}K$ and 0 pressure is not zero, but rather the heat of formation of ammonia at $0^{\circ}K$ and 0pressure (-16,860 BTU/lb-mole). All other ammonia values are transposed to conform to the enthalpy at $0^{\circ}K$ and 0 pressure. Numerical calculations are included in the section under ammonia.

With all the data on one basis, one can now calculate the heat involved in the cracking reaction at any temperature and pressure by a simple enthalpy balance, without accounting separately for the heat of reaction.

C. Use of the Graphs

To calculate the heat of the cracking reaction, it is necessary to know the equilibrium content at any temperature and pressure. MIT-D8 (1) is available for this purpose. It reports equilibrium ammonia mole fraction Y_{NH_3} versus temperature $^{\circ}F$ with pressure as a parameter.

Consider one mole of ammonia at a given temperature and pressure being cracked according to the reaction.

$$NH_3\ (g) \rightleftharpoons \frac{3}{2}H_2\ (g) + \frac{1}{2}N_2\ (g)$$

$$(1-x)\text{moles} \qquad (\tfrac{3}{2}x)\text{moles} \qquad (\tfrac{1}{2}x)\text{moles}$$

Let x be the number of moles cracked per mole of starting ammonia. Total number of moles at any instant is (1+x)moles.

Now, relate conversion x and the ammonia mole fraction Y_{NH_3}. The equilibrium or minimum (in the case of cracking) value of Y_{NH_3} is reported in MIT-D8.

$$Y_{NH_3} = \frac{1-x}{1+x}$$

or

$$x = \frac{1-Y_{NH_3}}{1+Y_{NH_3}}$$

Therefore, in terms of Y_{NH_3}, and based on one mole of starting ammonia, the change in the number of moles of each substance because of the ammonia cracking is:

Ammonia: $x = \dfrac{1-Y_{NH_3}}{1+Y_{NH_3}}$ moles per mole starting ammonia, decrease

Hydrogen: $\frac{3}{2}x = \frac{3}{2}\dfrac{1-Y_{NH_3}}{1+Y_{NH_3}}$ moles per mole starting ammonia, increase

Nitrogen: $\frac{1}{2}x = \frac{1}{2}\dfrac{1-Y_{NH_3}}{1+Y_{NH_3}}$ moles per mole starting ammonia, increase

Let i represent enthalpy, with the subscript indicating the substance involved. At any given temperature and pressure, enthalpy values are fixed and are easily read off the graphs in this report. Thus, heat of cracking at that temperature and pressure may be expressed as a function of the exit ammonia mole fraction Y_{NH_3}. Note that because the cracking reaction is endothermic, Q attains its maximum value when the maximum amount of ammonia is cracked, that is when Y_{NH_3} attains its equilibrium value, as reported in MIT-D8.

$$Q = \frac{3}{2}\frac{1-Y_{NH_3}}{1+Y_{NH_3}} i_{H_2} + \frac{1}{2}\frac{1-Y_{NH_3}}{1+Y_{NH_3}} i_{N_2} - \frac{1-Y_{NH_3}}{1+Y_{NH_3}} i_{NH_3}$$

$$= \frac{1-Y_{NH_3}}{1+Y_{NH_3}}\left[\frac{3}{2} i_{H_2} + \frac{1}{2} i_{N_2} - i_{NH_3}\right] \text{ Btu per mole starting ammonia.}$$

The graphs included in this report may also be used for ammonia synthesis calculations. In fact, as long as one is concerned only with changes in enthalpy, and as long as one is aware of the manner in which these graphs have been obtained, these graphs may prove useful, even for studies that have nothing to do at all with ammonia synthesis or cracking.

II HYDROGEN ENTHALPIES

A. Preparation of Curves

The graphs of hydrogen enthalpies have been obtained through private correspondence with Howard K. Rae of the Atomic Energy of Canada, Ltd. (2). Rae stated that the graphs are not too well documented but confirmed that they are adequate for preliminary calculations.

Another source, NBS Circular 564 (3), is available for hydrogen enthalpies, but the temperature range extends only from 60°K (-352°F) to 600°K (620°F). This NBS source is undoubtedly the more reliable of the two; but beyond 620°F, the only source available is the Canadian graphs. It becomes expedient, therefore, to compare the two sources for temperatures below 620°F.

Comparison between the two sources is summarized in Table 1, where the deviation indicated is based on the NBS value. All enthalpies are in Btu/lb-mol of hydrogen, with base zero at 0°K and 0 pressure.

From Table 1, the deviation between the two sources does not exceed 28.0 Btu/lb-mole between -100 and 620°F. So as to provide consistency, therefore, up to 1400°F, the Canadian graphs are accepted as the main source of data, being more extensive and reasonably accurate. This move eliminates the need for replotting the NBS data up to 620°F and then adjusting the curves at that temperature to coincide with the rest of the Canadian curves.

One slight observation must be added here. The NBS circular reports some curves crossing over one another between

Table 1

Comparison of Hydrogen Enthalpies from Canadian Graphs and from NBS Circular 564

t	P 1atm		100 atm
620°F	7410.	:Can:	7485
	7438.0	:NBS:	7506.4
(600°K)	-28.0	:Dev:	-21.4
440°F	6150	:Can:	6220
	6177.2	:NBS:	6240.9
(500°K)	-27.2	:Dev:	-20.9
260°F	4908	:Can:	4965
	4919.0	:NBS:	4974.7
(400°K)	-11.0	:Dev:	-19.7
80°F	3670	:Can:	3712
	3668.1	:NBS:	3709.1
(300°K)	+1.9	:Dev:	+2.9
-100°F	2430	:Can:	2445
	2452.2	:NBS:	2461.4
(200°K)	-22.2	:Dev:	-16.4

All Enthalpies in Btu/lb-mole

$-280^{\circ}F$ and $-100^{\circ}F$. This indicates that somewhere in this range, the Joule-Thompson coefficient vanishes. In the Canadian graphs, however, there is no crossing of curves at all. In using the Canadian graphs below $-100^{\circ}F$, one should therefore, be wary of any possible error. Fortunately, all calculations in the design of the ammonia cracking section involve only temperatures above $-100^{\circ}F$.

The Canadian curves follow immediately.

FIG. 1-1.

ENTHALPY OF HYDROGEN

1st Graph
-300 to 560°F

BASE:
IDEAL GAS AT -459.69° F

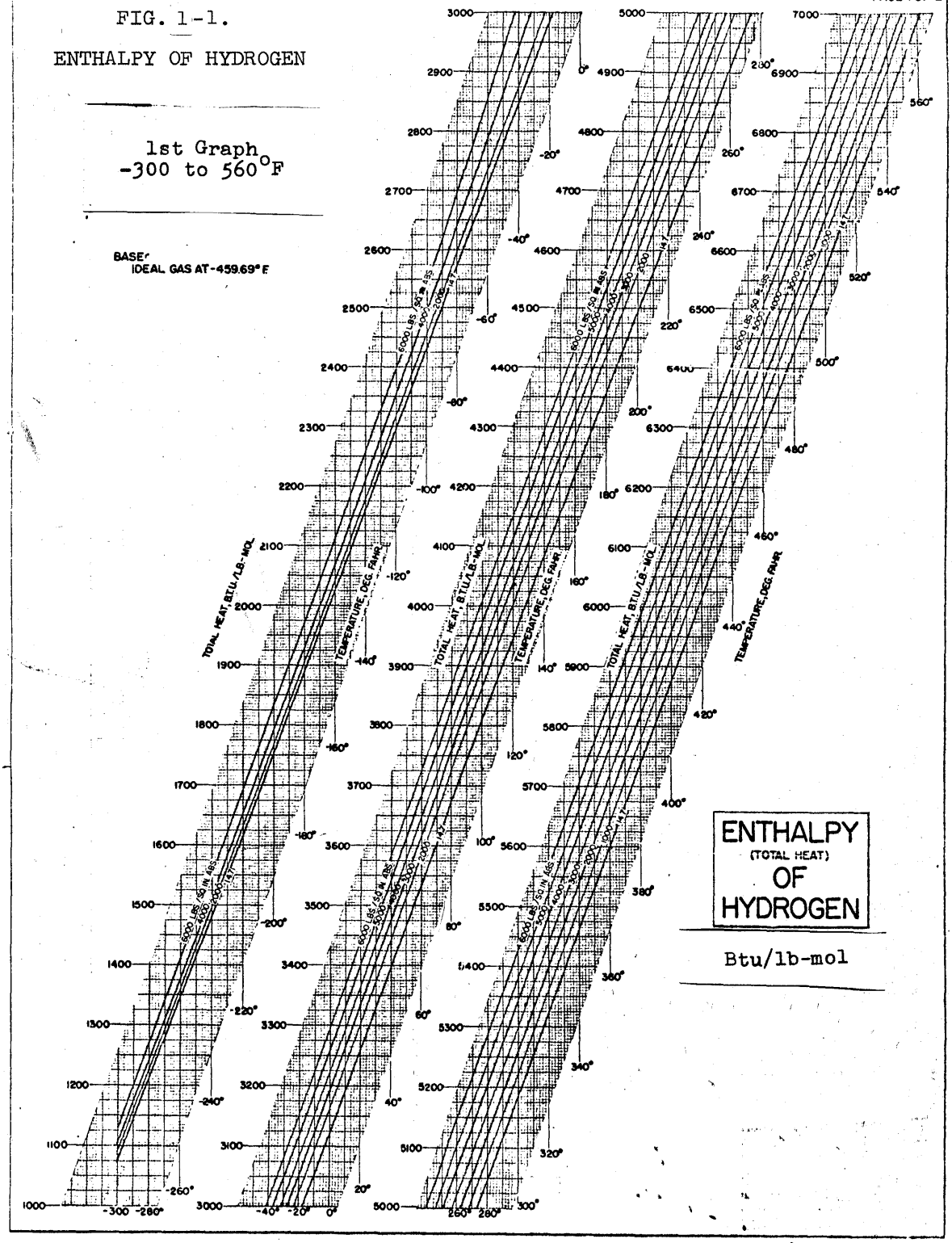

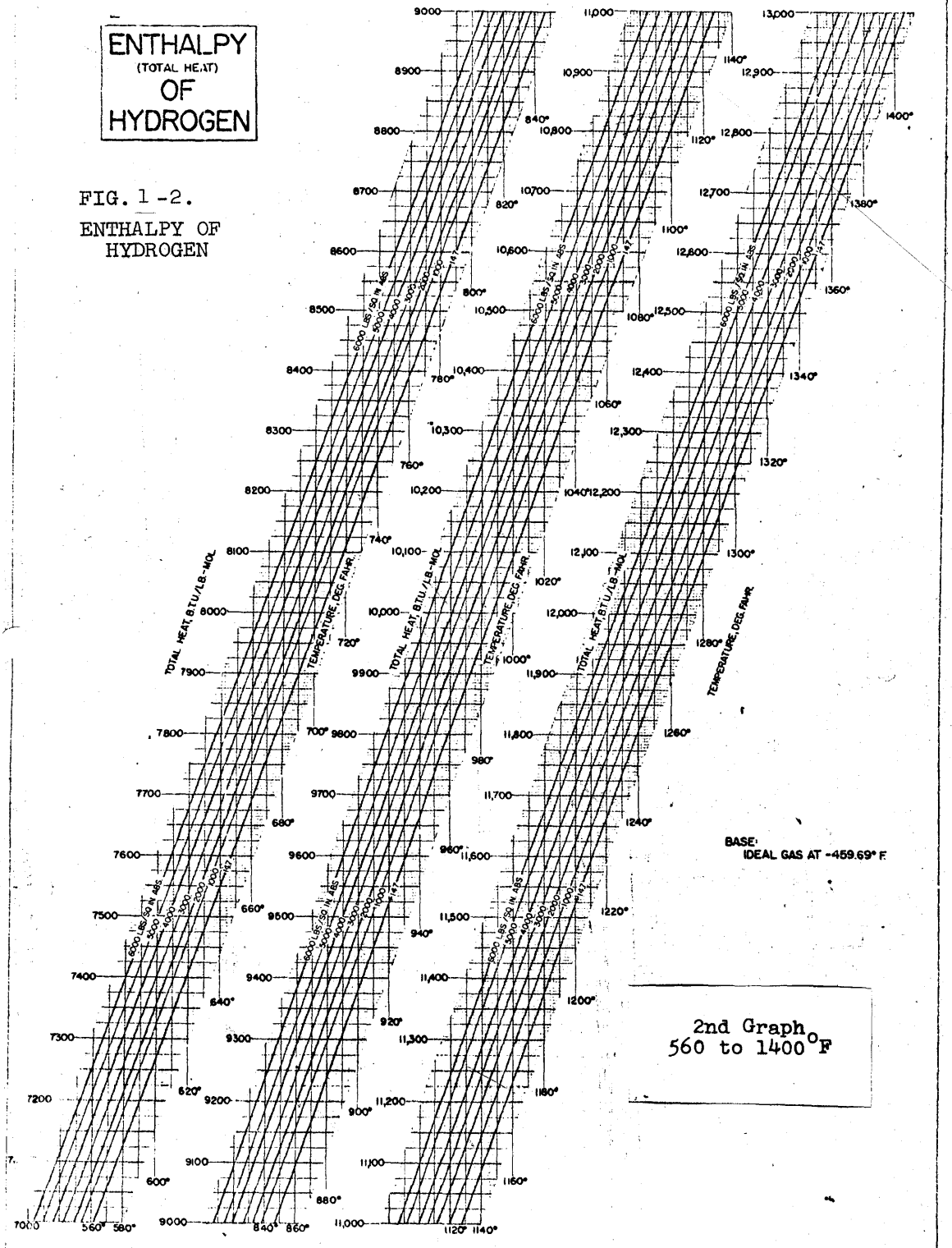

FIG. 1-2.
ENTHALPY OF
HYDROGEN

III NITROGEN ENTHALPIES

A. Source of Information

The nitrogen graphs are based entirely on NBS Circular 564 (3) Table 7-4. This time, reported data spans all the way from -280 to 4940°F and 0.01 to 100 atmospheres. The temperature range is certainly adequate. To extend the pressure range up to 200 atmospheres, extrapolations were necessary; and the details involved in such operations are explained in section B of this chapter.

Table 7-4 of NBS 564 reported nitrogen enthalpies as $(H-Eo^{\circ})/(RTo)$ where Eo° is the internal energy of the ideal gas at absolute zero, R is the universal gas constant, and To is 491.688°R (as 273.16°K). Transforming the enthalpies to Btu/lb-mole of nitrogen became a matter of multiplying all the NBS data by the constant factor RTo, since the basis was already the same; namely, ideal gas at absolute zero. Here, RTo was taken to be 976.984 Btu/lb-mole.

Table 2 of this report gives nitrogen enthalpies in Btu/lb-mole from -64°F to 1700°F at the NBS pressures: 0.01 atm, 10 atm, 40 atm, 70 atm, and 100 atm.

Table 2

Values of Nitrogen Enthalpies Based on Absolute Zero Temperature

Pressure: $t^{\circ}F$	0.01 atm	10 atm	40 atm	70 atm	100 atm
		Nitrogen Enthalpies, Btu/lb-mole			
-64	2750.8	2701.9	2553.1	2407	2267
-46	2876.1	2831.0	2695.2	2564	2442
-28	3001.4	2959.7	2835.4	2716	2609
-10	3126.5	3088.0	2973.8	2865	2765
+ 8	3251.8	3216.0	3110.4	3010	2911
26	3377.0	3343.9	3246.7	3155	3068
44	3482.6	3471.5	3381.7	3297	3222
62	3627.5	3598.9	3515.8	3438	3369
80	3752.8	3726.2	3649.1	3578	3513
98	3878.1	3853.4	3781.9	3715	3657
116	4003.5	3980.4	3914.1	3852	3799
134	4128.8	4107.3	4045.7	3989	3939
152	4254.2	4234.1	4177.1	4125	4078
170	4379.6	4360.9	4308.0	4259.7	4217
188	4505.2	4487.8	4438.6	4393.9	4354
206	4630.7	4614.6	4569.1	4527.6	4491
224	4756.2	4741.3	4698.9	4660.9	4627
242	4882.0	4868.1	4828.9	4793.9	4763
260	5007.7	4994.8	4958.8	4926.5	4898
278	5133.7	5121.7	5088.4	5058.8	5032
296	5259.6	5248.6	5217.9	5190.8	5167.5
314	5385.7	5375.6	5347.4	5322.8	5301.7
332	5511.9	5502.5	5476.7	5454.2	5435.1
350	5638.3	5629.7	5606.1	5585.7	5568.5
368	5764.7	5756.9	5735.4	5716.9	5701.5
386	5891.3	5884.2	5864.6	5848.2	5834.6
404	6018.1	6011.7	5994.0	5979.3	5967.6
422	6145.1	6139.3	6123.5	6110.6	6100.4
440	6272.2	6266.8	6252.9	6241.8	6233.1
458	6399.6	6394.8	6382.6	6373.0	6365.9
476	6527.1	6522.8	6512.2	6504.1	6498.4
494	6654.9	6651.1	6642.0	6635.4	6631.2
512	6782.9	6779.5	6772.0	6766.8	6763.7
530	6911.1	6908.2	6902.1	6898.2	6896.4
548	7039.5	7037.0	7032.2	7029.7	7029.1
566	7168.1	7166.2	7162.7	7161.4	7162.0
584	7297.0	7295.4	7293.2	7293.1	7294.7
602	7426.1	7425.0	7424.0	7425.1	7428.2

$t^{\circ}F$	0.01	10	40	70	100
620	7555.5	7555.1	7555.2	7557.4	7561.2
638	7685.1	7685.1	7686.3	7689.5	7694.3
656	7815.1	7815.4	7817.8	7821.9	7827.7
674	7945.3	7946.0	7949.4	7954.6	7961.3
692	8075.8	8076.8	8081.2	8087.2	8095.0
710	8206.5	8207.8	8213.2	8220.1	8228.7
728	8337.5	8339.2	8345.5	8353.4	8362.7
746	8468.8	8470.8	8478.0	8486.8	8496.9
764	8600.4	8602.6	8610.7	8620.4	8631.3
782	8732.2	8734.8	8743.7	8754.1	8765.9
800	8864.4	8867.3	8877.0	8888.3	8900.6
818	8996.9	9000.1	9010.4	9022.4	9035.5
836	9129.5	9132.9	9144.2	9157.0	9170.7
854	9262.6	9266.3	9278.3	9291.7	9306.2
872	9395.9	9399.9	9412.5	9426.6	9441.8
890	9529.5	9533.7	9547.1	9561.8	9577.7
908	9663.3	9667.7	9681.9	9697.2	9713.7
926	9797.6	9802.3	9816.9	9833.1	9850.0
944	9932.0	9936.9	9952.2	9968.9	9986.5
962	10,066.8	10,071.9	10,087.9	10,105.1	10,123.3
980	10,202.0	10,207.2	10,223.8	10,241.6	10,260.2
1160	11,568.4	11,575.5	11,597.3	11,620.0	11,643.4
1340	12,962.0	12,970.4	12,996.3	13,022.8	13,049.9
1520	14,380.5	14,390.0	14,419.1	14,448.7	14,478.6
1700	15,821.2	15,831.6	15,863.2	15,895.2	15,927.7

B. Extrapolation to Higher Pressures

Since the reported NBS pressures were 10, 40, 70, and 100 atmospheres, it became possible to extrapolate beyond 100 atm at regular intervals of 30 atm by the method of second differences. It was assumed that extrapolations up to 220 atm could be made without incurring significant errors. Furthermore, poltting the values would diminish any effect due to slight errors in extrapolating. As such, extrapolated enthalpies are taken at 130, 160, 190, and 200 atmospheres.

As an illustration, consider values at 422°F, shown in Table 3.

Table 3

Extrapolation to Higher Pressures at 422°F.

An Illustration of the Method of Second Differences

Pressure	Enthalpy Btu/lb-m	First Difference	Second Difference	Average of Second Differences
10 atm	6139.3			
		-15.8		
40 atm	6123.5		-2.9	
		-12.9		-2.8
70 atm	6110.6		-2.7	
		-10.2		
100 atm	6100.4			
		-7.4		
130 atm	6093.0			
		-4.6		
160 atm	6088.4			
		-1.8		
190 atm	6086.6			
		+1.0		
220 atm	6087.6			

The upper part of Table 3, using data from Table 2, should be self-explanatory. The average of second differences (in the case, 2.8) is then successively applied to the first differences to establish a continuous trend. Thus, the first difference between 100 atm and 130 atm is determined to be 2.8 Btu/lb-mole lower than the first difference between 70 atm and 100 atm. And so on, with succeeding extrapolations. Once the first differences have been fixed, the actual enthalpy values can be obtained by successive algebraic application of these first differences to the immediately preceding enthalpy.

Now, between 190 and 220 atm, the first difference reverses sign. This indicates that at 422°F between 0 and 190 atm, an increasing pressure causes a decreasing enthalpy effect; whereas above 220 atm, the opposite is true. The reversing trend is associated with a vanishing Joule-Thomson coefficient at 422°F between 190 and 220 atmospheres. For different temperatures, this coefficient vanishes at a different pressure. The pressure lines, therefore, on an enthalpy versus temperature graph are not concurrent, but rather, two pressure lines have a unique intersection. The 3rd Graph for nitrogen included here somewhat illustrates this concept, although not very clearly because of scale limitations.

Table 4 shows the extrapolated nitrogen enthalpies obtained by the methos of second differences just illustrated.

Table 4

Nitrogen Enthalpies Extrapolated for Higher Pressures

Pressure $t^{\circ}F$	Nitrogen Enthalpies Btu/lb-mole 130 atm	160 atm	190 atm	220 atm
-64	2131	2000	1873	1751
-46	2327	2219	2117	2023
-28	2512	2424	2343	2271
-10	2672	2585	2505	2431
+ 8	2815	2722	2631	2544
26	2986	2909	2838	2771
44	3154	3094	3041	2976
62	3308	3255	3210	3173
80	3454	3401	3354	3313
98	3607	3564	3530	3503
116	3753	3713	3680	3653
134	3895	3856	3824	3797
152	4036	3999	3967	3940
170	4179	4147	4119	4097
188	4319	4288	4262	4240
206	4459	4431	4408	4389
224	4597	4572	4550	4533
242	4726	4694	4666	4641
260	4873	4852	4834	4820
278	5008	4988	4971	4957
296	5147.9	5132.0	5119.8	5111.3
314	5284.2	5270.3	5260.0	5253.3
332	5419.4	5407.1	5398.2	5392.7
350	5554.5	5543.7	5536.1	5531.7
368	5689.1	5679.7	5673.3	5669.9
386	5824.0	5816.4	5811.8	5810.2
404	5958.9	5953.2	5950.5	5950.8
422	6093.0	6088.4	6086.6	6087.6
440	6227.0	6223.5	6222.6	6224.1
458	6361.4	6359.5	6360.1	6363.4
476	6495.1	6494.2	6495.7	6499.6
494	6629.4	6630.0	6633.0	6638.4
512	6762.8	6764.1	6767.6	6773.3
530	6896.6	6898.8	6903.0	6909.2
548	7030.6	7034.2	7039.9	7047.7
566	7164.6	7169.2	7175.8	7184.4
584	7298.2	7303.6	7310.9	7320.1
602	7433.3	7440.4	7449.5	7460.6

$t^{\circ}F$	130	160	190	220
620	7567.0	7574.8	7584.6	7596.4
638	7700.9	7709.3	7719.5	7731.5
656	7835.2	7844.4	7855.3	7867.9
674	7969.6	7979.5	7991.0	8004.1
692	8104.5	8115.7	8128.6	8143.2
710	8238.9	8250.7	8264.1	8279.1
728	8373.5	8385.8	8399.6	8414.9
746	8508.4	8521.3	8535.6	8551.3
764	8643.9	8658.2	8674.2	8691.9
782	8779.1	8793.7	8809.7	8827.1
800	8914.6	8930.0	8946.8	8965.0
818	9050.0	9065.9	9083.2	9101.9
836	9185.6	9201.7	9219.0	9237.5
854	9321.9	9338.8	9356.9	9376.2
872	9458.3	9476.1	9495.2	9515.6
890	9594.8	9613.1	9632.6	9653.3
908	9731.4	9750.3	9770.4	9791.7
926	9868.1	9887.4	9907.9	9929.6
944	10,005.3	10,025.3	10,046.5	10,068.9
962	10,142.6	10,163.0	10,184.5	10,207.1
980	10,279.8	10,300.4	10,322.0	10,344.6
1160	11,667.6	11,692.6	11,718.4	11,745.0
1340	13,077.6	13,105.9	13,134.8	13,164.3
1520	14,508.9	14,539.6	14,570.7	14,602.2
1700	15,960.6	15,993.9	16,027.6	16,061.7

C. Preparation and Use of the Nitrogen Graphs

The enthalpy values from Tables 2 and 4 are plotted, allowing the same degree of accuracy as the Canadian hydrogen curves; that is, four significant figures. Six graphs are constructed to cover the temperature range from -80 to 1560°F.

To facilitate the use of the curves, here is an index of the enthalpy and temperature ranges of each graph:

	Temperature Range °F	Enthalpy Range Btu/lb-m
First Graph	-80 to 200	1800 to 4000
Second Graph	100 to 420	4000 to 6000
Third Graph	400 to 720	6000 to 8200
Fourth Graph	700 to 980	8200 to 10,200
Fifth Graph	960 to 1280	10,200 to 12,400
Sixth Graph	1240 to 1560	12,400 to 14,600

Linear interpolation between pressures is accurate enough for all practical purposes. If greater accuracy is desired, interpolations should be applied to the values of Tables 2 and 4, instead of to the graphs.

Note that in the third Graph, the 0.01 atm, 100 atm, and 220 atmosphere lines cross one another because of the vanishing Joule-Thomson coefficient. The intersection temperatures have been determined to be around:

470°F for the 100 and 200 atm lines;

540°F for the 0.01 and 200 atm lines;

and 590°F for the 0.01 and 100 atm lines.

Scale limitations prohibit more precise plotting in this region.

Following are the six nitrogen enthalpy graphs.

FIG. 1-3. ENTHALPY OF NITROGEN

First Graph: -80 to 200°F

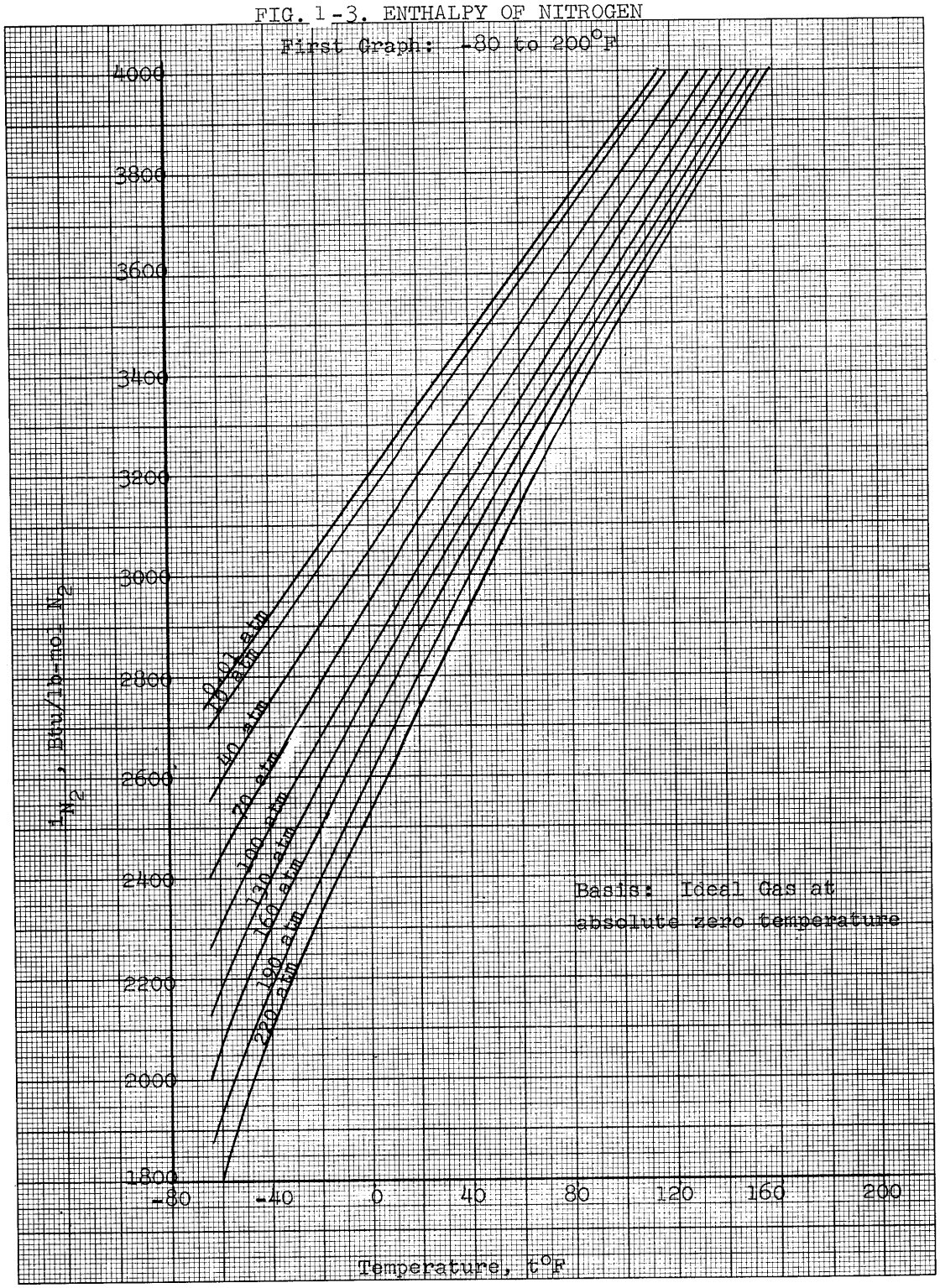

FIG. 1-4. ENTHALPY OF NITROGEN

Second Graph: 100 to 420°F

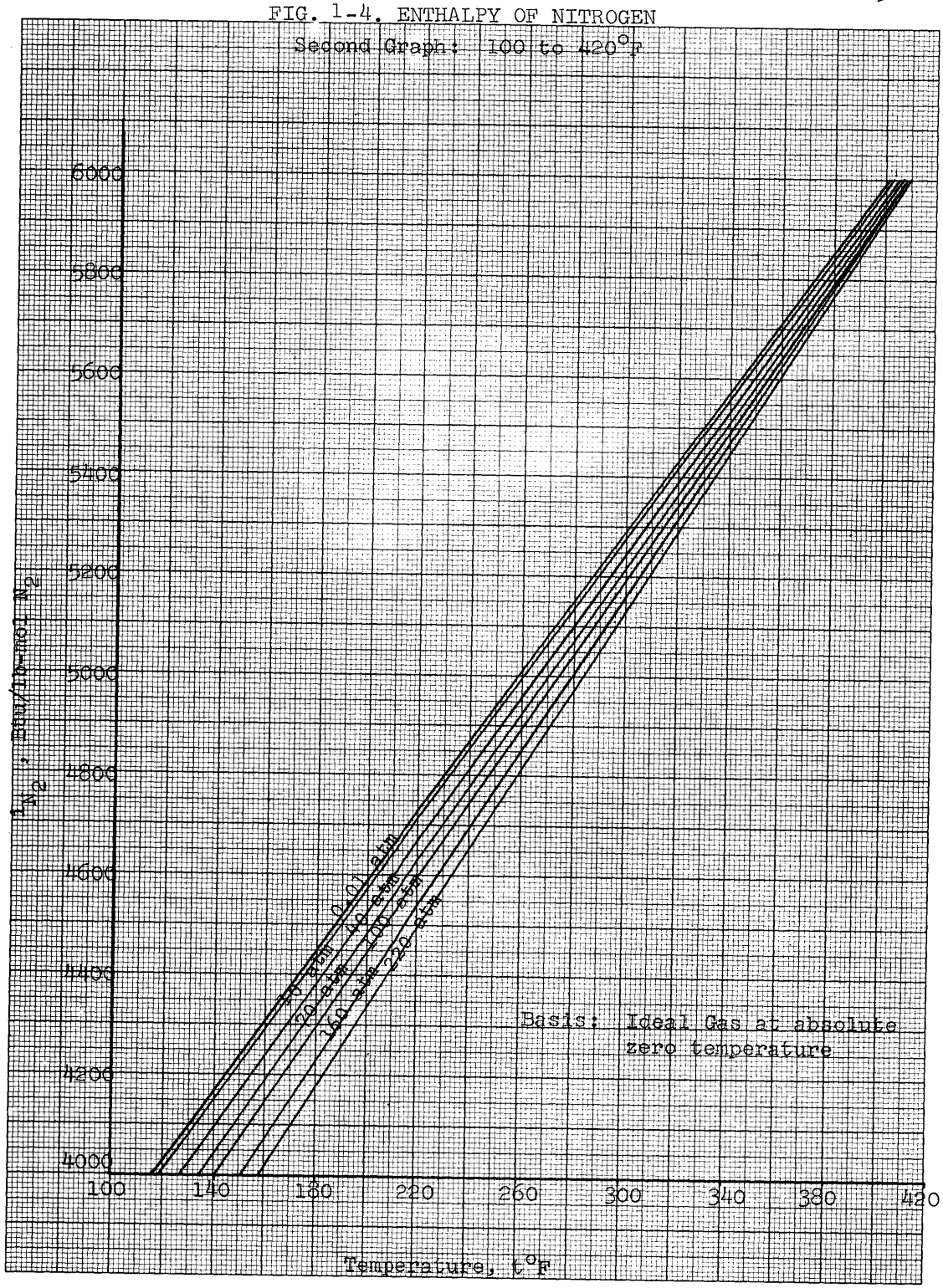

FIG. 1-5. ENTHALPY OF NITROGEN

Third Graph: 400 to 720°F

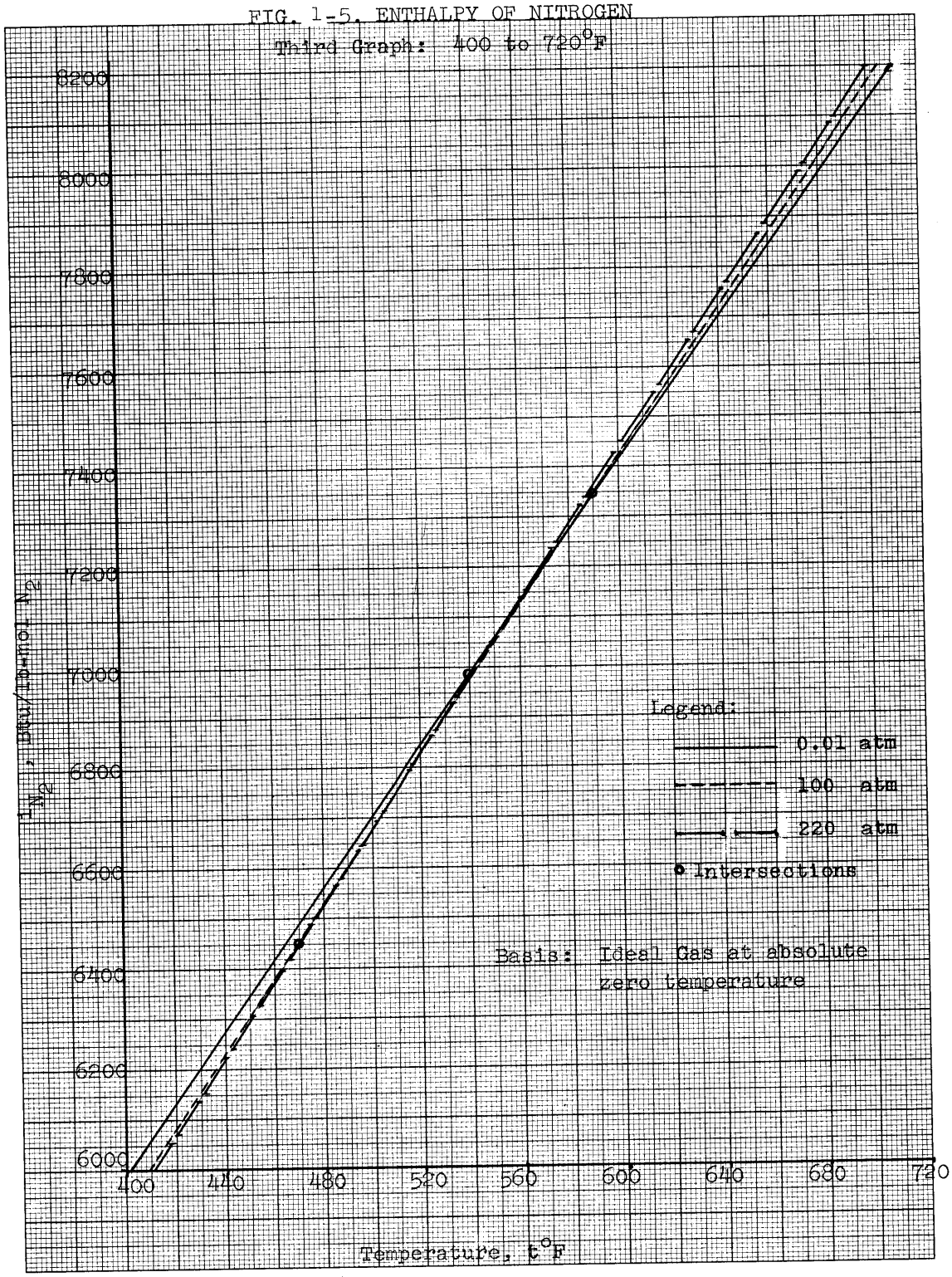

FIG. 1-6. ENTHALPY OF NITROGEN
Fourth Graph: 700 to 980°F

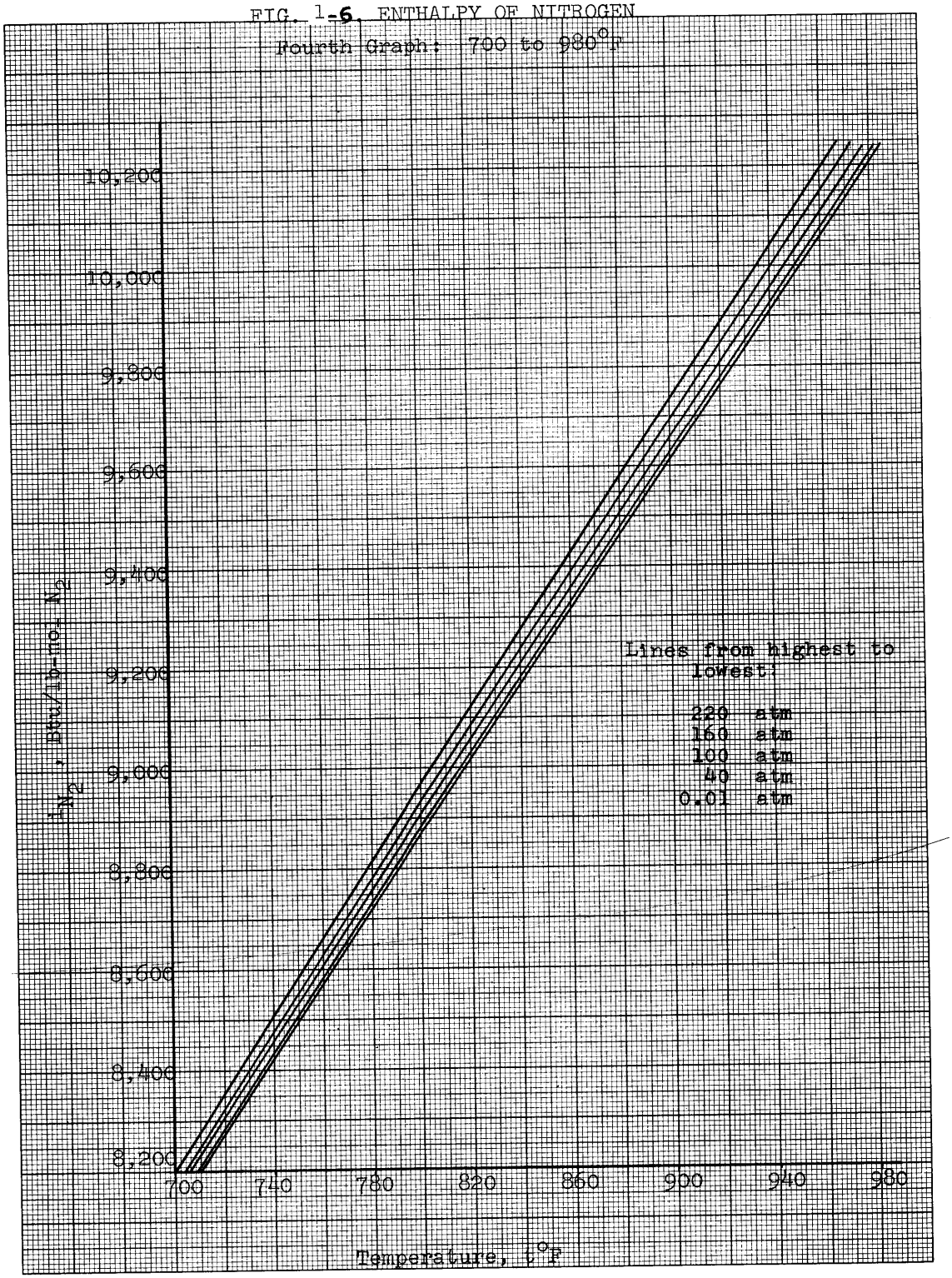

FIG. 1-7. ENTHALPY OF NITROGEN

Fifth Graph: 960 to 1280°F

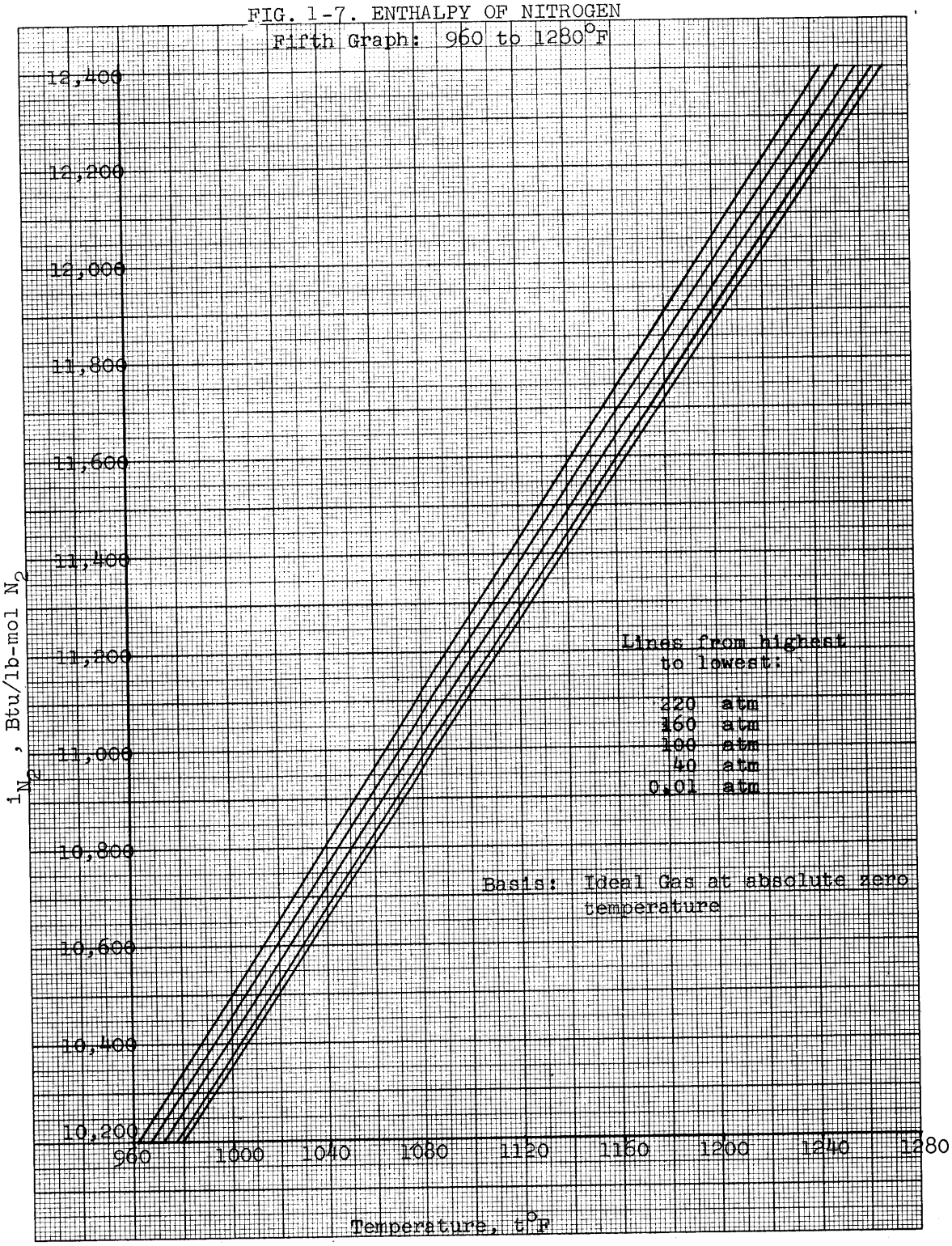

FIG. 1-8. ENTHALPY OF NITROGEN
Sixth Graph: 1240 to 1560°F

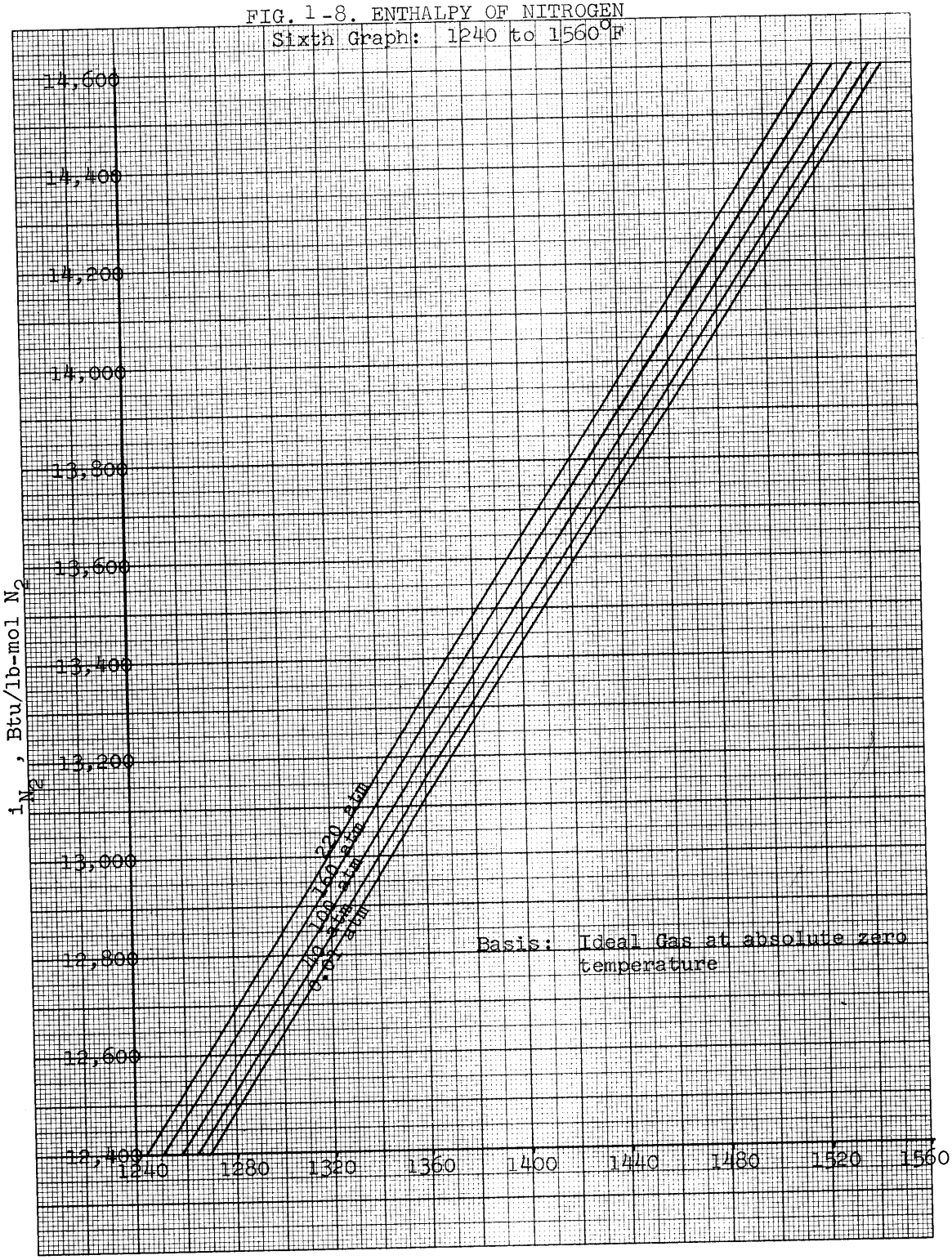

AMMONIA ENTHALPIES

A. List of Correlated Data

The pieces of information used to prepare the ammonia enthalpy graphs are the following:

1. Heat of formation of ammonia at absolute zero temperature and enthalpy of ammonia gas at zero pressure at 298°K relative to 0°K, needed to transpose all enthalpies to the chosen basis of ideal hydrogen and nitrogen gas at 0°K; from Lewis and Randall (4)

2. Specific heat of ammonia gas at zero pressure as a function of temperature for a wide temperature range; from Tsoiman (5)

3. Saturated and superheated ammonia tables, from refrigeration handbook (6)

4. Graphically determined ammonia enthalpy values from -100 to 700°F and from 0 to 1600 psia; from Grahl (7)

5. Beattie-Bridgeman equation of state; from Wolley, et al, (8) and original Beattie and Lawrence data (9)

The final results are given on eleven large-scale graphs spanning from -100°F to 1400°F, the scale of coordinates of the graphs being similar to the hydrogen and nitrogen curves. The shades of disagreements and discontinuities caused by the use of so many data sources are more than offset by the difficulty of plotting and reading more accurately than $\pm$ 5 Btu/lb-mol. Liquid enthalpies are no longer plotted but may be obtained easily from tabulated values included here.

B. Transposing Data to Report Basis

The term report basis refers to zero enthalpy level taken for this report----diatomic hydrogen and nitrogen gas

at absolute zero temperature and zero pressure. Lewis and Randall (4) gave the heat of formation of ammonia at zero pressure and absolute zero temperature as -9.37 kcal/g-mole. This figure therefore became the enthalpy of ammonia gas at zero pressure and zero absolute temperature relative to the report basis. Thus, in report notation,

$$(i_{NH_3})^{0}_{0} = 9.37 \text{ Kcal/g-mole or } -16{,}860 \text{ Btu/lb-mole.}$$

For this chapter of the report, the notation NH_3 will be dropped so that $i^0_0 = -16{,}860$ Btu/lb-mole, with the subscript representing absolute temperature and the superscript zero pressure. This figure now serves as the basis for correlating all ammonia sources.

Lewis and Randall (4) also gave enthalpy of ammonia at zero pressure at 298°K relative to 0°K as +2.37 kcal/g-mole. Therefore:

$$i^0_{298^\circ K} = -9.37 + 2.37 = -7.00 \text{ kcal/g-mole} \quad \text{or}$$

$$-12{,}600 \text{ Btu/lb-mole.}$$

Similarly, if enthalpies relative to either i^0_0 or $i^0_{298^\circ K}$ are available, they can be transposed to the report basis.

As a matter of convenience, the units of the subscripts and the superscripts are dropped when the temperature is in °F and the pressure in psia, since these are the common units used for ammonia data. Thus, i^0_{77} is the enthalpy of ammonia at 0 psia and 77°F. The symbols 0 and o are used here interchangeably so that i^0_{77} is the same as i^o_{77}.

C. Obtaining the Zero Pressure Line

G. I. Tsoiman (5) gave empirical equations for heat capacity Cp^0 of ammonia in the ideal-gas state as functions of temperature. Integration and basis transposition yield desired enthalpy values at any temperature within the range of validity. However, the valid temperature range for the equation extends only from 0^oC to 3000^oC. For zero-pressure enthalpies below 0^oC, it is necessary to use another source---superheated ammonia tables (6).

The superheated vapor tables report enthalpies down to 5 psia. An examination of the data reveals a linear pressure effect at low pressures. Linear extrapolation down to zero pressure is, therefore, justified as a means of determining ideal-gas points below 0^oC.

To transpose these enthalpies to the report basis, since the datum for the ammonia tables is saturated liquid at -40^oF, it is a matter of relating each particular value to the enthalpy at 77^oF (298^oK) which is already known to be -12,600 Btu/lb-m.

As an illustration, let us take the case of -50^oF. What is required is the enthalpy of ammonia at -50^oF and zero pressure relative to the report basis. Superheated tables give the following values relative to the table datum of saturated liquid at -40^oF:

At -50^oF: 5 psia-----595.2 Btu/lb
6 psia-----594.6 Btu/lb
7 psia-----594.0 Btu/lb

By linear extrapolation, enthalpy at -50^oF and 0 psia is 598.2Btu/lb. Similarly, enthalpy at 77^oF is determined to be 659.9Btu/lb.

Thus:

$$i^{\circ}_{(-50)} - i^{\circ}_{77} = 598.2 - 659.9 = -61.7 \text{ Btu/lb}$$

or -1050.9 Btu/lb-mole

using 17.032 as molecular weight of ammonia. Since $i^{\circ}_{77} = -12{,}600$ Btu/lb-mole, $i^{\circ}_{(-50)}$ is determined to be -13,650.9 Btu/lb-mole. This is the required piece of information needed.

Table 5 lists enthalpy values obtained in this manner.

Table 5

Ammonia Enthalpies at Zero Pressure, from Ammonia Tables

Temp	i°_F Btu/lb from tables	$i^{\circ}_t - i^{\circ}_{77}$ Btu/lb	$i^{\circ}_t - i^{\circ}_{77}$ Btu/lb-mole	i°_t Btu/lb-mole
-100	573.7	-86.2	-1,469.1	- 14069.1
- 50	598.2	-61.7	-1,050.9	-13,650.9
0	621.8	-38.1	- 648.9	-13,248.9
32	637.6	-22.3	- 379.8	-12,979.8
50	646.6	-13.3	- 226.5	-12,826.5
77	659.9	0	0	-12,600.0
100	671.4	+11.5	+ 195.9	-12,404.1
150	697.0	+37.1	+ 631.9	-11,968.1
200	723.1	+63.2	+1,076.4	-11,523.6

Note that the overlap, beyond 100°F will be used to compare with values from Tsoiman's equations.

Tsoiman gave two equations, the first of which was already sufficient to cover the desired range from 0 to 1500°C:

$$Cp^{\circ} = 0.4915 + 0.38 \times 10^{-3}\, t + 0.189834 \times 10^{-6} t^2 - 0.26 \times 10^{-9} t^3 + 0.072666 \times 10^{-12} t^4 \qquad (1)$$

where t is in $^{\circ}C$

Cp is in Btu/lb $^{\circ}R$ or cal/g $^{\circ}K$

and equation (1) valid from $0^{\circ}C$ to $1500^{\circ}C$.

Integrating and converting units to give enthalpy in Btu/lb-mole,

$$\Delta I(\text{based on } 32^{\circ}F) = 8.3712\,(F-32) + 1.79783 \times 10^{-3}\,(F-32)^2 + 0.332635 \times 10^{-6}\,(F-32)^3 - 0.189830 \times 10^{-9}\,(F-32)^4 + 0.023579 \times 10^{-12}\,(F-32)^5 \qquad (2)$$

where Δ I is enthalpy in Btu/lb-mole relative to ideal gas at $32^{\circ}F$ or equal to $i_F^{\circ} - i_{32}^{\circ}$

F is temperature in Fahrenheit and equation (2) valid from $32^{\circ}F$ to $2732^{\circ}F$

Table 5 gives i_{32}° as -12,979.8. Thus, i_t° may be computed by algebraically adding -12,979.8 to Δ I obtained from equation (2). Values of i_t° are shown in Table 6.

Table 6

Ammonia Enthalpies at Zero Pressure, from Tsoiman Equation

Temp $t^{\circ}F$	I from (2) Btu/lb-mole	i_t° Btu/lb-mole
100	577.6	-12,402.2
150	1,015.6	-11,964.2
200	1,458.5	-11,520.3
250	1,913.4	-11,066.4
300	2,378.1	-10,601.7
350	2,852.7	-10,127.1
400	3,337.3	- 9,642.5
450	3,832.0	- 9,147.8
500	4,337.0	- 8,642.8
550	4,852.1	- 8,127.7
600	5,377.5	- 7,602.3
650	5,913.0	- 7,066.8
700	6,456.0	- 6,523.8
750	7,014.2	- 5,965.6
800	7,580.4	- 5,399.4
850	8,156.3	- 4,823.5
900	8,742.1	- 4,237.7
950	9,337.7	- 3,642.1
1000	9,943.0	- 3,036.8
1050	10,557.8	- 2,422.0
1100	11,182.1	- 1,797.7
1150	11,815.6	- 1,164.2
1200	12,458.2	- 521.7
1250	13,109.7	+ 129.9
1300	13,770.0	+ 790.2
1350	14,438.8	+ 1,459.0
1400	15,116.0	+ 2,136.2
1450	15,801.4	+ 2,821.6
1500	16,494.8	+ 3,515.0
1550	17,195.9	+ 4,216.1

Comparison of i_t^o at 100°F, 150°F, and 200°F from Tables 5 and 6 reveals that the agreement between the steam tables and Tsoiman's equation is excellent. The deviation does not exceed 4 Btu/lb-mole. Furthermore, Grahl's data (7) , the use of which is explained in section D, deviates from Tsoiman's values by no more than 30 Btu/lb-mole. This deviation is practically unnoticeable when the numbers are plotted.

D. Plotting the Saturated Vapor and Liquid Lines

Ammonia tables (6) give enthalpies of the saturated vapor and liquid up to 125°F. For plotting values above 125°F, Grahl's thesis (7) was used. Table 7 gives saturated enthalpies derived from ammonia tables and solved for in the same manner as Table 5.

The final result of Grahl's thesis is a large graph of ammonia enthalpy in Btu/lb versus temperature with isobars up to 16,000 psia. Temperature range is -100 to 700°F, and base enthalpy is saturated liquid at -100°F. The difficulty with Grahl's graph is that enthalpies can be read off, at best, to ± 1 Btu/lb. On a molar scale, this deviation purports to be ± 17 Btu/lb-mole, or a total span of 34 Btu/lb-mole. Although the effect of this error is diminished in the plotting, Grahl's figures were still trusted less than other sources and were used extensively only when no other data are available.

The extension of the saturated curves up to the critical point is one case where no other data are available. The technique to transform Grahl's data to report basis is to algebraically add the saturated liquid enthalpy at -100°F, which is found to be -24,866.9 Btu/lb-mole from Table 7. Grahl's points are listed in Tables 8 and 9.

Table 7

Ammonia Enthalpies for Saturated Vapor and Liquid Lines, from Ammonia Tables

Temp °F	Enthalpy Sat. Vapor Btu/lb-mole	Enthalpy Sat. Liquid Btu/lb-mol
-100	-14,107.3	-24,886.9
- 90	-14,030.7	-24,714.9
- 80	-13,959.0	-24,542.8
- 70	-13,885.8	-24,369.1
- 60	-13,810.9	-24,195.4
- 50	-13,736.0	-24,018.3
- 40	-13,661.1	-23,839.4
- 30	-13,596.4	-23,657.2
- 20	-13,535.1	-23,474.9
- 10	-13,475.5	-23,292.7
0	-13,419.2	-23,108.7
10	-13,366.3	-22,923.1
20	-13,317.1	-22,737.4
30	-13,291.1	-22,550.1
40	-13,228.5	-22,361.0
50	-13,191.0	-22,172.0
60	-13,155.2	-21,979.5
70	-13,124.5	-21,787.1
80	-13,097.3	-21,591.2
90	-13,075.2	-21,395.4
100	-13,058.2	-21,196.1
110	-13,046.3	-20,995.2
120	-13,041.1	-20,790.7

Examination of Table 7 and 9 for overlapping temperature reveals a deviation not exceeding 26 Btu/lb-mol.

Table 8

Saturated Vapor Line up to Critical Point, from Grahl's Thesis

Absolute Pressure psia	Temp °F	Enthalpy Btu/lb-mole	
200	96	-12,845.3	
400	146	-13,032.6	
600	178	-13,168.9	
800	200	-13,356.2	
1000	221	-13,611.7	
1200	238	-13,986.4	
1400	253	-14,446.3	
1600	267	-15,331.9	
1638	270	-16,370.9	critical pt.

Table 9

Saturated Liquid Line up to Critical Point, from Grahl's Thesis

Temp °F	Enthalpy Btu/lb-mole
60	-21,957.4
80	-21,565.7
100	-21,173.9
120	-20,782.2
140	-20,339.4
160	-19,913.6
180	-19,453.7
200	-18,976.8
220	-18,465.8
240	-17,903.8
250	-17,563.2
260	-17,222.5

E. Use of the Beattie-Bridgeman Equation of State

The Beattie-Bridgeman equation of state (8) may be written as:

$$P = RT\left(\frac{1}{V}\right) + \left(RTB_o - \frac{RC}{T^2} - A_o\right)\left(\frac{1}{V}\right)^2 - \left(RTbB_o + \frac{RCB_o}{T^2} - aA_o\right)\left(\frac{1}{V}\right)^3 + \frac{RCbB_o}{T^2}\left(\frac{1}{V}\right)^4 \quad (3)$$

For units of atmospheres for pressure, liters per mole for volume, and ^oK for temperature, the constants used for ammonia gas are the following, taken from original evaluation of Beattie and Lawrence (9)

$$A_o = 2.3930$$
$$a = 0.17031$$
$$B_o = 0.03415$$
$$b = 0.19112$$
$$c = 476.87 \times 10^4$$
$$R = 0.08206$$

This equation of state is valid above the critical temperature, as long as the specific volume is greater than 20 cc/gram. This limiting volume corresponds to a maximum density or $\left(\frac{1}{V}\right)$ of 2.94 g-moles/liter.

Let Δ Ip represent the difference in enthalpy at a fixed temperature between the ideal-gas state (zero pressure) and the actual state (at actual pressure). Once Δ Ip is known, it may be added algebraically to i_t^o (which is calculated by the method of section C) to obtain the actual gas enthalpy i_t^p. In short:

$$i_t^p = i_t^o + \Delta I_p \quad (4)$$

To relate ΔI_p and the equation of state, it is necessary to use the thermodynamic relation:

$$I_p = \int_{\infty}^{V} \left[T \left(\frac{\partial p}{\partial T}\right)_V + V \left(\frac{\partial p}{\partial V}\right)_T \right] dV \qquad (5)$$

Taking the proper derivatives from (3) and substituting into (5) gives:

$$\Delta I_p = -\left[2A_o + \frac{4Rc}{T^2} - RTB_o\right]\left(\frac{1}{V}\right) - \left[RTbB_o + \frac{5RcB_o}{2T^2} - \frac{3}{2}aA_o\right]\left(\frac{1}{V}\right)^2 + \frac{2RcbB_o}{T^2}\left(\frac{1}{V}\right)^3 \qquad (6)$$

At any fixed temperature, P from (3) and ΔI_p from (6) become polynomial functions of $(\frac{1}{V})$. Therefore, the ΔI_p at the given temperature and at any pressure P may be found by a trial and error procedure in which $(\frac{1}{V})$ is determined from (3) and substituted into (6) to give I_p. The actual enthalpy of ammonia at the given temperature and pressure is solved for by (4).

Note that using the Beattie-Bridgeman constants results in enthalpy units of (atm liter)/g-mole. To convert these units to Btu/lb-mole, multiply by the factor 43.6223. Likewise, multiplying the value of P from (3) by the factor 14.696 converts atmospheres to psia.

Table 10 gives enthalpies calculated in this manner.

Note that the only values of $(\frac{1}{V})$ listed are those below 2.94g-moles/li, which is the upper limit for the Beattie-Bridgeman valid for all pressures up to 3000 psia. At lower temperatures and high pressures, some values of $(\frac{1}{V})$ exceed the acceptable

limit and are then dropped from the tables as unreliable.

The seven reported temperatures in Table 10 represent typical enthalpy data derived from the Beattie-Bridgeman equation. It must be understood that the same procedure can be carried out for any temperature and gas density for which the equation is valid.

Table 10

Superheated Ammonia Enthalpies, from the Beattie-Bridgeman Equation of State

i_t^p Btu/lb-mole

Temperature, t°F → / Pressure, psia ↓	300	440	620	850	1000	1200	1400
0	-10,601.7	- 9,247.5	-7,368.9	-4,823.5	-3,036.8	-521.7	+2,136.2
200	-10,821.1	- 9,388.9	-7,459.0	-4,880.0	-3,080.2	-553.3	+2,112.7
400	-11,056.7	- 9,534.2	-7,549.5	-4,936.3	-3,123.5	-584.8	+2,089.4
600	-11,311.2	- 9,683.5	-7,640.3	-4,992.3	-3,166.4	-616.0	+2,066.0
800	-11,587.9	- 9,835.8	-7,731.1	-5,047.9	-3,209.1	-647.1	+2,042.8
1000	-11,889.8	- 9,991.6	-7,822.0	-5,103.0	-3,251.3	-677.9	+2,019.6
1200		-10,149.9	-7,912.6	-5,157.8	-3,293.2	-708.6	+1,996.5
1400		-10,309.7	-8,002.7	-5,212.0	-3,345.3	-739.1	+1,973.4
1600			-8,092.0	-5,265.6	-3,376.0	-769.4	+1,950.4
1800			-8,180.3	-5,318.6	-3,434.3	-799.5	+1,927.5
2000				-5,406.3	-3,457.1	-829.4	+1,904.6
2500					-3,555.8	-903.1	+1,847.7
3000						-975.4	+1,791.2

F. Completion of Superheated Curves by Grahl's Data

The Beattie-Bridgeman equation was unable to supply reliable figures up to 3000 psia, especially at low temperatures. To complete the curves at these high pressures and low temperatures, especially around the critical region, Grahl's thesis was relied upon. In fact, Grahl's data was the only source of the 2000, 2500, and 3000 psia lines below 700°F. Some typical Grahl points are listed in Table 11. A certain overlap with the Beattie-Bridgeman region was allowed for comparison.

Table 11 consists of two parts, the first one covering 1200 to 3000 psia, and the second covering 200 to 1000 psia. Table 11 contains some representative data, although actually more points have been read off from Grahl's data, especially in the region of great corvature.

The footnotes attached to Table 11 verify that in spite of the difficulty in reading Grahl's chart accurately, there is a remarkable agreement between Grahl's data and the Beattie-Bridgeman equation, especially for low pressures.

Table 11

Superheated Ammonia Enthalpies, from Grahl's Thesis

Part A. 1200 to 3000 psia

Pressure, psia → / Temp t°F ↓	1200	1400	1600	1800	2000	2500	3000
260	-13,134.8	-14,105.7	liquid-vapor	-17,443.9	-17,529.1	-17,648.3	-17,733.5
280	-12,623.9	-13,288.1	-14,207.8	-15,689.7	-16,456.1	-17,035.1	-17,239.5
300*	-12,198.1	-12,692.0	-13,254.1	-14,071.6	-14,957.2	-16,268.7	-16,711.5
320	-11,857.4	-12,249.2	-12,589.8	-13,220.0	-13,816.1	-15,280.9	-16,115.4
340	-11,516.8	-11,823.4	-12,061.8	-12,589.8	-13,015.6	-14,293.0	-15,434.1
360	-11.193.2	-11,465.7	-11,670.0	-12,061.8	-12,436.5	-13,407.3	-14,531.4
380	-10,903.6	-11,125.1	-11,312.3	-11,601.9	-11,942.6	-12,623.9	-13,390.3
400	-10,631.1	-10,818.5	-10,971.7	-11,193.2	-11,499.7	-11,976.6	-12,538.7
420	-10,358.6	-10,511.9	-10,648.1	-10,835.5	-11,091.0	-11,516.8	-11,925.5
440**	-10,120.2	-10,256.4	-10,341.6	-10,494.9	-10,750.3	-11,125.0	-11,465.7
460	- 9,864.7	- 9,983.9	-10,069.1	-10,188.3	-10,409.7	-10,784.4	-11,091.0
480	- 9,626.2	- 9,728.4	- 9,813.6	- 9,898.7	-10,086.1	-10,460.8	-10,750.3
500	- 9,387.8	- 9,473.0	- 9,558.1	- 9,643.3	- 9,796.5	-10,154.2	-10,460.8
600	- 8,178.6	- 8,297.7	- 8,348.8	- 8,417.0	- 8,502.1	- 8,825.7	- 9,149.3
620***	- 7,940.1	- 8,032.3	- 8,105.0	- 8,171.8			
700	- 6,986.3	- 7,105.5	- 7,139.6	- 7,190.7	- 7,241.7	- 7,616.5	- 7,923.0

* No comparison possible because Beattie-Bridgeman equation does not work at 300°F for 1200 psia or higher pressures (see part B)

** Comparison with Table 10 at 440°F shows 53 Btu/lb-m deviation at 1400 psia and 30 Btu/lb-m at 1200 psia. Deviation further decreases, coming to as close as 4 Btu/lb-m at 400 psia (see part B)

*** Four values at 620°F have been inserted to compare with Table 10. Maximum deviation is 30 Btu/lb-mole. Deviation decreases to around 20 Btu/lb-m at lower pressures, with Grahl's data being consistently lower, that is, larger negative value.

Table 11

Part B 200 to 1000 psia

i_t^p Btu/lb-mole

Pressure, psia → / Temp, $t^\circ F$ ↓	200	400	600	800	1000
120	-12,709.0	wet-region	wet-region	wet-region	wet-region
140	-12,470.6	wet-region	wet-region	wet-region	wet-region
160	-12,266.2	-12,794.2	wet-region	wet-region	wet-region
180	-12,061.8	-12,504.6	-13,100.9	wet-region	wet-region
200	-11,857.4	-12,232.1	-12,640.9	-13,356.2	wet-region
300*	-10,818.5	-10,059.0	-11,312.4	-11,567.9	-11,857.4
400	- 9,779.5	- 9,966.9	-10,154.2	-10,324.6	-10,460.8
440**	- 9,365.0	- 9,530.9	- 9,698.2	- 9,861.4	- 9.983.9
500	- 8,740.6	- 8,876.8	- 9,013.1	- 9,166.4	- 9,268.6
600	- 7,684.6	- 7,786.8	- 7,889.0	- 8,008.2	- 8,093.4
620***	- 7,476.8	- 7,568.8	- 7,664.2	- 7,756.2	- 7,858.4
700	- 6,645.6	- 6,696.7	- 6,764.9	- 6,833.0	- 6,918.2

* Comparison with Table 10 part A shows excellent agreement at 200, 400, and 600 psia with increasing deviations at 800, and 1000 psia. At 300°F, Beattie-Bridgeman equation is no longer valid at 1200 psia and above.

** At 440°F and *** 620°F, comparison with Table 10 respectively indicates excellent agreement, the deviation being smaller than the allowable tolerance for reading off Grahl's chart and for plotting.

G. Enthalpy of Compressed Liquid Ammonia

Liquid ammonia under compression has slightly different enthalpies from the saturated liquid at the same temperature. The calculation of these corrections is handled in the following manner.

From basic enthalpy relations,

$$\left(\frac{\partial i_l}{\partial P}\right)_T = \frac{1}{\rho}\left[1+\frac{T}{\rho}\left(\frac{\partial \rho}{\partial T}\right)_{sat}\right]$$

where ρ is the saturated liquid density, $ft^3/$

T is the absloute temperature at which the correction is applied, ^oR

i_l is the enthalpy of liquid ammonia at T in Btu/lb-mol

With these units, the right side of the equation must be multiplied by a factor of 46.3 to give $\left(\frac{\partial i_l}{\partial P}\right)$ in Btu/ -mol-atm. In Table 12, this quantity is reported for temperatures from -100 to +100°F. To obtain the correction factor at any given temperature for a desired pressure P atmospheres, the listed quantity $\left(\frac{\partial i_l}{\partial P}\right)_T$ at that temperautre is multiplied by the factor (P-Psat)atmospheres. And this product must be added algebraically to the saturated liquid enthalpy at the given temperature to yield the actual compressed liquid enthalpy under P atmospheres. Note that for large pressures P, the small Psat may be neglected.

To illustrate the manner in which Table 12 was obtained, consider the case of 0°F. Properties of saturated liquid ammonia at 0°F are:

ρ = 41.34 ft^3/

Psat = 30.42 psia = 2.07 atm

T = 460°R;

The quantity $(\frac{\partial \rho}{\partial T})_{sat}$ may be taken as simply $(\frac{\Delta \rho}{\Delta T})_{sat}$ in the immediate vicinity of 0°F; here, it is convenient to take the temperature interval from -5 to +5°F, so that:

$$(\frac{\partial \rho}{\partial T})_{sat} = (\frac{\Delta \rho}{\Delta T})_{sat} = -0.045 \text{ ft}^3/\text{lb-}^\circ\text{R}$$

Solving for $(\frac{\partial i_l}{\partial P})_T$ and taking care of the units, this value turns out to be 0.559 Btu/lb-m-atm.

Now, for example, to evaluate the enthalpy of liquid ammonia at 0°F and 150 atmospheres, the correction factor is:

(0.559 Btu/lb-m-atm)(150 - 2.07 atm)

= 82.6 Btu/lb-m

At 0°F, saturated enthalpy is -23, 108.7 Btu/lb-m from Table 7.

Therefore, the enthalpy at 0°F and 150 atm is:

(-23,108.7) + (82.6)

= 23,026.1 Btu/lb-m

Similarly, values at other temperatures and pressures may be obtained. For intermediate temperatures, Table 12 may be interpolated linearly for $(\frac{\partial i_l}{\partial P})_T$ before multiplying the (P - Psat) factor. No graphs are given for liquid enthalpies, so that Tables 7 and 12 must be used to evaluate liquid enthalpies.

Table 12

Correction Term for Compressed Liquid Ammonia

$t^{\circ}F$	P_{sat}, atm	$\left(\frac{\partial i_l}{\partial P}\right)_T$ Btu/lb-m-atm
-100	0.082	0.705
- 90	0.136	0.691
- 80	0.186	0.680
- 70	0.268	0.669
- 60	0.378	0.656
- 50	0.522	0.643
- 40	0.709	0.629
- 30	0.945	0.615
- 20	1.244	0.594
- 10	1.616	0.576
0	2.07	0.559
10	2.62	0.540
20	3.28	0.521
30	4.07	0.492
40	4.99	0.450
50	6.06	0.425
60	7.31	0.390
70	8.75	0.351
80	10.40	0.291
90	12.30	0.244
100	14.41	0.197

H. Construction of the Ammonia Graphs

All the data tabulated in sections A to F have been summarized in eleven large-scale graphs. Preceding the eleven graphs are three index graphs, drawn on a smaller scale and showing the boundaries of each large-scale relative to the next ones. Liquid enthalpies below 180°F may be found only by using Tables 7 and 12.

Interpolations may be taken linearly for intermediate pressures.

The temperature and enthalpy ranges for all graphs is as follows:

	Temperature Range °F	Enthalpy Range Btu/lb-mole
First Index	-100 to 700	-19,000 to -7,000
Second Index	600 to 1000	- 9,250 to -3,000
Third Index	1000 to 1400	- 3,750 to +2,000
Graph I	180 to 340	-18,800 to -16,400
	Liquid Region	
Graph II	180 to 380	-16,400 to -14,200
	Critical Region	
Graph III	-100 to 220	-14,200 to -12,000
	Saturated Vapor Region	
Graph IV	Vapor, 180 to 460	-14,200 to -12,000
Graph V	Vapor, 140 to 460	-12,000 to - 9,800
Graph VI	Vapor, 340 to 620	-11,000 to - 9,000
Graph VII	Vapor, 460 to 700	- 9,000 to -6,800
Graph VIII	Vapor, 680 to 880	- 7,800 to - 5,400
Graph IX	Vapor, 800 to 1080	- 5,400 to - 3,000
Graph X	Vapor, 1000 to 1240	- 3,000 to - 600
Graph XI	Vapor, 1200 to 1400	- 600 to + 1,800

FIG. 1-9. ENTHALPY OF AMMONIA

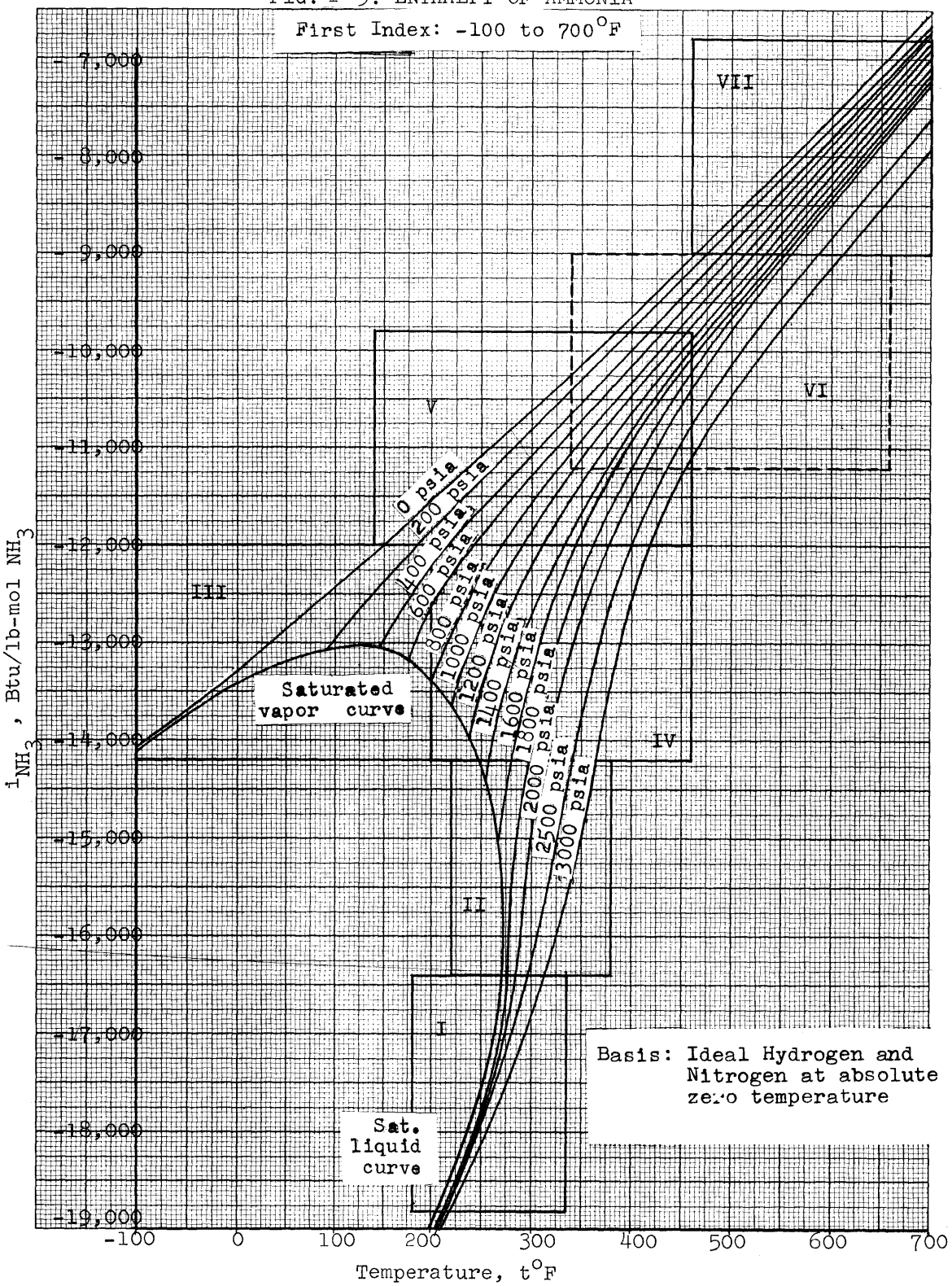

FIG. 1-10. ENTHALPY OF AMMONIA

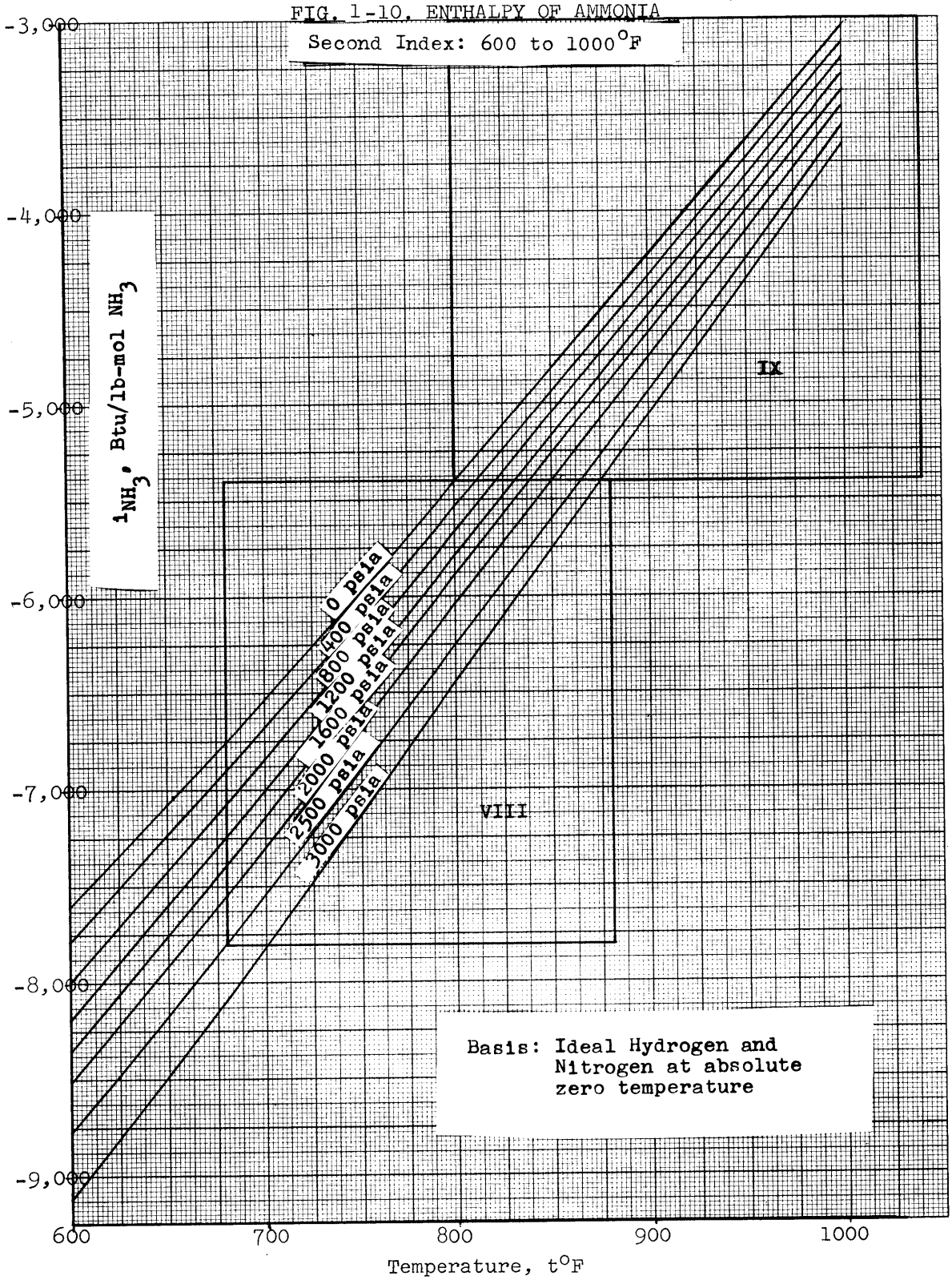

FIG. 1-11. ENTHALPY OF AMMONIA

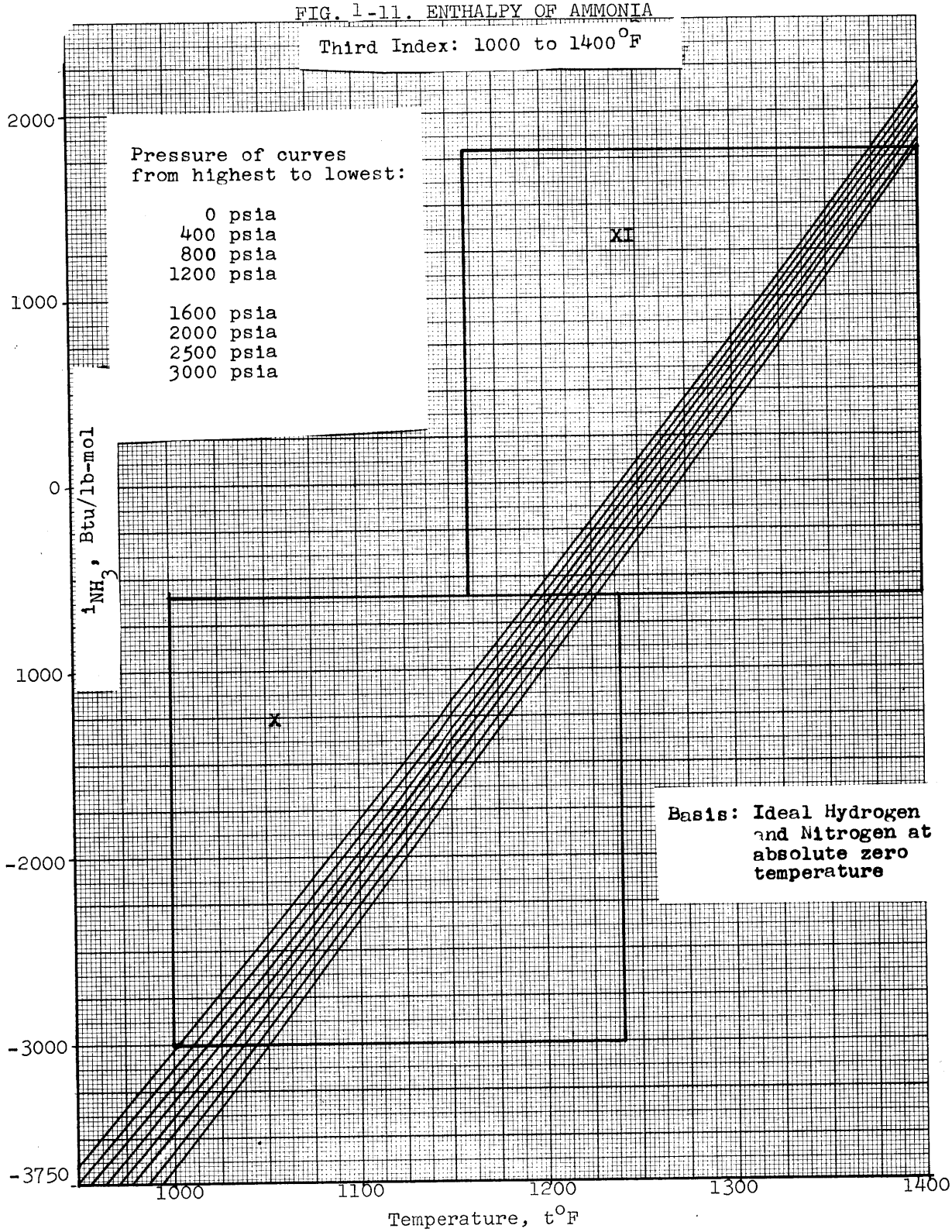

FIG. 1-12. ENTHALPY OF AMMONIA

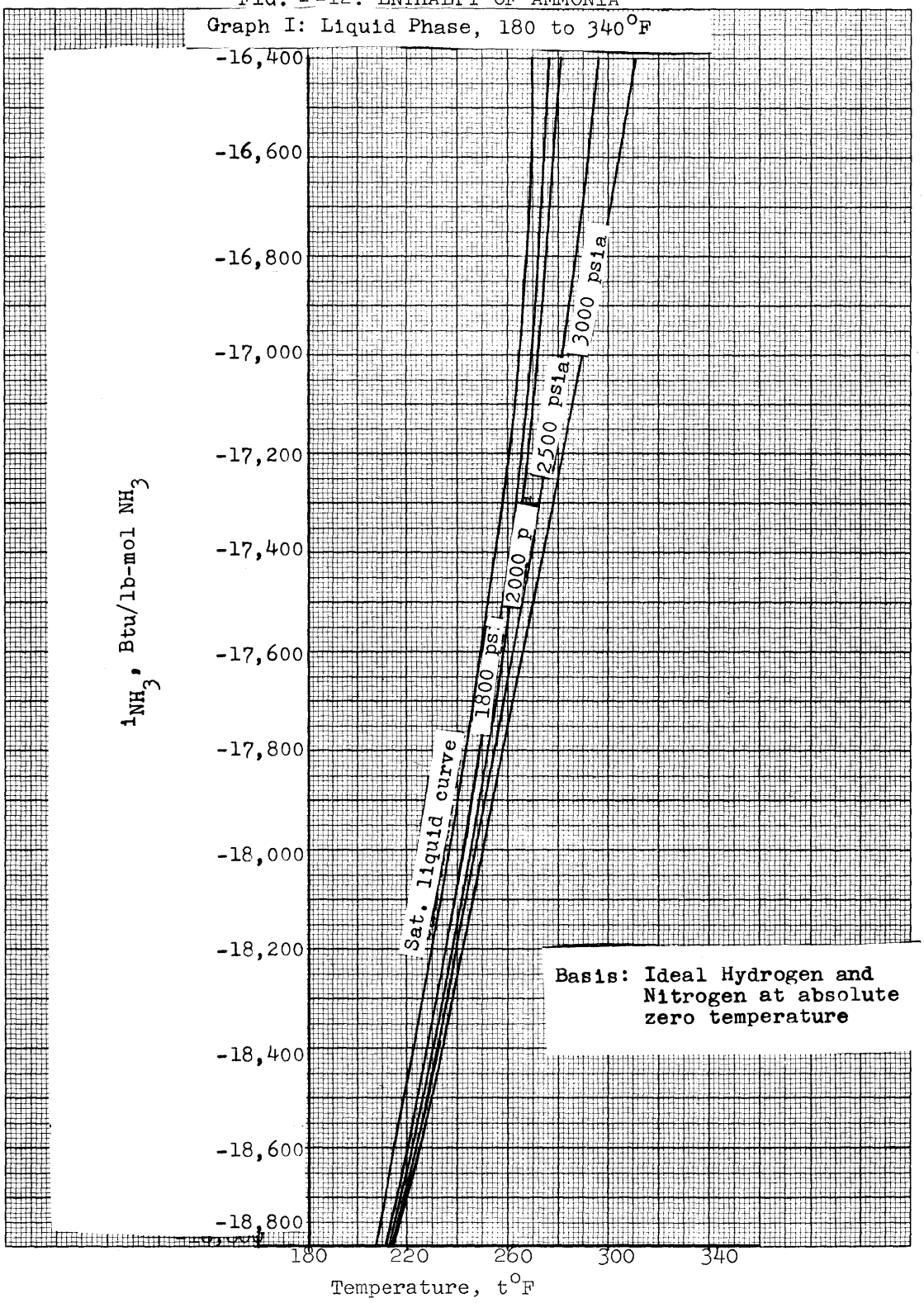

FIG. 1-13. ENTHALPY OF AMMONIA

Graph II: Critical Region, 180 to 380 °F

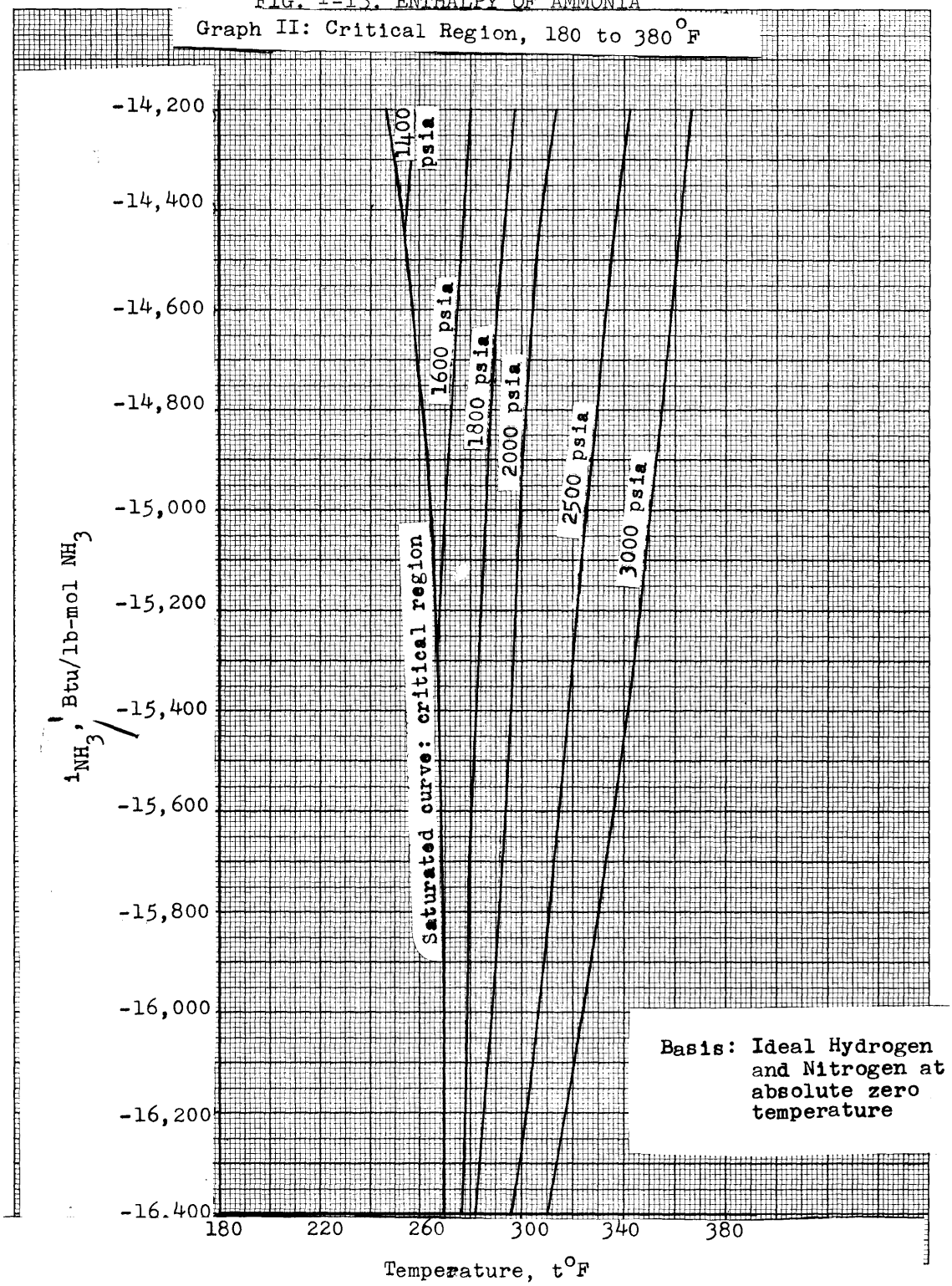

FIG. 1-14. ENTHALPY OF AMMONIA

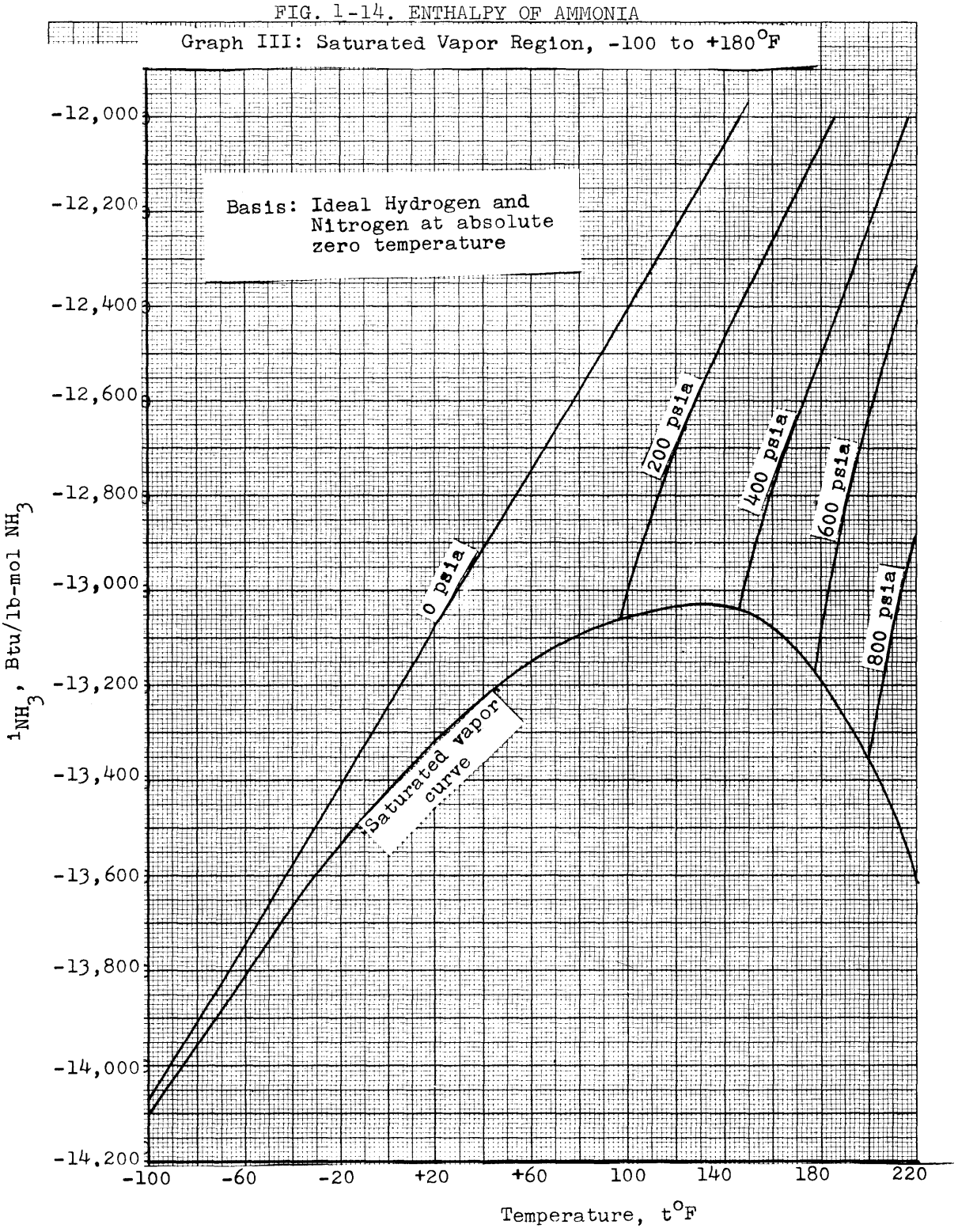

FIG. 1-15. ENTHALPY OF AMMONIA

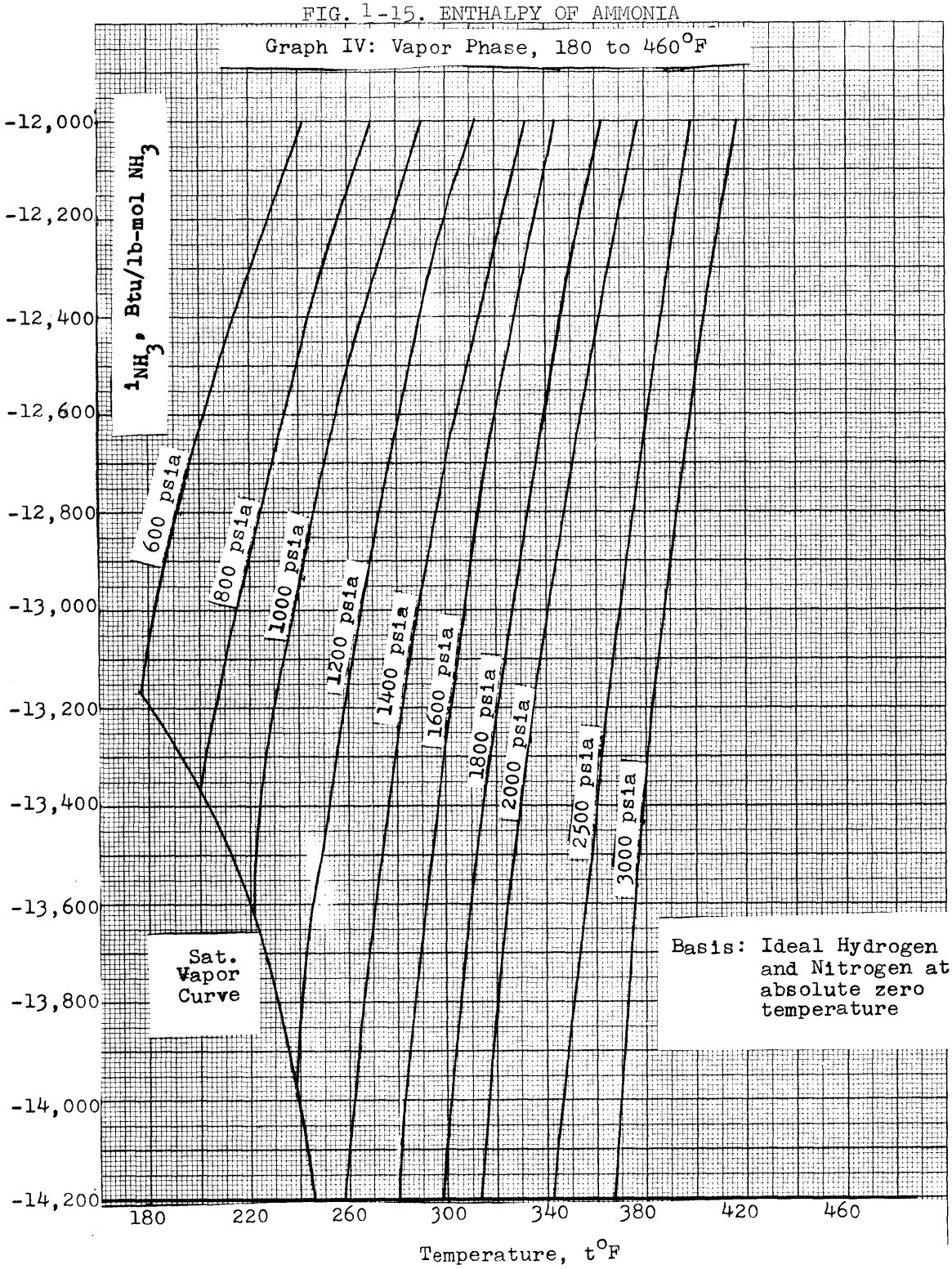

FIG. 1-16. ENTHALPY OF AMMONIA

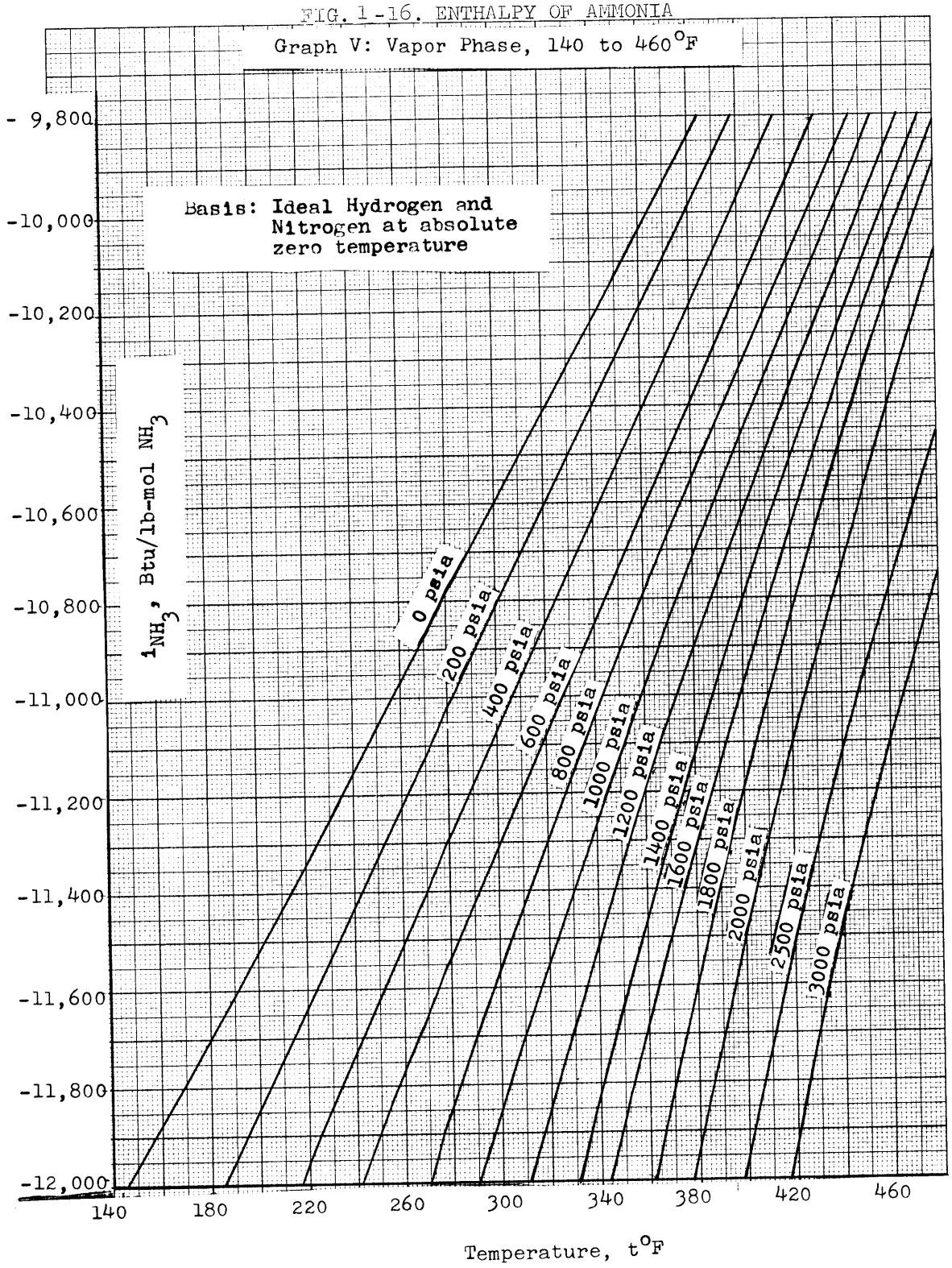

FIG. 1-17. ENTHALPY OF AMMONIA

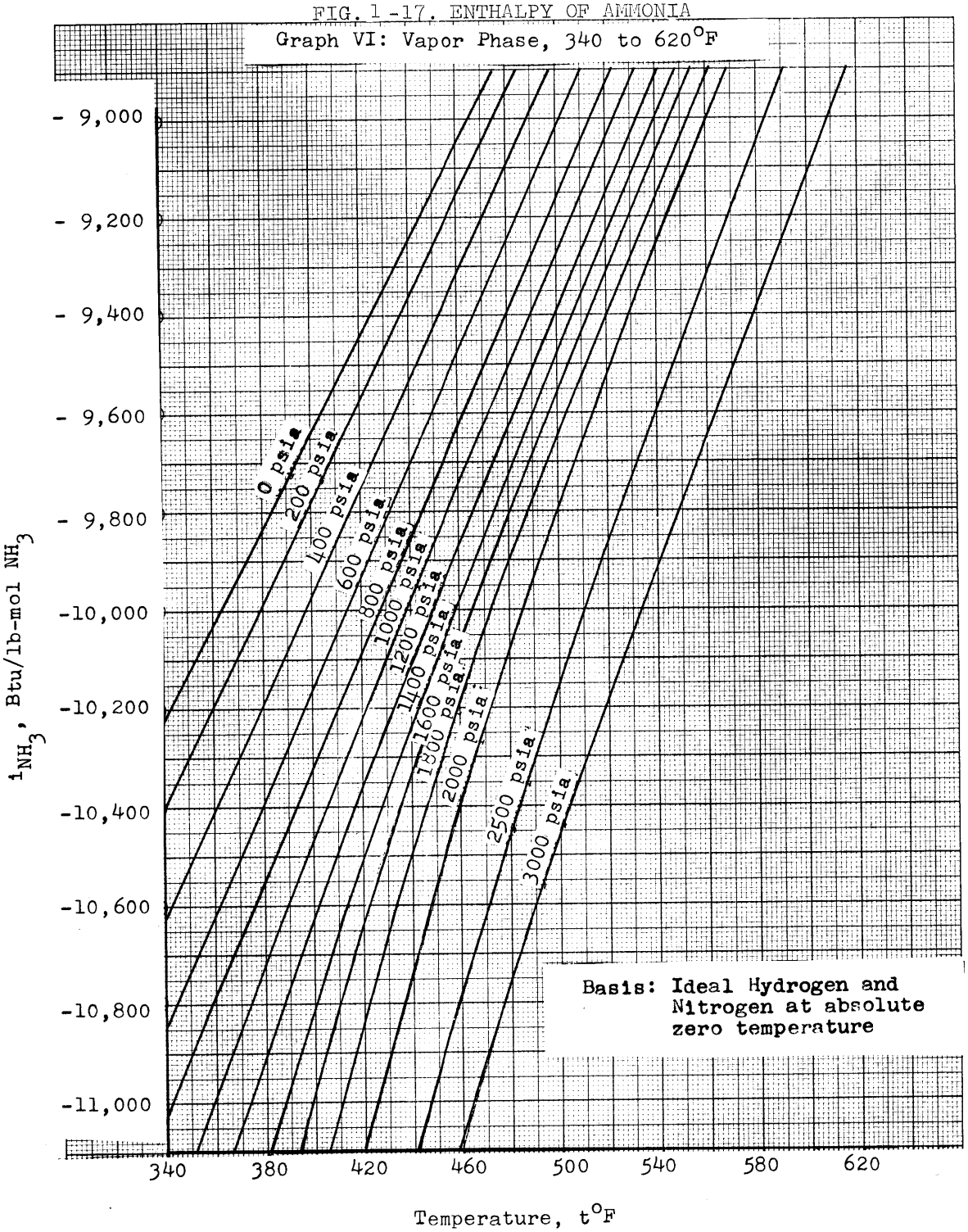

FIG. 1-18. ENTHALPY OF AMMONIA

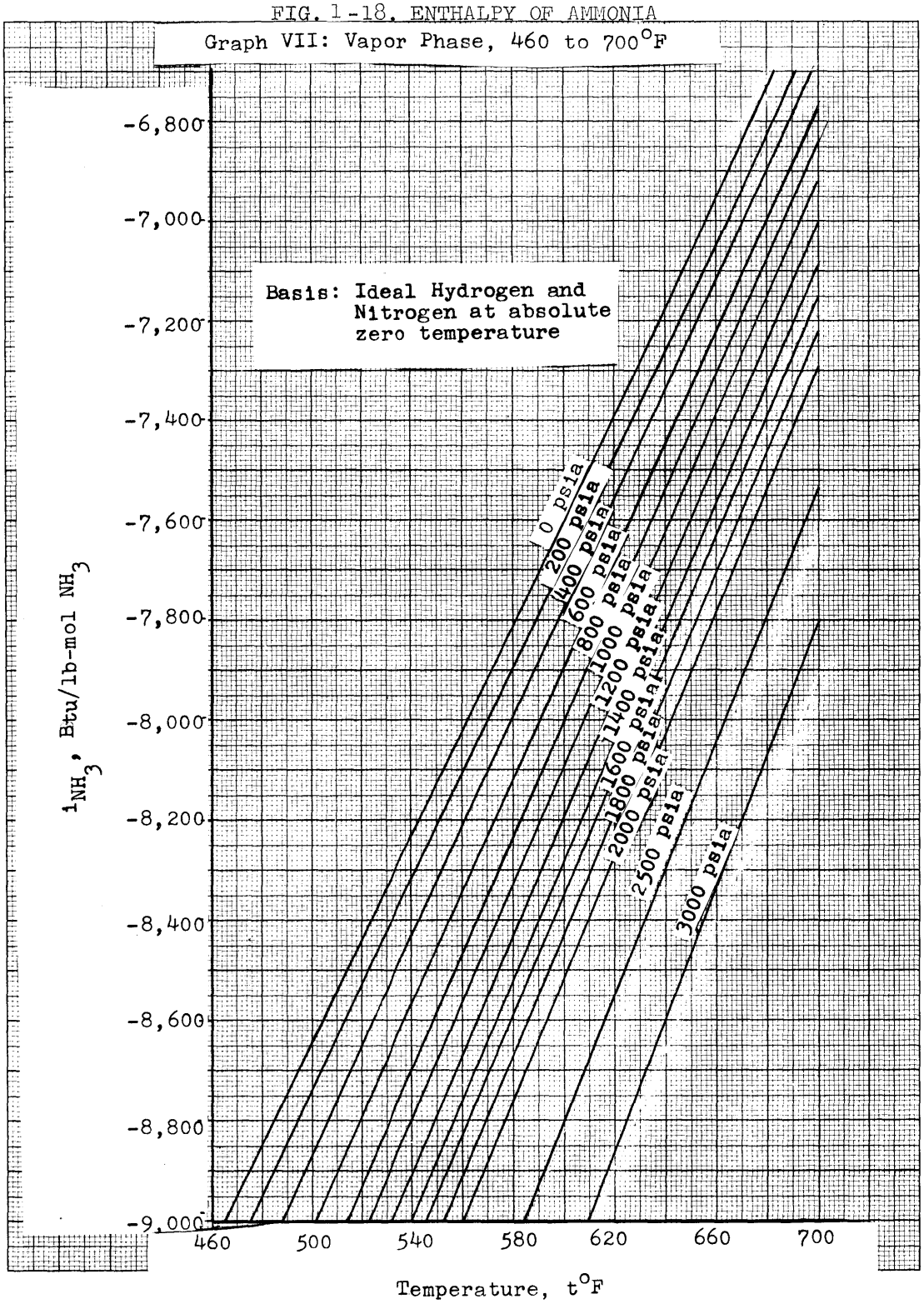

FIG. 1-19. ENTHALPY OF AMMONIA

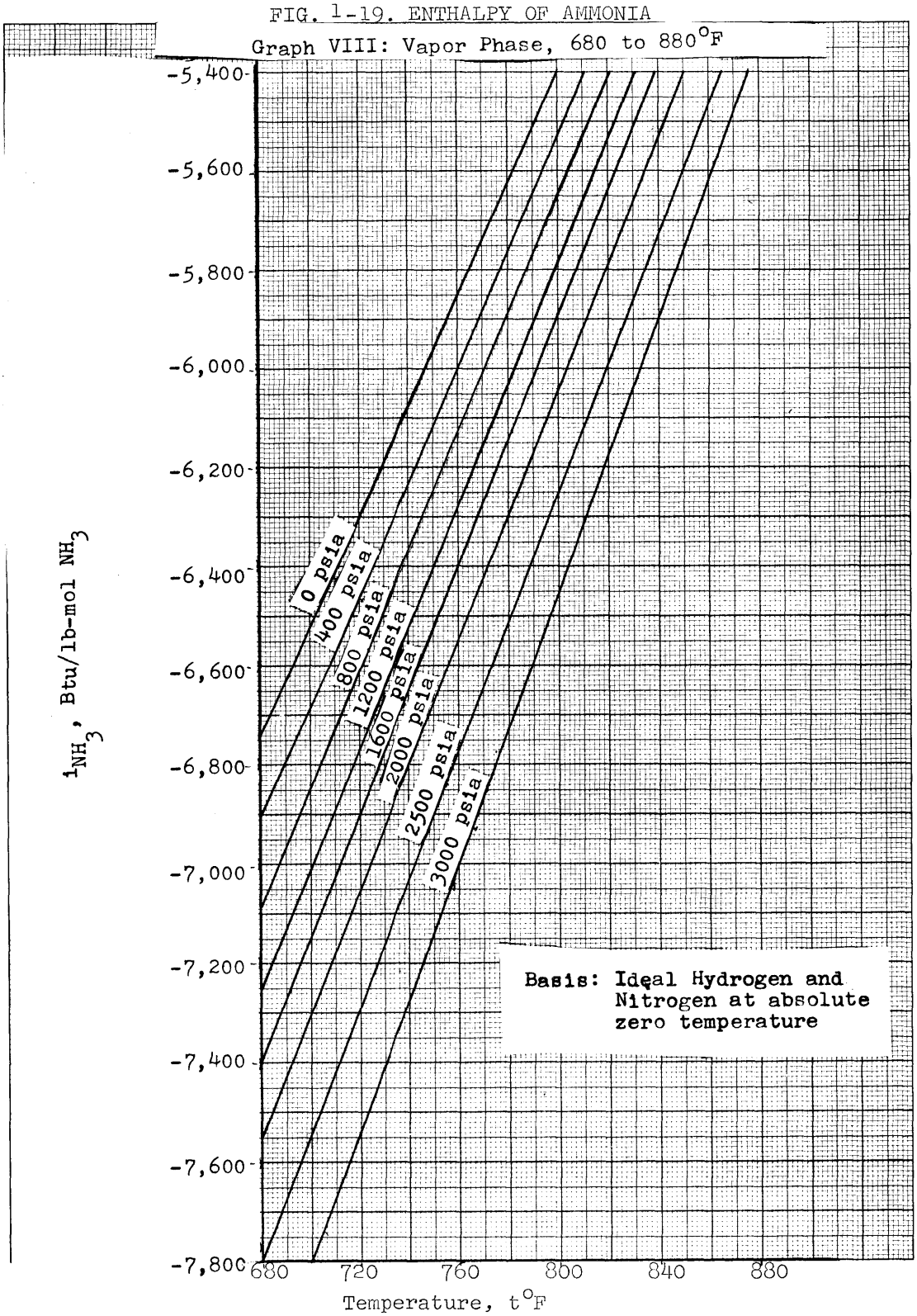

FIG. 1-20. ENTHALPY OF AMMONIA

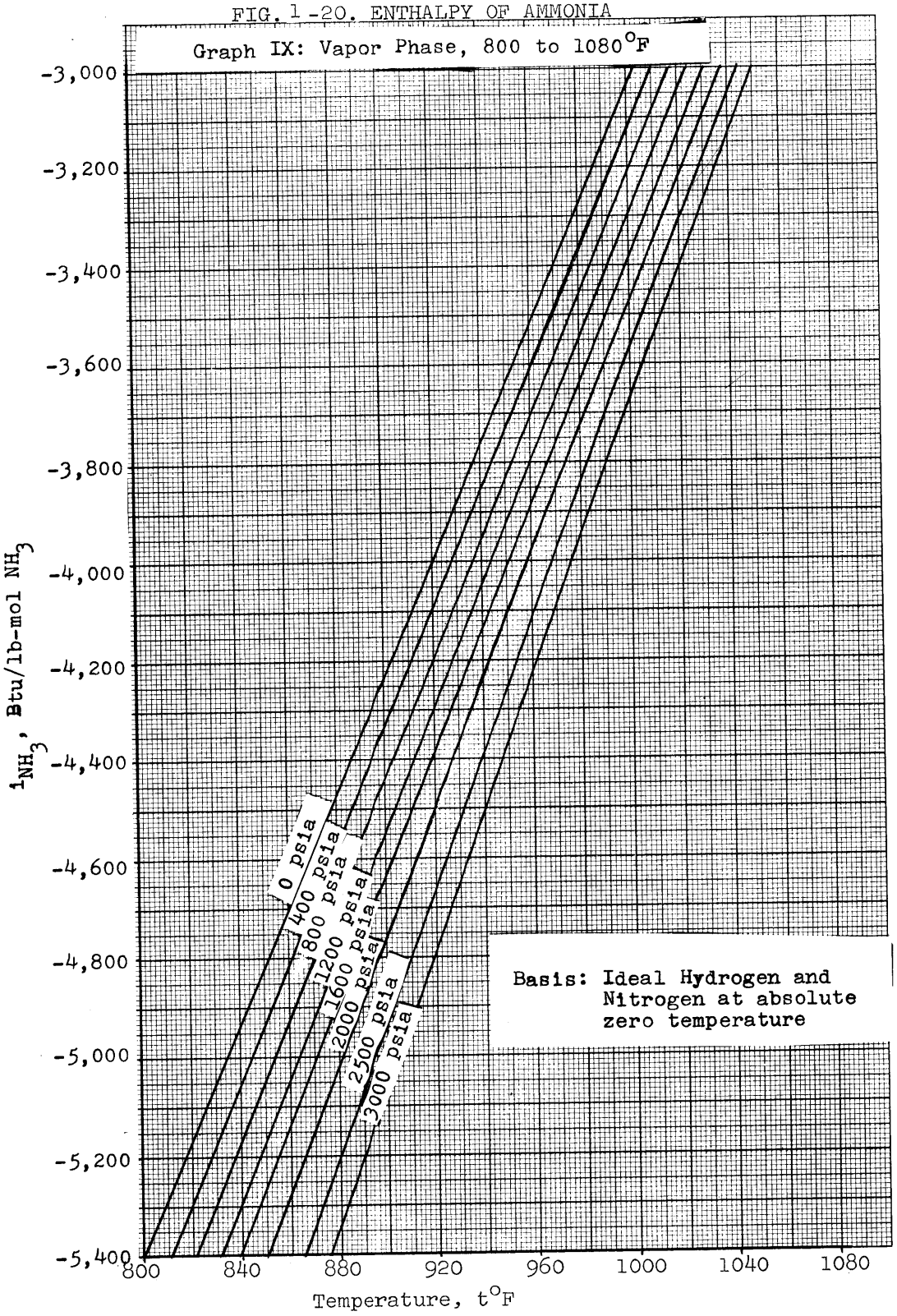

FIG. 1-21. ENTHALPY OF AMMONIA

Graph X : Vapor Phase, 1000 to 1240°F

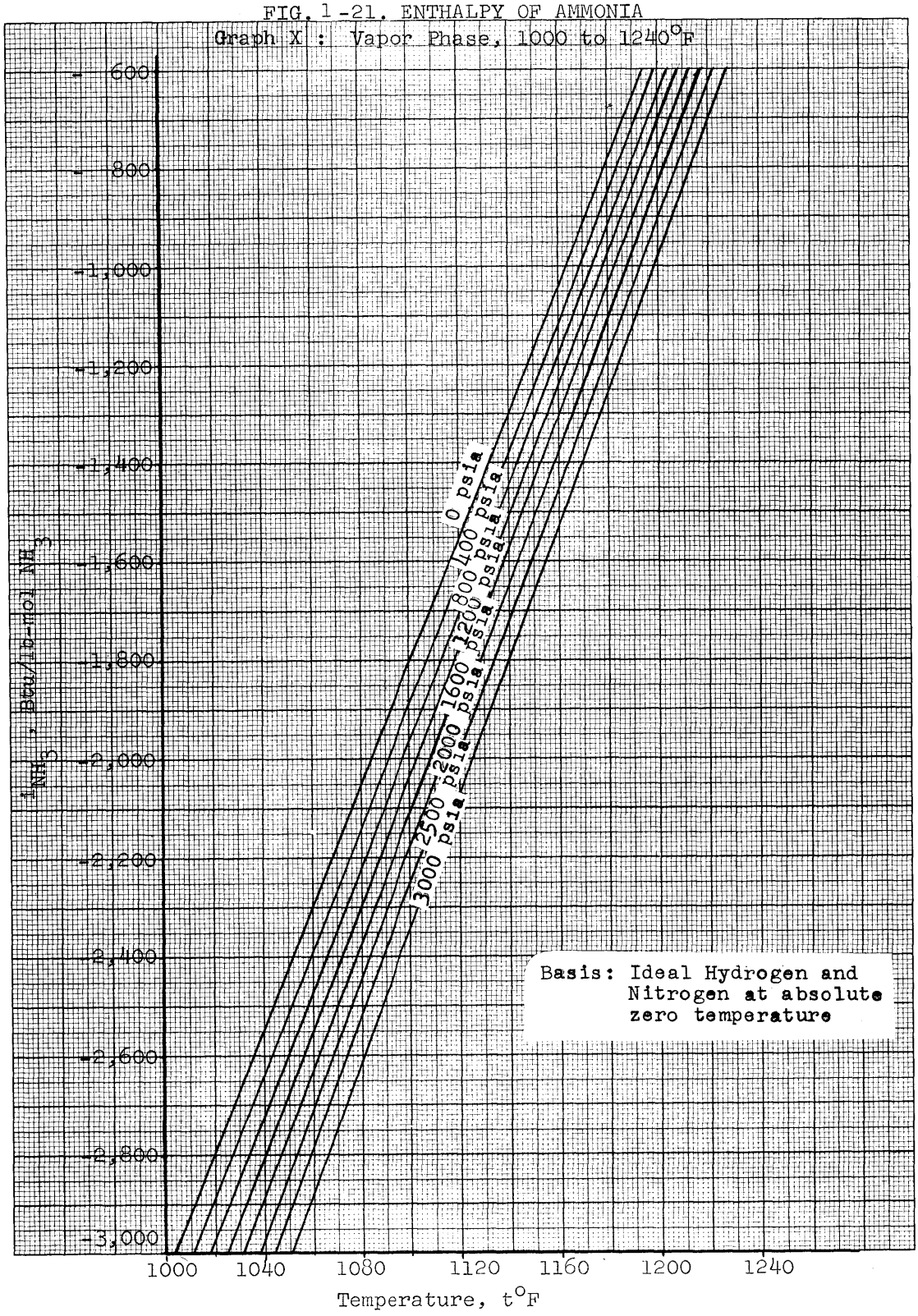

FIG. 1-22. ENTHALPY OF AMMONIA

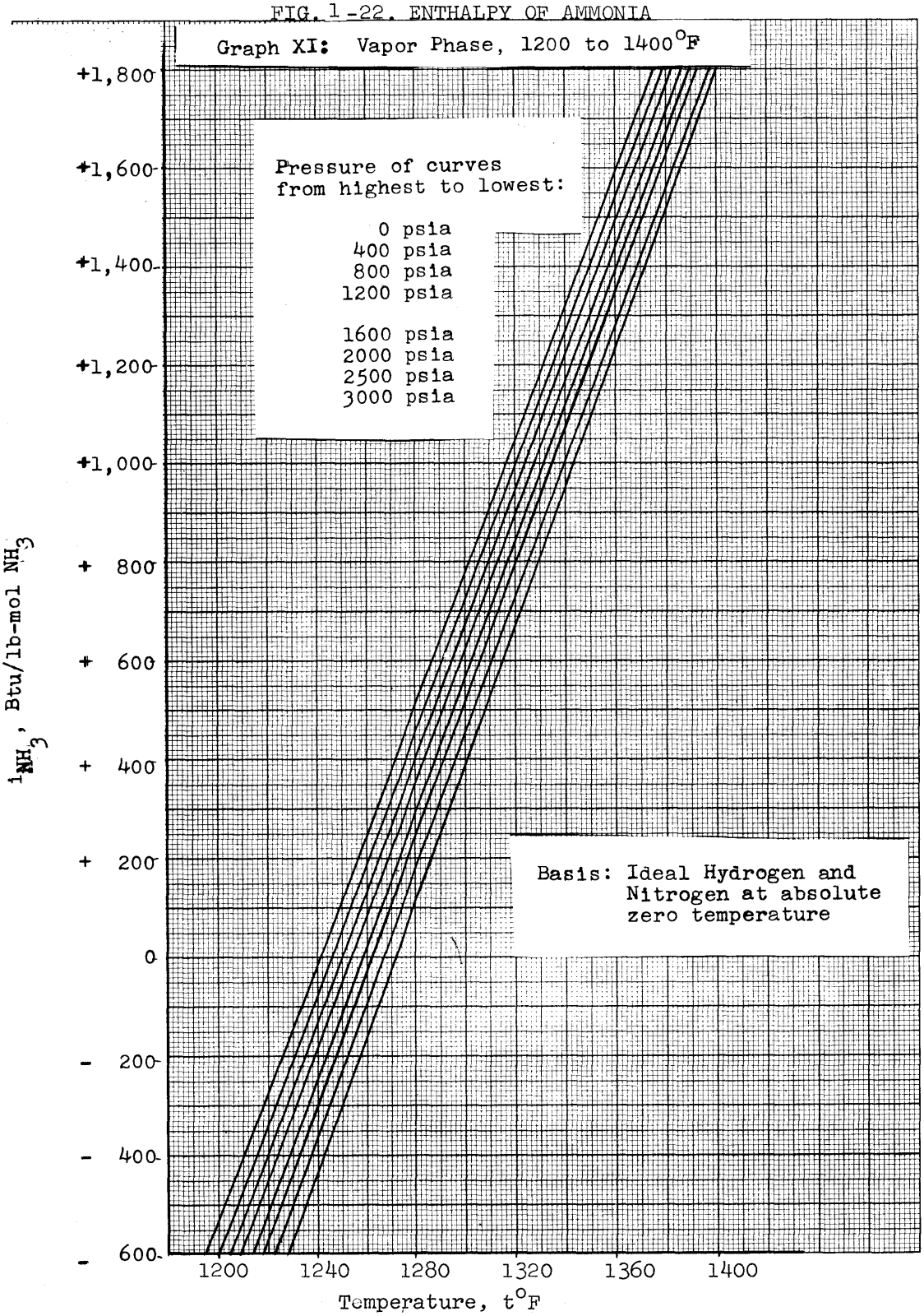

BIBLIOGRAPHY

1. Chow, Edward R., Thermodynamic Equilibria for Ammonia Synthesis and Cracking, Report MIT-D8, Nuclear Engineering Department, MIT, 26 May 1968

2. Private Communication with Mr. Howard K. Rae, Head of the Chemical Engineering Division of the Atomic Energy of Canada, Ltd, Chalk River, Ontario, 26 April 1968

3. Hilsemath, Joseph, and others, Tables of Thermal Properties of Gases, National Bureau of Standards Circular 564, U. S. Department of Commerce, 1 November 1955

4. Lewis, Gilbert N., and Randall, Merle., Thermodynamics, Second Edition, Appendix A7-10, McGraw Hill Book Co., Inc., New York, 1961

5. Tsoiman, G. I., Thermodynamic Properties of Undissociated Ammonia, Russian Journal of Physical Chemistry, 35, 1048-1049, September 1961

6. Refrigeration Data Handbook, The American Society of Refrigerating Engineers, Part II Tables 1 to 4, 110-125, Menasha, Wisconsin, 1943

7. Grahl, Edward R., Thermodynamic Properties of Ammonia at High Temperatures and Pressures, A Thesis Presented to the Faculty of Clarkson College of Technology for the Degree of Professional Engineering, 1 June 1952

8. Wolley, Jr., C. E., Worlton, W. J., and Zeigler, R. K., Compressibility Factors and Fugacity Coefficients Calculated from the Beattie-Bridgeman Equation of State for Hydrogen Nitrogen, Oxygen, Carbon Dioxide, Ammonia, Methane, and Helium, Los Alamos Scientific Laboratory, Report LA-2271, 17 March 1959

9. Beattie, James A., and Lawrence, Charles K., Some of the Thermodynamic Properties of Ammonia. I. The Compressibility of and An Equation of State for Gaseous Ammonia. Journal of the American Chemical Society 52, 6-14, January 1930

SUPPLEMENT C
THERMODYNAMIC EQUILIBRIUM FOR AMMONIA SYNTHESIS AND CRACKING

1. Introduction

In the monothermal ammonia-hydrogen chemical exchange process for production of heavy water, chemical reflux is provided by the simultaneous synthesis of stripped tower gas into ammonia and the dissociation of enriched liquid ammonia into hydrogen and nitrogen. The complete study of this exchange process, being undertaken at MIT under subcontract No. AX 210280 with E. I. du Pont de Nemours and Co., therefore requires information on the thermodynamic equilibrium for ammonia synthesis and cracking at different temperatures and pressures. This report presents values for the equilibrium constants and the equilibrium ammonia concentration at 50, 100, 150, and 200 atmospheres for temperatures from 500 to 1500°K.

2. Sources of Information

The primary source of information for the equilibrium constant of the ammonia synthesis reaction was the article of Harrison and Kobe,[1] written as a correlation for most of the experimental data available up to 1953. Harrison and Kobe came up with an equation expressing the ideal gas equilibrium as a function of absolute temperature. This equation was derived from thermodynamic first principles and later adjusted, by the method of curve-fitting outlined by Kobe and Arnold,[2] to compare excellently with the experimental findings of Haber,[3] Larson and Dodge,[4] and Stephenson and McMahon.[5] Harrison and Kobe claim for their equation an average deviation of 0.00055 and a maximum deviation of 0.0016 in log K over the temperature range from 500 to 1300°K. In view of this small deviation and also considering that

Harrison and Kobe derived their equation with industrial applications in mind, it was deemed satisfactory to dispense with a full literature survey and to use their equation extensively.

To proceed from the ideal gas constants to actual gas concentrations, Harrison and Kobe recommended the use of fugacity coefficients at the temperatures and pressures studied. Values of these coefficients were taken from Smith and Van Ness[6] and from Lydersen, Greenkorn, and Hougen.[7]

3. Calculation of Equibibrium Constants

The ammonia synthesis reaction is written as:

$$\frac{3}{2} H_2 (g) + \frac{1}{2} N_2 (g) \rightleftharpoons NH_3 (g) \qquad (1)$$

Harrison and Kobe's equation for this reaction is:

$$\log K = \frac{2250.322}{T} - 0.85340 - 1.51049 \log T - 25.8987 \times 10^{-5} T + 14.8961 \times 10^{-8} T^2 \qquad (2)$$

where K is the ideal gas equilibrium constant, atm^{-1}
T is the absolute temperature, ^{o}K

From thermodynamic principles the ideal gas constant K may be expressed as:

$$K = K_{\phi} K_y \frac{1}{\pi} \qquad (3)$$

where $K_{\phi} = \frac{\phi_{NH_3}}{(\phi_{H_2})^{3/2}(\phi_{N_2})^{1/2}}$ and ϕ is the fugacity coefficient of a gas component, given in references 6 and 7 as functions of reduced pressure and temperature

$$K_y = \frac{y_{NH_3}}{(y_{H_2})^{3/2}(y_{N_2})^{1/2}}$$ and y is the equilibrium mole fraction of a gas component

π is total pressure of the system

Table 1 gives values of log K and K at temperatures from 298.16 to 1500°K. These were obtained from Harrison and Kobe's equation.

Table 2 contains values of K_ϕ at the same temperatures and at 50, 100, 150, and 200 atm total pressure. To evaluate K_ϕ the fugacity coefficients ϕ for each of the three components for each pair of conditions had to be read out of a generalized graph or table.

By knowing K and K_ϕ and π atm, the quantity K_y can be obtained by equation (3). K_y expresses the combination of the mole fractions of the three gas components at equilibrium. Values of K_y are listed under Table 3.

4. Calculation of Equilibrium Ammonia Mole Fraction

To see how the equilibrium ammonia mole fraction varied with the parameters, three equations were written down relating y_{NH_3}, y_{H_2}, and y_{N_2}. The first is the expression

$$K_y = \frac{y_{NH_3}}{(y_{H_2})^{3/2}(y_{N_2})^{1/2}} \qquad (4)$$

The second may be written as

$$y_{H_2} = 3y_{N_2} \qquad (5)$$

This condition is satisfied when 3:1 hydrogen to nitrogen synthesis gas is used or when pure ammonia is to be cracked. In most cases of synthesis or cracking to be considered in this work this condition is satisfied.

The third equation is

$$y_{NH_3} + y_{N_2} + y_{H_2} = 1 \qquad (6)$$

This is assuming that there are no inerts, a condition that may have to be altered slightly for industrial applications.

These three equations were combined to solve for y_{NH_3}. The resulting values are given in Table 4.

Included is a plot of the equilibrium mole fraction of ammonia against temperature at constant pressure, on semilog paper.

Table 1. Ideal Gas Equilibrium Constant K

T, °K	Log K	K, atm^{-1}
500	-0.52178	0.3008
600	-1.39940	0.03987
700	-2.04342	0.009048
800	-2.53646	0.002908
900	-2.92783	0.001181
1000	-3.24477	0.0005692
1100	-3.50578	0.0003121
1200	-3.72488	0.0001884
1300	-3.91091	0.0001228
1400	-4.07197	0.00008473
1500	-4.21177	0.00006141

Table 2. Values of K_ϕ or Constant Relating Fugacity Coefficients

	K_ϕ			
Pressure, π, atm.	50	100	150	200
T, °K				
500	0.912	0.800	0.725	0.624
600	0.944	0.880	0.838	0.775
700	0.964	0.945	0.910	0.851
800	0.990	0.965	0.951	0.905
900	1.00	0.975	0.965	0.926
1000	1.00	0.985	0.974	0.951
1100	1.00	0.990	0.980	0.970
1200	1.00	0.995	0.990	0.982
1300	1.00	0.996	0.990	0.986
1400	1.00	0.997	0.993	0.990
1500	1.00	0.998	0.994	0.990

Table 3. Values of K_y or Constant Relating Mole Fractions of Components

	K_y			
Pressure, π, atm	50	100	150	200
T, °K				
500	16.50	37.6	62.3	96.5
600	2.12	4.53	7.15	10.30
700	0.470	0.957	1.491	2.13
800	0.1470	0.302	0.459	0.644
900	0.0591	0.1212	0.1840	0.255
1000	0.0285	0.0574	0.0876	0.1196
1100	0.0156	0.0312	0.0473	0.0643
1200	0.00940	0.01891	0.0284	0.0384
1300	0.00614	0.01232	0.01850	0.0248
1400	0.00423	0.00851	0.01279	0.01711
1500	0.00317	0.00617	0.00925	0.01240

Table 4. Values of y_{NH_3}, Equilibrium Ammonia Mole Fraction

		y_{NH_3}			
Pressure, π, atm		50	100	150	200
T, °K	t, °F				
500	440	0.651	0.751	0.800	0.837
600	620	0.320	0.449	0.525	0.583
700	800	0.1171	0.1990	0.263	0.320
800	980	0.0438	0.0825	0.1161	0.1511
900	1160	0.0185	0.0365	0.0534	0.0711
1000	1340	0.00909	0.01798	0.0270	0.0362
1100	1520	0.00501	0.00994	0.01491	0.0201
1200	1700	0.00303	0.00606	0.00906	0.01215
1300	1880	0.001986	0.00397	0.00594	0.00794
1400	2060	0.001370	0.00274	0.00411	0.00511
1500	2240	0.001029	0.00199	0.00298	0.00400

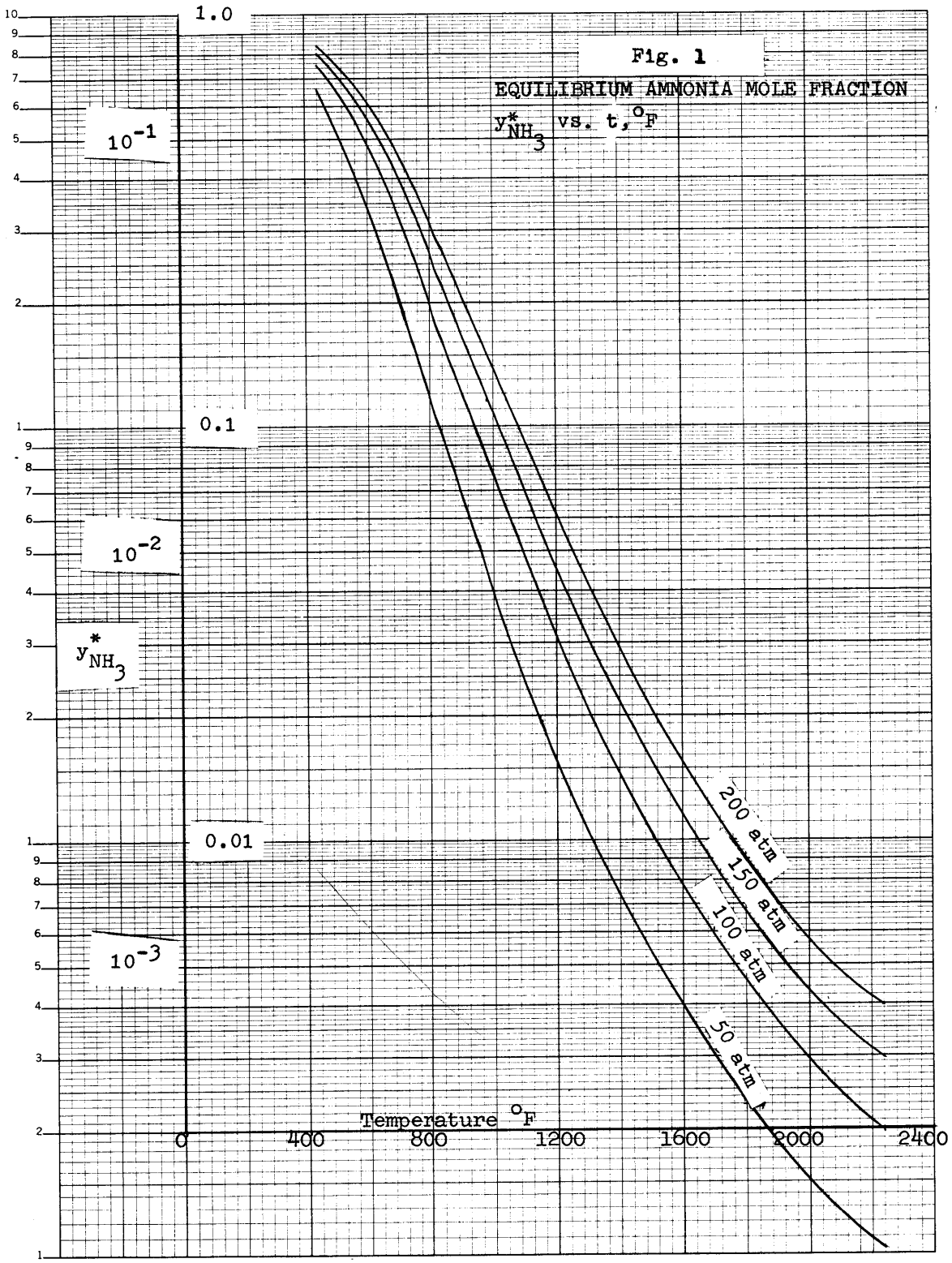
Fig. 1
EQUILIBRIUM AMMONIA MOLE FRACTION
$y^*_{NH_3}$ vs. t, °F
1.0
0.1
0.01
10^{-1}
10^{-2}
10^{-3}
$y^*_{NH_3}$
200 atm
150 atm
100 atm
50 atm
Temperature °F
0
400
800
1200
1600
2000
2400

BIBLIOGRAPHY

1. Harrison, Roland H. and Kobe, Kenneth A., Thermodynamics of Ammonia Synthesis and Oxidation, Chemical Engineering Progress 49, 349-353, July 1953.

2. Kobe, Kenneth A. and Arnold, Charles W., Curve Fitting: A Method for Minimum Percentage Deviation, Petroleum Refiner 30, 123-124, April 1951.

3. Haber, Fritz, Untersuchungen uber Ammoniak Sieben Mitteilungen, Zeitschrift fur Elecktrochemie 20, 597, Dec. 1914; 21, 89, March 1915; 21, 128, April 1915; 21, 191, May 1915; 21, 206, May 1915; 21, 228, May 1915; 21, 241, May 1915.

4. Larson, Alfred T. and others, The Ammonia Equilibrium, 45, 2918-2930, Dec. 1923; The Ammonia Equilibrium at High Pressures 46, 367-372, Feb. 1924.

5. Stephenson, C.C. and McMahon, H.O., The Free Energy of Ammonia, Journal of the American Chemical Society 61, 437-440, Feb. 1939.

6. Smith, J.M., and Van Ness, H. C., Introduction to Chemical Engineering Thermodynamics, Second Edition, Chapter 12, McGraw Hill Book Co., New York 1959.

7. Lydersen, Aksel L., Greenkorn, Robert A. and Hougen, Olaf A. Generalized Thermodynamic Properties of Pure Fluids, Engineering Experiment Station Report No. 4, University of Wisconsin, October 1955.

Supplement D

PREDICTION OF PLATE EFFICIENCY IN THE HYDROGEN DEUTERIUM AMMONIA-EXCHANGE REACTION

I. Introduction

The future use of heavy water as a moderator in nuclear power reactors is mainly dependent upon its cost. Several processes for the large-scale production of heavy water exist; however, there is still a need for new processes to be developed in order to bring down the cost. One of the more promising methods for separating deuterium is the chemical exchange between hydrogen and liquid ammonia

$$NH_3(\ell) + HD(g) \rightleftharpoons NH_2D(\ell) + H_2(g) \qquad (1)$$

The equilibrium constant causes the deuterium to concentrate selectively in the liquid phase. This reaction occurs only in the liquid phase and, then, only in the presence of a catalyst such as potassium amide.

Since the efficiency of a hydrogen-ammonia contactor is low due to the low solubility of hydrogen in liquid NH_3, accurate estimates of contactor efficiencies are crucial in the successful design of a deuterium absorption tower. It is the purpose of this memorandum to derive an expression for the prediction of the over-all Murphee plate efficiency of a bubble-plate contactor for the absorption of HD in solutions of potassium amide in ammonia. This derivation is a modification of the correlations developed for simple physical absorption in a bubble-plate contactor as presented in the "Bubble-Tray Design Manual"[4] published by the American Institute of Chemical Engineers in 1958.

II. Effect of a Chemical Reaction on the Mass Transfer Rate

A. General Theory

Mass transfer with chemical reaction may occur when two phases not in chemical equilibrium with each other are brought into contact. The phenomenon which takes place consists of a number of basic, simple steps.

1. The diffusion of one or more of the reactants from the bulk of the first phase to the interface between them. Physical equilibrium is usually assumed to exist at the interface.

2. The diffusion of the reactants to the bulk of the second phase from the interface.

3. Chemical reaction within the second phase.

4. The diffusion of reactants and reaction products in the second phase due to concentration gradients set up by the chemical reaction.

The analysis of the relative importance of these steps allows an evaluation of the effect chemical reaction has on the mass transfer rate.

When the kinetics of a chemical reaction are such that the reaction rate in a volume of liquid with unit interfacial area is slow compared to the physical absorption rate (with identical driving force), it is easy to see that mass transfer rate with chemical reaction is identical to that of physical absorption and that the bulk concentration will be greater than the equilibrium concentration, i.e.,

$$\psi \cdot \kappa (C_0' - C') \ll K_L^0 (C_0' - C') \tag{2}$$

$$K_L = K_L^0 \tag{3}$$

$$C_0 > C' \tag{4}$$

where

ψ is the volume of liquid per unit interfacial area; length

$\kappa(C_0'-C')$ is the reaction rate with driving force $(C_0'-C')$; mole $\cdot$ (length)$^{-3}$ $\cdot$ (time)$^{-1}$

K_L^0 is the physical absorption mass transfer coefficient; (length) $\cdot$ (time)$^{-1}$

K_L is the apparent mass transfer coefficient with chemical reaction, i.e., the mass transfer coefficient required to transfer the experimentally determined number of moles under a $(C_0'-C')$ driving force; (length) $\cdot$ (time)$^{-1}$

C_0' is the interfacial concentration of the gas being absorbed; (moles) $\cdot$ (length)$^{-3}$

C_0 is the bulk liquid concentration of the gas being absorbed; (moles) $\cdot$ (length)$^{-3}$

C' is the equilibrium concentration of the gas being absorbed; (moles) $\cdot$ (length)$^{-3}$

As the chemical reaction rate increases, the gradient at the gas-liquid interface also increases since some of the gas diffusing into the liquid boundary layer is removed by chemical reaction. Thus the mass transfer rate is enhanced by the chemical reaction and the bulk concentration begins to approach the equilibrium value.

$$K_L = \phi K_L^0 \tag{5}$$

$$C_0 \longrightarrow C' \tag{6}$$

where

ϕ is the apparent increase in the physical absorption coefficient caused by the increased concentration gradient at the gas-liquid interface; dimensionless.

B. Determination of ϕ for the HD(ℓ)-NH_3(ℓ) Exchange Reaction

In the absence of diffusion, the rate of change with time t of HD concentration C_{HD} in the liquid phase due to the reaction

$$HD + NH_3 \longrightarrow NH_2D + H_2$$

is given by

$$\frac{dC_{HD}}{dt} = k_1 C_{NH_2D} C_{H_2} - k_2 C_{HD} C_{NH_3} \tag{7}$$

But

$$\frac{k_1}{k_2} = \frac{C'_{HD} C'_{NH_3}}{C'_{NH_2D} C'_{H_2}} \tag{7a}$$

where C' is the concentration of the indicated species at equilibrium. For the solutions present in the exchange towers of an ammonia-hydrogen deuterium exchange plant

$$C_{HD} << C_{H_2}$$

$$C_{NH_2D} << C_{NH_3}$$

and

$$C_{H_2} << C_{NH_3}$$

Thus, as C_{HD} approaches its equilibrium concentration C'_{HD}, the only concentration in Eq. (7) which changes by a significant fraction is C_{HD}, and we may regard the other three concentrations as remaining constant at their equilibrium values. Then (7a) may be approximated by

$$k_1 C_{NH_2D} C_{H_2} = k_2 C_{HD} C_{NH_3} \tag{7b}$$

and (7) by

$$\frac{dC_{HD}}{dt} = k_2 C_{NH_3}(C'_{HD} - C_{HD}) = k (C'_{HD} - C_{HD}) \tag{7c}$$

where

$$k \equiv k_2 C_{NH_3} \tag{8}$$

Here

k_2 is the kinetic constant for the 2nd order HD-NH_3 exchange reaction; $(\text{mole})^{-1} \cdot (\text{time})^{-1} \cdot (\text{length})^3$

k is the kinetic constant for pseudo first-order HD-NH_3 exchange reaction; $(\text{time})^{-1}$

When HD diffuses into the liquid, the differential material balance on this component may be expressed by

$$\frac{\partial C}{\partial t} = k(C'-C) + D_1 \frac{\partial^2 C}{\partial z^2} \tag{9}$$

where

z is the distance from the interface; length

D_1 is the diffusivity of the absorbing component; $(\text{length})^2 \cdot (\text{time})^{-1}$

This equation is to be solved subject to the boundary conditions

$$\begin{array}{lll} t = 0 & C = C_0 \\ t > 0 \begin{cases} z = 0 & C = C'_0 \\ z \to \infty & C \neq \pm \infty \end{cases} \end{array} \tag{10}$$

Solution of equation (9) with its associated boundary conditions by the method of Laplace transforms yields:

$$\frac{C - C'}{C_0' - C'} = \frac{1}{2}\left\{ e^{(z\sqrt{k/D_1})} \cdot \operatorname{erfc}\left[\frac{z}{2\sqrt{D_1 t}} + \sqrt{kt}\right] + e^{-(z\sqrt{k/D_1})} \cdot \operatorname{erfc}\left[\frac{z}{2\sqrt{D_1 t}} - \sqrt{kt}\right] \right\} + \frac{C_o - C'}{C_o' - C'} e^{-(kt)} \cdot \operatorname{erf}\left[\frac{z}{2\sqrt{D_1 t}}\right] \tag{11}$$

where

$$\operatorname{erf}(\zeta) = \frac{2}{\sqrt{\pi}} \int_0^{\zeta} e^{-(\eta^2)}\, d\eta$$

$$\operatorname{erfc}(\zeta) = 1 - \operatorname{erf}(\zeta)$$

$$e = 2.71828 \ldots\ldots$$

The instantaneous absorption rate, R, can be found by differentiating equation (11) and evaluation at the interface.

$$R(t) = -D_1 \left(\frac{\partial C}{\partial z}\right)_{z=0} = (C_0' - C')\sqrt{kD_1}\left\{ \operatorname{erf}(\sqrt{kt}) + \frac{e^{-(kt)}}{\sqrt{\pi kt}} \right\} - (C_0 - C')e^{-(kt)} \cdot \sqrt{D_1/\pi t} \tag{12}$$

where

R(t) is the instantaneous absorption rate; $(\text{mole}) \cdot (\text{length})^{-2} \cdot (\text{time})^{-1}$.

It is now possible to calculate a mean absorption rate, $\bar{R}$, if we are willing to model the hydrodynamic conditions in the liquid phase close to the gas-liquid interface. In the calculations that follow, a model proposed by Danckwerts (2) will be used.

This model is similar to that of the Higbie penetration model (3) except that it does not accept the hypothesis of an equal lifetime for all surface elements.

A brief summary of the relevant hypotheses in Higbie's model is as follows:

1. The gas-liquid interface is made up of a variety of small liquid elements.

2. These surface elements are continuously brought to the surface from the bulk liquid and returned to it by the motion of the liquid phase.

3. Each element is considered stagnant as long as it remains on the surface.

4. The initial dissolved gas concentration is equal to that of the bulk.

5. Absorption takes place by unsteady molecular diffusion.

6. The lifetimes of the surface elements are identical.

Danckwerts' model differs in Hypothesis 6 ; he proposed an age-distribution function, I, which assumed that the probability a surface element would be removed from the surface is independent of its age. Thus,

$$-\frac{dI}{dt} = sI \tag{13}$$

and

$$\int_0^\infty I(t)dt = 1 \tag{14}$$

where

I(t) is called the age, distribution function; $(\text{time})^{-1}$

I(t)dt is the fraction of the total surface which is made up of surface elements whose age is larger than t and smaller than (t+dt); dimensionless.

s is the Danckwerts' model parameter, a proportionality constant; $(\text{time})^{-1}$

Solving equations (13) and (14) yields

$$I(t) = se^{-st} \tag{15}$$

for the distribution function. Calculation of a mean absorption rate, $\bar{R}$, is now possible.

$$\bar{R} = \int_0^\infty I(t)R(t)dt$$

$$= (C_0'-C')\sqrt{D_1(s+k)} - (C_0-C')\sqrt{D_1 s}\ \sqrt{s/(s+k)} \tag{16}$$

where

$\bar{R}$ is the mean absorption rate; $(\text{mole})\cdot(\text{length})^{-2}\cdot(\text{time})^{-1}$

Since the average physical absorption rate, $\overline{R^0}$, can be calculated from equation (16) by setting k = 0,

$$\overline{R^0} = \sqrt{D_1 s}\ (C_0'-C_0) \tag{17}$$

the ratio ϕ of the absorption rate with chemical reaction to the absorption rate with just physical absorption is

$$\phi \equiv \frac{\bar{R}}{\overline{R^0}} = \frac{C_0'-C'}{C_0'-C_0}\sqrt{\frac{s+k}{s}} - \frac{C_0-C'}{C_0'-C_0}\sqrt{\frac{s}{s+k}} \tag{18}$$

If we assume that the reaction rate is sufficiently high to maintain the bulk concentration C_0 close to the equilibrium concentration C', the last term may be neglected

$$C_0 \sim C' \tag{18a}$$

and

$$\phi \sim \sqrt{1 + \frac{k}{s}} \tag{19}$$

As the average physical absorption rate in the absence of chemical reaction is related to the physical absorption mass transfer coefficient K_L^0 by

$$\overline{R_0} = K_L^0\ (C_0'-C_0) \tag{19a}$$

comparison of (17) and (19a) shows that the constant s of the Danckwerts theory is related to K_L^0 by

$$s = \frac{(K_L^0)^2}{D_1} \tag{19b}$$

so that

$$\phi = \sqrt{1 + \frac{kD_1}{(K_L^0)^2}} \qquad (20)$$

III. Efficiency Correlation

A. Literature Survey

A literature survey was made of methods used in the prediction of tray efficiencies. Except for the case of bubble-trays, no generally reliable correlations were found. For the case of bubble-trays, the A.I.Ch.E. correlation[4,14] was found to yield predictions in agreement with experimental plate efficiencies from a large number of fractionating systems. Work was done to modify this correlation to predict efficiencies in absorbing systems with accompanying chemical reaction.

The predictions from this modified correlation were then tested against HD-NH_3 exchange data obtained in experiments, with good results.

B. Modification of the A.I.Ch.E. Correlation

In order to modify the existing A.I.Ch.E. correlation for stage efficiency prediction, it is necessary to operate in a region where the chemical reaction proceeds sufficiently rapid to maintain the bulk liquid concentration of HD equal to the equilibrium concentration.

If the usual conventions are used in defining the steady-state equations for mass transfer per unit area, we can write

$$dN_{HD} = K_{OG}(y^*-y)_{HD} P_\pi AdZ = k_G a(y_i-y)_{HD} P_\pi AdZ = K_{OL}(x-x^*)_{HD}\rho_L AdZ$$

$$= k_L a(x-x_i)_{HD}\rho_L AdZ \qquad (21)$$

where

a is the interfacial area per unit volume of gas and liquid holdup; $(ft)^{-1}$

A is the cross-sectional area of contact volume, bubbling area; $(ft)^2$

K_{OG} is the over-all gas phase mass-transfer coefficient; (lb moles) $\cdot$ $(hr)^{-1} \cdot (ft)^{-2} \cdot (atm)^{-1}$

K_{OL} is the over-all liquid phase mass transfer coefficient; $(ft) \cdot (hr)^{-1}$

k_G is the mass-transfer gas-film coefficient; (lb moles) $\cdot$ $(hr)^{-1} \cdot (ft)^{-2} \cdot (atm)^{-1}$

k_L is the mass-transfer liquid-film coefficient; $(ft) \cdot (hr)^{-1}$

dN_{HD} is the rate of transfer of HD at steady-state from liquid phase to vapor phase;(lb moles) $\cdot$ $(hr)^{-1}$, in height dZ

P_π is the total pressure; atm

x is the mole fraction of a given component in the liquid phase at a given point. Subscript i denotes the value at the vapor-liquid interface; dimensionless

x* is the mole fraction in the liquid which would exist if the bulk liquid phase were in equilibrium with the bulk vapor phase; dimensionless

y is the mole fraction of a given component in vapor phase at a given point. Subscript i denotes the value at vapor-liquid interface; dimensionless

y* is the mole fraction of the diffusing component which would exist in the bulk vapor phase if the vapor were in equilibrium with the bulk liquid phase; dimensionless

Z is the height of contact volume; (ft)

ρ_L is the molar density of the liquid phase; (lb moles) $\cdot$ $(ft)^{-3}$

Under the assumption of equilibrium in the bulk liquid, it is possible to say that for every mole of HD transferred from the gas phase a mole of NH_2D appears (this is approximately true since the holdup of HD in the liquid phase is small and in the region we are interested in

$$\frac{dx_{HD}}{dx_{NH_2D}} \sim 10^{-3}).$$

Thus the material balance on the amount of HD transferred can be simply written

$$dN_{HD} = G_M A dy_{HD} = L_M A dx_{NH_2D} \tag{22}$$

where

G_M is the molar gas flow rate per bubbling area; (lb moles)$\cdot$ $(hr)^{-1}\cdot(ft)^{-2}$

L_M is the molar liquid flow rate per bubbling area; (lb moles)$\cdot(hr)^{-1}\cdot(ft)^{-2}$

The equilibrium equation for the reaction

$$NH_3(\ell) + HD(g) \rightleftharpoons H_2(g) + NH_2D(\ell) \tag{1}$$

is normally written

$$K = \frac{P_{H_2}}{P_{HD}} \cdot \frac{C_{NH_2D}}{C_{NH_3}} \tag{23}$$

where

K is the equilibrium constant for the reaction; dimensionless

The value of the equilibrium constant is given by (5)

$$\text{Log}_{10}\ K = -.0667 + \frac{237}{T} \tag{24}$$

where

T is the absolute temperature; ^{o}K

Assuming that the solubility of HD in $NH_3(\ell)$ is that of H_2

$$\frac{P_{HD}}{P_{H_2}} = \frac{C_{HD}}{C_{H_2}} \tag{25}$$

the equilibrium constant can be referred to the liquid phase where the reaction takes place in the presence of a catalyst.

$$K = \frac{C_{H_2}}{C_{HD}} \cdot \frac{C_{NH_2D}}{C_{NH_3}} \tag{26}$$

or in terms of mole fractions

$$K = \frac{x_{H_2}}{x_{HD}} \quad \frac{x_{NH_2D}}{x_{NH_3}} \tag{27}$$

Since in the system under study

$$x_{H_2} >> x_{HD} \tag{28}$$

$$x_{NH_3} >> x_{NH_2D} \tag{29}$$

small changes in the deuterium concentration will leave the ratio, x_{H_2} / x_{NH_3}, relatively unchanged, the value x_{HD} can be

represented by

$$x_{HD} = \frac{x_{NH_2D}}{K'} \tag{30}$$

and

$$dx_{HD} = \frac{dx_{NH_2D}}{K'} \tag{31}$$

where K' is a constant equal to

$$K' = K \Big/ \left[x_{H_2} \Big/ x_{NH_3} \right] \tag{32}$$

Combination of the material balance, Equation (22), with each of the four rate equations, Equation (21), followed by an integration from Z=0 to Z=Z (G_M, L_M, P_π, ρ_L, and the mass-transfer coefficients are assumed constant) gives

$$\frac{k_G a P_\pi}{G_M} Z = \int \frac{dy_{HD}}{(y_i - y)_{HD}} = N_G \tag{33a}$$

$$\frac{k_L a \rho_L}{K' L_M} Z = \int \frac{dx_{NH_2D}}{K'(x - x_i)_{HD}} = N'_L \tag{33b}$$

$$\frac{K_{OG} a P_\pi}{G_M} Z = \int \frac{dy_{HD}}{(y^* - y)_{HD}} = N_{OG} \tag{33c}$$

$$\frac{K_{OL} a \rho_L}{K' L_M} Z = \int \frac{dx_{NH_2D}}{K'(x - x^*)_{HD}} = N'_{OL} \tag{33d}$$

where

N_G is the number of vapor-film transfer units; dimensionless

N'_L is the number of liquid-film transfer units; dimensionless

N_{OG} is the number of over-all vapor transfer units; dimensionless

N'_{OL} is the number of over-all liquid transfer units; dimensionless

A transfer unit is accomplished when the change in a stream concentration equals the mean driving force over the interval in which the change in concentration occurs. However, when a chemical reaction takes place, material is reacted, thereby reducing the change in stream concentration (for the HD-NH_3 exchange case by a factor of K'). Thus for our case of HD reacting, N'_L and N'_{OL} should be redefined

$$N_L = K'N'_L = \int \frac{K'dx_{HD}}{(x-x_i)_{HD}} = \frac{k_L a \rho_L}{L_M} Z \qquad (34)$$

$$N_{OL} = K'N'_{OL} = \int \frac{K'dx_{HD}}{(x-x^*)_{HD}} = \frac{K_{OL} a \rho_L}{L} Z \qquad (35)$$

If we add up the resistances to mass transfer, we obtain, after some algebraic manipulation,

$$\frac{1}{N_{OG}} = \frac{1}{N_G} + \frac{m_{HD}G_M}{L_M N_L} = \frac{m_{HD}G_M}{L_M N_{OL}} \qquad (36)$$

where

$$m_{HD} = \frac{H}{P_\pi} \qquad (37)$$

m is the slope of the equilibrium curve, $\frac{dy}{dx}$, and in this particular case corresponds to that of physical absorption, dimensionless. H is the Henry's law constant; atm.

The A.I.Ch.E. correlation presents expressions for the calculation of N_L and N_G from the operating conditions of the tower. However since the expression for N_L is based on pure physical absorption, it does not take into account the increased mass transfer due to increased concentration gradients at the liquid interface. Thus N_L in Equation (36) should be replaced by $\emptyset N_L$ and the value of N_{OG} to be used is

$$\frac{1}{N_{OG}} = \frac{1}{N_G} + \frac{m_{HD} G_M}{L_M \emptyset N_L} \tag{38}$$

An equilibrium stage produces an exit vapor stream which is in thermodynamic equilibrium with the exit liquid stream. The approach to equilibrium on such a tray has been expressed by Murphree as the ratio of the actual change in the vapor concentration through the tray to the change which would have occurred if equilibrium had been reached. The Murphree tray efficiency is

$$E_{MV} = \frac{y_n - y_{n-1}}{y_n^* - y_{n-1}} \tag{39}$$

where the subscripts n and n-1 refer to the outlet and inlet vapor streams respectively. However the Murphree tray efficiency represents physical reality only in the case of a completely mixed liquid on the tray. When the liquid on the tray is incompletely mixed Equation (39) cannot apply except at a point in the liquid pool. A point Murphree efficiency is defined as

$$E_{OG} = \frac{y - y_{n-1}}{y^* - y_{n-1}} \tag{40}$$

where the lack of a subscript on y* denotes the actual vapor or liquid concentration at a given point in the pool. While it is possible to obtain N_{OG} from the A.I.Ch.E. correlations, it is necessary to postulate a tray model in order to relate N_{OG} and E_{OG}. Using a tray model (see Figure I) possessing the following 3 assumptions:

1) The liquid is assumed to be completely mixed in the vertical direction

2) The vapor entering the tray is of uniform composition y_{n-1} and

3) The vapor passing upward through the liquid along any vertical line in plug flow,

it is possible to integrate Equation (33c)

$$N_{OG} = \int \frac{dy}{y^*-y} \tag{33c}$$

on any vertical line from the tray deck to the top of the froth. Since the liquid composition is constant, y* is a constant

$$N_{OG} = -\ell n \frac{y^*-y}{y^*-y_{n-1}} \tag{41}$$

$$e^{-N_{OG}} = 1 - E_{OG} \tag{42}$$

We would now like to relate this point efficiency, E_{OG}, to the tray Murphree efficiency, E_{MV}. If the liquid is completely mixed the relationship is trivial:

$$E_{OG} = E_{MV} \tag{43}$$

However if no horizontal mixing occurs, the liquid can be said to be in plug flow across in tray. Combination of a material

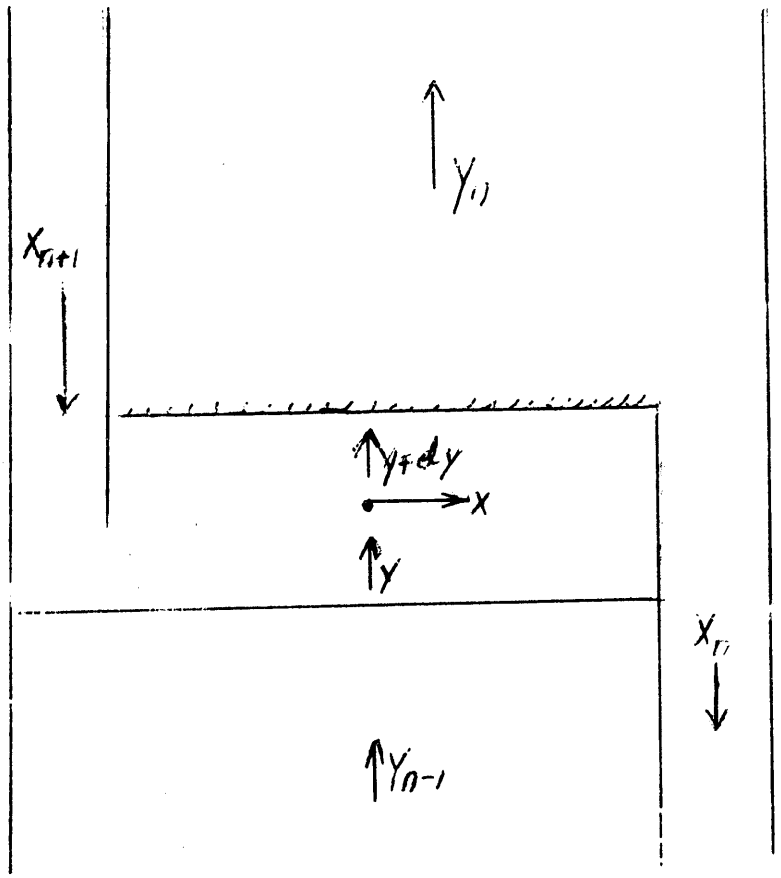

FIGURE 1. Tray Model in Vapor Terms.

balance (equilibrium)

$$(y-y_{n-1})_{HD} dG_M = L_m K' dy_{HD} \quad (44)$$

and Henry's law

$$y^*_{HD} = m_{HD} x_{HD} \quad (45)$$

gives

$$(y-y_{n-1})_{HD} = \frac{K' L_M}{m_{HD} G_M} \frac{dy^*_{HD}}{dw} \quad (46)$$

where a new variable, $dw = \frac{dG_M}{G_M}$, is defined. (47)

From the definition of E_{OG} [Equation (40)]

$$dy^*_{HD} = \frac{dy_{HD}}{E_{OG}} \quad (48)$$

$$\frac{m_{HD} G_M}{K' L_M} E_{OG} dw = \frac{dy_{HD}}{(y-y_{n-1})_{HD}} \quad (49)$$

it is now possible to integrate Equation (49) assuming E_{OG} is constant, from the overflow weir ($w = 0$ and $y = y_{w=0}$) across the tray to some point where $w = w$ and $y = y$

$$y = y_{n-1} + (y_{w=0} - y_{n-1})\, e^{\frac{m_{HD}}{k'} \frac{G_M}{L_M} E_{OG} w} \quad (50)$$

Using Equation (50) to find the average composition, y_n, of the vapor leaving the n^{th} stage

$$y_n = \int_0^{1.0} y\, dw \quad (51)$$

and

$$\frac{y_n - y_{n-1}}{y_{w=0} - y_{n-1}} = \frac{K'L_M}{m_{HD}G_M E_{OG}} \left[e^{\frac{M_{HD}G_M E_{OG}}{K'L_M}} - 1 \right] \qquad (52)$$

Since E_{OG} is assumed constant across the tray, if E_{OG} is defined at the overflow weir where w=0 ($y^*_{w=0} = y^*_n$)

$$E_{OG} = \frac{y_{w=0} - Y_{n-1}}{y^*_n - y_{n-1}} \qquad (53)$$

Combining Equations (52) and (53) yields the formulation for the Murphree tray efficiency, E_{MV},

$$E_{MV} = \frac{y_n - y_{n-1}}{y^*_n - y_{n-1}} = \frac{K'L_M}{m_{HD}G_M} \left[e^{\frac{M_{HD}G_M E_{OG}}{K'L_M}} - 1 \right] \qquad (54)$$

Almost every case in practice, however, is a mixture of these two cases; i.e. the liquid is neither completely mixed nor completely non-mixed. Reference (4), p. 10, gives the relationship between the tray and point efficiency as:

$$\frac{E_{MV}}{E_{OG}} = \frac{1 - e^{-\left[n + (Pe)\right]}}{\left[n + (Pe)\right] \left[1 + \frac{n+(Pe)}{n}\right]} + \frac{e^n - 1}{n\left[1 + \frac{n}{n+(Pe)}\right]} \qquad (55a)$$

where

$$n = \left(\frac{Pe}{2}\right) \left(\sqrt{1 + \frac{4\lambda E_{OG}}{(Pe)}} - 1\right) \qquad (55b)$$

Pe is the Peclet number and a measure of the degree of mixing $\frac{Z_\ell^2}{D_e t_L}$ dimensionless.

D_e is the eddy diffusion coefficient; $(ft)^2 \cdot (sec)^{-1}$

$$D_e = \left[1 + .044\ (d-3)\right]^2 \left(.0124 + .0150h_w + .017U_a + .0025L\right)^2 \quad (55c)$$

d is the bubble cap diameter; inch

h_w is the weir height; inch

U_a is the superficial gas velocity based on bubbling area; $(ft) \cdot (dec)^{-1}$

L is the liquid volume flow factor; $(gal) \cdot (min)^{-1} \cdot (ft)^{-1}$

$$\lambda = \frac{m_{HD} G_M}{K' L_M} \quad (55d)$$

t_L is the average residence time for the liquid on the tray; sec.

IV. Absorption System Design

A. Choice of Operating Conditions

In the design of a plant for concentrating deuterium by means of the H_2-NH_3 exchange reaction, a plentiful supply of cheap hydrogen and ammonia is required. An ideal solution would be to add the exchange towers to an existing ammonia synthesis plant. However this imposes certain restrictions on what the operation conditions may be, if the ammonia-synthesis plant is not to have its operating conditions greatly disturbed or modified.

TABLE I

Proposed Operating Conditions

Pressure	150 atm.
Temperature	$-20^\circ C$
Catalyst (KNH_2) concentration	0.5g mole/liter

The major restriction imposed would be on the maximum pressure employable without additional compressors. Since the ammonia synthesis plant of Air Products and Chemicals Inc. was used as a basis for process and cost confirmation, the maximum pressure available was 150 atm. As it is desirable to use the maximum pressure possible in order to minimize tower volume, an operating pressure of 150 atm was chosen.

Due to the low solubility of hydrogen in liquid ammonia, it is necessary that the exchange reaction occur within the absorption tower; otherwise the degree of deuterium concentration will be very small (limited to the amount that can be physically absorbed in the tower). Therefore a design requirement of the tower operating in the chem-absorption region rather than the physical-absorption region was made. This implies that the reactions e-folding time (first order reaction) is approximately equal to the time it takes a molecule of HD to be transported from the liquid's surface to its bulk.

$$\frac{1}{k} \backsim \frac{D_1}{(K_L^0)^2} \tag{56}$$

($D_1/K_L^{0^2}$ is the average surface renewal time in Danckwerts' model). Using typical values of D_1 and K_L^0, a value of about 1600 min^{-1} was found for k. Any catalyst concentration - temperature combination giving a value of $k > 1600$ min^{-1} was felt to be acceptable. The effect of increasing temperature for a given catalyst concentration was to increase the plate efficiency (9,10,12) and the exchange rate (1,2,10,12). Increasing temperature, however, raised the partial pressure of the liquid ammonia, thus requiring an extensive dehumidification section in addition to reducing the separation factor.

If the temperature was kept low in order to keep the ammonia content of the gas stream down the catalyst concentration had to be raised in order to maintain k above 1600 min^{-1}. Reborra (9,10)

found that additional catalyst became ineffective after .5 gm mole/liter. Thus a catalyst concentration of .5 gm mole/liter was chosen with a temperature, $-20^{\circ}C$, which would give a reaction rate constant of about 2000 $min.^{-1}$.

These values of temperature, pressure and catalyst concentration are a first guess as to what might prove the optimum values and keep the bulk liquid HD concentration close to equilibrium.

B. Physical and Phase Properties

Values of the physical and phase properties of an H_2-N_2-NH_3 system were obtained by either literature search (7) or estimation (8). Table 2 is a summary of the important physical data used in designing an exchange tower.

TABLE II

Design Data for Exchange Tower

Gas Phase

y_{H_2} (mole fraction)	0.73425
y_{N_2}	0.24475
y_{NH_3}	0.021
y_{CH_4} and y_A	assumed 0
Viscosity	0.04 lb /ft hr
Henry's Law Constant (H_2)	25700 atm
Diffusivity (HD in gas mixture)	$2.347.10^{-2}$ ft^2/hr
Density a) Mass b) Molar	 62.71 g/ℓ 7.226g mole/ℓ

Table II cont.

Liquid Phase	
k reaction	2000 min^{-1}
K for $HD + NH_3 \rightleftharpoons H_2 + NH_2D$	7.414
x_{NH_3}	0.9875
x_{KNH_2}	0.0125
Surface Tension	30.4 dynes/cm
Viscosity	0.246 cp.
Diffusivity (HD in NH_3)	$1.773 \cdot 10^{-4}$ ft^2 /hr
Density a) Mass	700 g/ℓ
Density b) Molar	40.0 g mole/ℓ

C. Determination of Flow Rates in Exchange Towers

A mass balance was drawn around the primary counter-current exchange tower operating in conjunction with a 1530 T/d ammonia - synthesis plant. The various inlet and exit concentrations were set (see Table 3) and the relative flow rates determined.

TABLE III

Inlet and Exit Compositions in Exchange Tower
(Mole Fraction)

Gas	
Inlet	
y_{NH_3}	0.021
y_{NH_2D}	$3.721 \cdot 10^{-5}$
y_{HD}	$1.98 \cdot 10^{-4}$
Outlet	
y_{NH_3}	0.021
y_{NH_2D}	$3.041 \cdot 10^{-7}$
y_{HD}	$7.343 \cdot 10^{-6}$

Table III cont.

Liquid	
Inlet	
$x_{NH_2D + KNHD}$	$1.5 \cdot 10^{-5}$
Outlet	
$x_{NH_2D + KNHD}$	$1.836 \cdot 10^{-3}$

The criteria used in setting the values found in Table 3 are

1) The gas stream enters with a $\frac{D}{D+H}$ ratio of 132 PPM for the gaseous hydrogen and an ammonia deuterium content in equilibrium with the exiting liquid stream.

2) The exiting gas stream has a $\frac{D}{D+H}$ ratio of 5 PPM for the gaseous hydrogen and the NH_2D content is in equilibrium with entering liquid.

3) The exiting liquid stream has its deuterium tied up in NH_2D and KNHD and is in equilibrium with a fictitious gas stream with a D/D+H ratio of 124 PPM.

4) The entering liquid stream has a $\frac{D}{D+H}$ ratio of 5 PPM due to its formation from the exiting gas stream.

With these operating conditions the molar gas-to-liquid-flow rate is 8 or for a synthesis gas flow rate of 360,000 lb moles/day (367,722 lb moles/day total gas flow rate), the liquid flow rate was 45,965 lb moles/day.

D. Tray Characteristics

Using standard design procedures (11), a model tower was designed as part of the study in order to determine how closely the efficiency equations would predict values determined experimentally and to determine the feasibility of using bubble-tray contactors in the HD-NH_3 exchange towers. Table 4 gives a summary of the physical layout of the tray to be used, while Table 5 gives the tower's design parameters.

TABLE IV

Physical Characteristics of Proposed Tray Design

Tray Diameter	4.4 ft
Tray Spacing	24 in
Tray Type	Single cross-flow tray with segmental downcomer
Downflow Area	1.83 ft^2
Bubble Cap Size	3" cap, triangular cap pitch; rows normal to flow of liquid
Total Area	15.2 ft^2
Active area (Bubbling area)	11.6 ft^2
Net Area	13.4 ft^2
Cap Spacing	1 in.
Cap S Clearance	1 in.
Outlet weir height	5.25 in.
Weir length	3.38 ft
Liquid flow path	2.82 ft
Average liquid flow width	4.1 ft

TABLE V

Exchange Tower Operating Parameters

Vapor Flow Rate	9.435 ft^3/sec
Liquid Flow Rate	93.626 gpm
Superficial vapor velocity based on bubbling area, U_a	0.813 fps
Flooding vapor velocity	1.176 fps
Approach to flooding, based on net area	60%

E. Evaluation of the Efficiency Prediction and Comparison with Experiment

The efficiency E_{OG}, of the proposed design was calculated to be 1.8%. The acceleration factor, $\emptyset$, was determined using the Ward correlation (13) for a completely"mobile" bubble

$$Sh = 0.61\ (Sc)_L^{.5}(Re)^{.5} \qquad (57)$$

where

Sh is the Sherwood number ($K_L^0\ d_b/D_L$); dimensionless

d_b is the diameter of the bubble; ft

Sc is the Schmidt number based on the liquid properties $\left(\frac{\mu_L}{\rho_L D_L}\right)$; dimensionless

μ_L is the liquid viscosity; $(lb)\cdot(ft)^{-1}\cdot(hr)^{-1}$

ρ_L is the mass density of the liquid; $(lb)\cdot(ft)^{-3}$

Re is the Reynolds number for the gas bubble, $\left(\frac{w\rho_L d_b}{\mu_L}\right)$ dimensionless

w is the velocity of the gas bubble through the liquid taken to be 21 cm/sec

The diameter of the gas bubble was estimated from Leiboon's (13) study

$$d_b' = 0.713\ (Re)^{-.05} \qquad (58)$$

where

d_b' is the bubble diameter; cm

$(Re)_o$ is the orifice Reynolds number $\left(\frac{d_o \rho_L U_a}{\mu_L}\right)$

d_o is the diameter of the orifice; ft

U_a is the active area superficial gas velocity; fps

The values obtained

From Eq. (58): $d_b' = 0.485$ cm

From Eq. (57): $K_L^0 = 3.2$ ft/hr

From Eq. (20): $\phi = 1.74$

made it possible to use the A.I.Ch.E. correlations.

$$N_G = (Sc)_G^{-.5}\left[0.776 + 0.116\ h_w - 0.290\ F_{va} + 0.0217\ Q/\ell\right]$$

$$N_L = \left[(4.13\ 10^4)\ (D_L)\right]^{.5}\ (0.26F_{va} + 0.15)\ t_L$$

$$t_L = \frac{37.4\ h_\ell Z_\ell}{Q/\ell}$$

---

* Note: The University of Delaware report (14) done for the A.I.Ch.E. suggested that the constant in N_L be changed from 1.065 to 4.13 for a better correlation of data, this suggestion was followed here.

$$h_{\ell} = 1.65 + 0.19\, h_w - 0.65\, F_{va} + 0.020\, Q/\ell$$

where

h_w is the weir height; in.

F_{va} is the F factor ($=U_a \sqrt{\rho_v}$), (fps) $\sqrt{\text{lb/ft}^3}$

Q is the actual clear liquid flow rate, gpm

ℓ is the average liquid flow width, ft

t_L is the residence time of liquid in the aerated mass on tray, sec

h_{ℓ} is the liquid holdup on the tray in cubic inches per square inch of bubbling area

Z_{ℓ} is the length of liquid travel from the inlet downcomer to the outlet weir, ft

Using the model tray, the point efficiency was calculated for conditions similar to those used by J. Bigeleisen et al (15). The efficiency equation was modified to account for Bigeleisen's use of a single slot of a bubble cap in a stagnant pool at a pressure of about 15 atm. The calculated value of E_{OG} was 2.3% while that taken from a graph of Bigeleisen's results was

$$2.6 \pm 1\% \text{ at } T = -20^{\circ}C$$

The Canadians (16) developed a correlation for the prediction of point efficiencies for the HD - NH_3 exchange process from experimental data in interphase mass transfer in sieve trays. (1, 9, 10, 12, 17, 18) The Canadian sieve tray correlation was applied to the model bubble cap tray investigated in this report and compared to the A.I.Ch.E. correlation. Because of the form of the Canadian correlation it was necessary to make the comparison for an $\frac{G_M}{L_M}$ ratio of 3.43, a potassium amide concentration of 0.65 molar and a bubble diameter of 0.433 cm. With the exception of an increased tray diameter to account for the changed $\frac{G_M}{L_M}$ ratio the tray characteristics remained unchanged.
The results of this comparison were

$$E_{OG\ \text{Canadian}} = 4.7\%$$

$$E_{OG\ \text{A.I.Ch.E.}} = 4.55\%$$

V. Conclusions

The above comparisons indicate that the A.I.Ch.E. tray efficiency correlation, extended as described in this report, provides a satisfactory means for predicting efficiencies of bubble plate trays in the ammonia-hydrogen exchange tower. The low efficiency thus predicted however, suggests that either a more efficient contactor or quite different operating conditions will be needed for a practical process.

VI. References

1. Bourke and Lee "Exchange of Deuterium Between Hydrogen and Liquid Ammonia", Trans. Institute of Chem. Eng. 39, 280-8 (1961).

2. Danckwerts, P.V., Trans Faraday Soc. 46, 300 (1950).

3. Higbie, R., "Rate of Absorption of a Pure Gas into a Still Liquid during Short Periods of Exposure", Trans. A.I.Ch.E., 31, 365-89.

4. A.I.Ch.E. "Bubble-Tray Design Manual", N.Y. (1958).

5. Perlman, M., Bigeleisen, J., and Elliott, N., J. Chem. Phys., 21, 70 (1953).

6. Wehner, J.F., and Wilhelm, R.H., Chem. Eng. Sci., 6, 89 (1956).

7. Chow, E. "Liquid-Vapor Equilibrium in the system NH_3-H_2-N_2" MITD-6, 4/1/68.

8. Reid and Sherwood, The Properties of Gases and Liquids, New York, McGraw-Hill, 2nd Edition (1966).

9. Reborra, P.L., "The Isotroic Exchange Between Gaseous Hydrogen and Liquid Ammonia, Part I. The Kinetics of the Exchange in a Bubbling Contactor", Energia Nucleare, 9, (7), 388 (1962).

10. Reborra, P.L. and Duranti-Valentini, "Part II The Kinetics of the Exchange in a Packed Column", Energia Nucleare, 9, (11), 621-7 (1962).

11. Smith, B.D., Design of Equilibrium Stage Processes, New York, McGraw-Hill, (1963).

12. Bouke, P.J. and Pepper, D., Trans. Instn. Chem. Engs., 41, 40 (1963).

13. Valentin, F.H.H., Absorption in Gas-Liquid Dispersions, London, E. and F.N. Spon. Ltd., (1967).

14. Gerster, J.A. et al, "Tray Efficiencies in Distillation Columns", Final Report from University of Delaware, A.I.Ch.E., New York (1958).

15. J. Bigeleisen et al, "The Ammonia-Hydrogen and Phosphine-Water Processes for the Production of D_2O", Proc. Int'l Symp on Isotope Separation, 133-45 (1958).

16. Bancroft, A.R. editor, "400 Ton per Year Water-Based Bithermal Hydrogen-Ammonia Exchange Heavy Water Plant" CRCE-1241 (1966).

17. R. Haul et al, Chemie-Ingenieur-Technik, 33, (11) 713 (1961).

18. G. Dirian et al, J. Chim. Phys, 60, 139 (1963).

Supplement E

ANALYSIS OF STIRRED CONTACTORS FOR GAS-LIQUID EXCHANGE REACTIONS

1.0 INTRODUCTION

Previous work (1, 2) has indicated that conventional gas-liquid contactors such as bubble plates and sieve trays are inherently inefficient when used in systems in which the gas is sparingly soluble. A design study has been conducted of an agitated vessel in which mixing impellors are used to subdivide the gas into small bubbles in order to provide a means of obtaining a higher contact efficiency.

Recent studies (3 - 7) of gas absorption with or without simultaneous chemical reaction have been usually based on extension of the Higbie penetration model (9). The mathematical solutions of this model require a knowledge of the rate with which the liquid surface renews itself at the bubble-liquid interface or of the bubble velocity relative to the liquid. Both these quantities are extremely difficult to measure or estimate.

The following analysis uses a basis similar to that of Gal-Or and Resnick (8) in which the average residence time of the gas bubble in the liquid is one of the prime variables.

2.0 PROPOSED MODEL

The system investigated is that in which a sparingly soluble gas mixture (H_2 - HD) is distributed throughout an agitated liquid phase (liquid ammonia). The following assumptions are involved:

(1) There is no gas phase resistance to mass transfer.

(2) There is a uniform distribution of gas bubbles throughout the liquid phase.

(3) The radius of a gas bubble remains constant.

(4) There is a singular distribution of gas bubble sizes.

(5) The equilibrium concentration of the dissolved gas is a constant in each stirred contactor.

(6) The concentration of dissolving gas at the gas-liquid interface above the equilibrium concentration decreases exponentially with time.

(7) Each bubble is surrounded by a shell of liquid through the outer boundary of which no dissolved gas passes.

(8) The agitation is adequate to insure no gross variation in liquid composition from one point in the stirred vessel to another.

(9) The dissolved gas is removed by a first-order, or pseudo-first-order, reaction with respect to the dissolved gas.

(10) The mixer is operating at steady state.

Since the results of this model are to be applied to the hydrogen deuterium-ammonia exchange reaction

$$HD(\ell) + NH_3(\ell) \overset{KNH_2}{\rightleftharpoons} NH_2D(\ell) + H_2(\ell) \qquad (1)$$

a comparison of the model and the physical system was made.

Both kinetic studies and empirical prediction made for this system show that the gas phase resistance contributed about 1% to the overall resistance to mass transfer between the phases (Assumption 1).

Sufficient agitation will insure that there is a uniform distribution of the gas throughout the liquid and that there will be no gross variations in liquid compositions under conditions of continuous operation (Assumption 2, 8, and 10).

Due to the exchange reaction (1), for every molecule of HD removed from the gas phase and reacted, a molecule of H_2 enters the gas phase; hence the volume of each bubble remains the same throughout its residency in the stirred vessel (Assumption 3). Although all the bubbles were assumed to be the same size (Assumption 4), this condition could be relaxed and a bubble size distribution inserted. However for calculational ease this was not done here.

The assumption of constant equilibrium concentration of HD per mixer stage (Assumption 5) is shown to be a very close approximation to reality since a small change in the equilibrium concentration of HD requires about a thousand fold change in the concentration of deuterated ammonia.

$$\Delta x_{HD} \sim .001\, \Delta x_{NH_2D} \tag{2}$$

The exponential decrease of the amount of HD above the equilibrium concentration is one of the weaker assumptions (Assumption 6). However, if the time dependent diffusion equation without chemical reaction is examined

$$D\nabla^2 C = \frac{\partial C}{\partial t} \tag{3}$$

it is seen that the time dependent part of the infinite series product solution is an exponential. Thus the assumption that the representation of the decreasing HD concentration above equilibrium in the gas phase as a single exponential appears reasonable as a first approximation.

Identical unit cells (Fig. 1) subdivide the entire vessel (Assumption 7) and the net flow of matter across

boundary b is assumed to be zero.

The hydrogen deuterium-ammonia exchange reaction

$$\frac{dC_{HD}}{dt} = k_1 C_{NH_2D} C_{H_2} - k_2 C_{HD} C_{NH_3} \tag{4}$$

is a second order reaction in the liquid phase with respect to the concentration of the dissolved gas, HD and of ammonia NH_3. But at steady state

$$\frac{k_1}{k_2} = \frac{C'_{HD}\, C'_{NH_3}}{C'_{NH_2D}\, C'_{H_2}} \tag{5}$$

where C' is the equilibrium concentration of the indicated species. For solutions present in the exchange towers of an ammonia-hydrogen exchange plant

$$C_{HD} \ll C_{H_2}$$

$$C_{NH_2D} \ll C_{NH_3} \tag{6}$$

and

$$C_{H_2} \ll C_{NH_3}$$

Thus, as C_{HD} approaches its equilibrium concentration, C'_{HD}, the only term in Equation (4) which changes significantly is C_{HD}, and we may regard the other three concentrations as remaining constant at their equilibrium values. Then Equation (5) may be approximated by

$$k_1 C_{NH_2D} C_{H_2} = k_2 C'_{HD} C_{NH_3} \tag{7}$$

and Equation (4) by (Assumption 9)

$$\frac{dC_{HD}}{dt} = k_2 C_{NH_3} (C'_{HD} - C_{HD})$$

$$= k (C'_{HD} - C_{HD}) \qquad (8)$$

where

$$k = k_2 C_{NH_3} \qquad (9)$$

Here

k_2 is the kinetic constant for the 2nd order $HD\text{-}NH_3$ exchange reaction;
$(mole)^{-1} \cdot (time)^{-1} \cdot (length)^3$

k is the kinetic constant for the pseudo first-order $HD\text{-}NH_3$ exchange reaction.

3.0 MASS TRANSFER WITH CHEMICAL REACTION

3.1 Model

In the case of mass transfer with chemical reaction, the time-dependent diffusion equation is

$$D\nabla^2 C_{HD} - k[\, C_{HD} - C'_{HD}\,] = \frac{\partial C_{HD}}{\partial t} \qquad (10)$$

where

D is the effective average diffusivity of HD in liquid ammonia; $(\text{length})^2 \cdot (\text{time})^{-1}$

and

k is the pseudo first-order reaction constant; $(\text{time})^{-1}$.

In spherical coordinates Equation (10) becomes

$$D\left[\frac{1}{r^2}\frac{\partial}{\partial r}\left(r^2\frac{\partial C_{HD}}{\partial r}\right)\right] - k\,[C_{HD} - C'_{HD}] = \frac{\partial C_{HD}}{\partial t} \qquad (11)$$

with

$$\frac{\partial C_{HD}}{\partial \theta} = \frac{\partial C_{HD}}{\partial \phi} = 0 \qquad (12)$$

due to symmetry.

3.2 Solution

Equation (11) was solved with the following initial and boundary conditions **(refer to Figure 1)**

at $t = 0$ and $r > a$ $\qquad C_{HD} = C'_{HD}$ $\qquad (13a)$

at $t > 0$ and $r = a$ $\qquad C_{HD} = (C_{i,HD} - C'_{HD})e^{-\beta t} + C'_{HD}$ $\qquad (13b)$

at $t > 0$ and $r = b$ $\qquad \frac{\partial C_{HD}}{\partial r} = 0$ $\qquad (13c)$

where

a is distance from the center of the bubble to the bubble-liquid interface; (length)

b is the distance from the center of the gas bubble to the edge of the unit cell; (length)
and β is constant to be determined by mass transfer considerations, $(\text{time})^{-1}$

Equation (11) was simplified by a change in variables

$$M = C_{HD} - C'_{HD} \tag{14}$$

$$D\left[\frac{1}{r^2}\frac{\partial}{\partial r}\left(r^2\frac{\partial M}{\partial r}\right)\right] - kM = \frac{\partial M}{\partial t} \tag{15}$$

The corresponding initial and boundary conditions would be

$$\text{at } t = 0 \text{ and } r > a \qquad M = 0 \tag{16a}$$

$$\text{at } t \geq 0 \text{ and } r = a \qquad M = M_i e^{-\beta t} \tag{16b}$$

$$\text{at } t \geq 0 \text{ and } r = b \qquad \frac{\partial M}{\partial r} = 0 \tag{16c}$$

Applying Laplace transformsto Equation(15) one obtains

$$r^2\frac{\partial^2 \bar{M}}{\partial r^2} + 2r\frac{\partial \bar{M}}{\partial r} - \bar{M}\left(\frac{k+S}{D}\right)r^2 = -\frac{M_i}{D}\mathbf{P}(0\rightarrow a)r^2 \tag{17}$$

where

$\mathbf{P}(0\rightarrow a)$ is a unitary function, dimensionless.
Solving this equation with its corresponding boundary conditions (16b)and (16c) yields

$$\bar{M} = \frac{M_i a}{r}\left[\frac{\sinh F(b-r) - Fb\cosh F(b-r)}{\sinh F(b-a) - Fb\cosh F(b-a)}\right]$$

$$\left[\frac{(S+k) - (S+\beta)\mathbf{P}(0\rightarrow a)}{(S+k)(S+\beta)}\right] + \frac{M_i}{S+k}\mathbf{P}(0\rightarrow a) \tag{18a}$$

where

$$F = \sqrt{\frac{S+k}{D}} \tag{18b}$$

For r > a, Equation (18a) reduces to

$$\bar{M} = M_i \frac{a}{r}\left[\frac{\sinh F(b-r) - Fb \cosh F(b-r)}{\sinh F(b-a) - Fb \cosh F(b-a)}\right] \frac{1}{S+\beta} \tag{19}$$

and for r = a

$$\bar{M} = M_i \frac{1}{S+\beta} \tag{20}$$

Since Equation (19) reduces to Equation (20) at r = a, Equation (19) was said to hold for $r \geq a$.

To find the inverse of $\bar{M}$, Equation (19) was represented as a polynomial

$$\bar{M} = \frac{f(S)}{\ell(S)} \tag{21}$$

where the degree of $\ell(S)$ was greater than that of f(S), thus the method of residues was able to be used.

The method of residues allows the inverse transform to be given as

$$M(t) = \sum_{n=1}^{n=N} \rho_n(t) \tag{22}$$

where

$\rho_n(t)$ is the "residue" of M at the pole S_n

Simple poles occur at

$$S_1 = -\beta \tag{23a}$$

and at solutions of the transcendental equation

$$\sinh\left[\sqrt{\frac{k+S_n}{D}}\,(b-a)\right] = b\sqrt{\frac{k+S_n}{D}}\,\cosh\left[\sqrt{\frac{k+S_n}{D}}(b-a)\right]$$

$$S_n \geq 2 \qquad (23b)$$

From examination of the equation, $S_n (n \geq 2)$ must be less than $-k$.

NOTE: $S = -k$ is not an acceptable solution since $k+S$ would be cancelled from both numerator and denominator of M in Equation (19)

$$\tan\left[\sqrt{\left|\frac{k+S_n}{D}\right|}\,(b-a)\right] = b\sqrt{\left|\frac{k+S_n}{D}\right|}$$

$$S_n \geq 2 \qquad (23c)$$

Since S_n is a simple pole of $\bar{\rho}$

$$\rho_n(t) = \frac{f(S_n)}{\ell'(S_n)}\, e^{S_n t} \qquad (24)$$

where

$\ell'(S_n)$ denotes the value of

$\frac{d\,\ell(s)}{dS}$ at $S = S_n$

thus

$$M(r,t) = \frac{M_i a}{r}\,\frac{\sinh\left[\sqrt{\frac{k-\beta}{D}}(b-r)\right] - b\sqrt{\frac{k-\beta}{D}}\cosh\left[\sqrt{\frac{k-\beta}{D}}(b-r)\right]}{\sinh\left[\sqrt{\frac{k-\beta}{D}}(b-a)\right] - b\sqrt{\frac{k-\beta}{D}}\cosh\left[\sqrt{\frac{k-\beta}{D}}(b-a)\right]}\, e^{-\beta t}$$

$$- \frac{M_i a}{r}\sum_{n=2}^{\infty}\left\{\frac{\sin\left[\sqrt{\left|\frac{k+S_n}{D}\right|}\,(b-r)\right] - b\sqrt{\left|\frac{k+S_n}{D}\right|}\cos\left[\sqrt{\left|\frac{k+S_n}{D}\right|}\,(b-r)\right]}{\cos\left[\sqrt{\left|\frac{k+S_n}{D}\right|}\,(b-a)\right]\left(\frac{S_n+\beta}{2D}\right)\left(a\sqrt{\left|\frac{k+S_n}{D}\right|} + b^2(b-a)\sqrt{\left|\frac{k+S_n}{D}\right|}\right)}\right\} e^{S_n t} \qquad (25)$$

3.3 Determination of β

In order to determine a value for β, a material balance requires that

$$4\pi a^2 D\left(\frac{\partial C_{HD}}{\partial r}\right)_{r=a} = \frac{4}{3}\pi a^3\left(\frac{\partial C_{HD}}{\partial t}\right)_{r=a} \tag{26}$$

i.e., the change in concentration of HD in the gas bubble must equal the amount of HD diffusing into the liquid.
Now since

$$\frac{\partial C_{HD}}{\partial r} = \frac{\partial M}{\partial r} \tag{27a}$$

and

$$\frac{\partial C_{HD}}{\partial t} = \frac{\partial M}{\partial t} \tag{27b}$$

Equation(26)becomes

$$\left(\frac{\partial M}{\partial r}\right)_{r=a} = \frac{a}{3D}\left(\frac{\partial M}{\partial t}\right)_{r=a} \tag{28}$$

Now from Equation (25)

$$\left(\frac{\partial M}{\partial t}\right)_{r=a} = -M_i \beta e^{-\beta t} \tag{29a}$$

$$\frac{\partial M}{\partial r}_{r=a} = M_i e^{-\beta t}\left\{-\frac{1}{a} + \frac{b\sqrt{\frac{k-\beta}{D}}\sinh\left[\sqrt{\frac{b-\beta}{D}}(b-a)\right] - \cosh\left[\sqrt{\frac{k-\beta}{D}}(b-a)\right]\sqrt{\frac{k-\beta}{D}}}{\sinh\left[\sqrt{\frac{k-\beta}{D}}(b-a)\right] - b\sqrt{\frac{k-\beta}{D}}\cosh\left[\sqrt{\frac{k-\beta}{D}}(b-a)\right]}\right\}$$

$$+ M_i \sum_{n=2}^{\infty}\left\{\frac{1 + \left[\left|\frac{k+S_n}{D}\right|\right] b^2}{\left[\frac{S_n+\beta}{2D}\right]\left[a\sqrt{\left|\frac{D}{k+S_n}\right|} + b^2(b-a)\sqrt{\left|\frac{k+S_n}{D}\right|}\right]}\right\} e^{S_n t} \tag{29b}$$

Inserting (29a) and (29b) into Equation (28) and gathering like terms yields

$$0 = e^{-\beta t}\left\{\frac{a\beta}{3D} - \frac{1}{a} + \frac{b\sqrt{\frac{k-\beta}{D}}\sinh\left[\sqrt{\frac{k-\beta}{D}}(b-a)\right] - \cosh\left[\sqrt{\frac{k-\beta}{D}}(b-a)\right]}{\sinh\left[\sqrt{\frac{k-\beta}{D}}(b-a)\right] - b\sqrt{\frac{k-\beta}{D}}\cosh\sqrt{\frac{k-\beta}{D}}(b-a)}\sqrt{\frac{k-\beta}{D}}\right\}$$

$$+ \sum_{n=2}^{\infty}\frac{1 + \left[\left|\frac{k+S_n}{D}\right|\right] b^2}{\left[\frac{S_n+\beta}{2D}\right]\left[a\sqrt{\left|\frac{D}{S_n+k}\right|} + b^2(b-a)\sqrt{\left|\frac{k+S_n}{D}\right|}\right]} e^{S_n t} \qquad (30)$$

β was approximated by setting the coefficient of $e^{-\beta t}$ equal to zero. This approximation seemed reasonable since the other exponentials decrease more rapidly than $e^{-\beta t}$ and after a short time the other coefficients' contributions are extremely small.

3.4 Bubble Gas Distribution Function

Cholette and Cloutier (10) used a mixed model to describe the behavior of a real stirred tank reactor under various conditions of agitation. Their data was best fitted by a model which consisted of a backmix region and of a deadwater region with a portion of the fluid bypassing the vessel.

The exit age distribution function determined by their experiments was

$$E = \left[\frac{v_1}{v}\right]^2 \frac{V}{V_b} \exp\left[-\frac{v_1}{v}\frac{V}{V_b}\frac{t}{\tau} + \frac{v_2}{v}\delta\left(\frac{t}{\tau}=0\right)\right] \qquad (31)$$

where

$\frac{v_1}{v}$ is the fraction of gas entering the backmix region,

$\frac{v_2}{v}$ is the fraction which bypasses the vessel

$\frac{V_b}{V}$ is the active fraction of the vessel

τ is the mean residence time of the gas in the vessel; (time)

δ is the Dirac delta function

Cholette and Cloutier (10)found that the agitation rate influenced the model's parameters i.e., increased agitation decreases both the bypassing rate and the size of deadwater regions and, if the mixing is vigorous enough, backmix flow is achieved.

For the efficiency calculations here complete backmixing is assumed.

4.0 DETERMINATION OF EFFICIENCY EQUATION

If gas phase resistance is neglected the concentration of dissolved HD at the interface is directly proportional to the (uniform) gas phase concentration following Henry's Law. Thus the time dependency of interface HD concentration can be used in the determination of the gas phase efficiency.

For a gas entering with composition $y_{i,HD}$, there exists an initial liquid composition at the interface $C_{i,HD}$

$$y_{i,HD}\,\pi = H' C_{i,HD} \tag{32}$$

where

π is the total pressure, atm.

H' is the Henry Law constant, (atm) · (liter) · $(mole)^{-1}$

The quantity M_i is related to $C_{i,HD}$ by Equation (14).

Setting r = a in Equation (25) gives the time dependent HD concentration at the liquid interface, M(a,t); the gas phase composition is then obtained using Henry's Law. If an exit age distribution function, E(t), is multiplied by M(a,t) and the product integrated over time

$$\bar{M}\,(a,\tau) = \int_0^\infty M(a,t)\,E(t)\,dt \tag{33}$$

where

$$\int_0^\infty E(t)dt = 1 \tag{34}$$

The result is the average interfacial concentration of HD as a function of the gas residence time, τ, where

$$\tau = \int_0^\infty tE(t)\,dt \tag{35}$$

From this point, derivation of the efficiency equation is straightforward.

$$\frac{\bar{M}(a,\tau)}{M_i} = \frac{C_{HD}(a,\tau) - C'_{HD}}{C_{i,HD} - C'_{HD}} \tag{36}$$

$$1 - \frac{\bar{M}(a,\tau)}{M_i} = \frac{C_{HD}(a,\tau) - C_{i,HD}}{C'_{HD} - C_{i,HD}} \tag{37}$$

By Henry's Law the interfacial concentration is directly proportional to the gas phase composition

$$1 - \frac{M(a,\tau)}{M_i} = \frac{y_{HD}^{(\tau)} - y_{i,HD}}{y'_{HD} - y_{i,HD}} = E_{mv} \tag{38}$$

5.0 POSSIBLE DESIGN NUMBERS

In the stirred contactors presently available the gas holdup is usually 20 to 30% of the total volume and the bubble diameters are 0.2 to 0.4 cm.

The stage efficiency as a function of time is given in Table 1 for the case where:

$r = a = 0.2$cm
$r = b = 0.342$ cm (gas holdup = 20% of system volume)
$\beta = 0.584$ sec^{-1} (from Equation (30)
$D = 4.575$ cm^2/sec (See Supplement D, Table II)
$k = 33\ 1/3$ sec^{-1} (See Supplement D, Table II)

$$E(t) = \frac{e^{-t/\tau}}{\tau} \quad \text{(perfect mixing).}$$

Table 1

Efficiency As A Function of Average Retention Time

τ (sec)	Efficiency (%)
.3	15.0
.5	22.6
1	36.8
2	52.5
3	63.6
4	70.1
6	77.8

For a gas flow rate of 9.5 ft^3/sec, a height to diameter ratio of 1, and a retention time of 3 sec, a volume of 142.5 ft^3 or a tank with a diameter of 5.7 ft results. Sieve trays employed to do the separation of one stirred contactor would require about 30 plates with a corresponding volume of about 750 ft^3 since the sieve trays would have an efficiency of about 2%. A look at the volume required for sieve trays (750 ft^3) and for a stirred reactor (140 ft^3)

shows the possible savings in high pressure construction. However the design of the agitated vessel plus its operating power will tend to increase the price of the stirred contactor. A lack of cost information precluded a decision favoring one type or the other.

6.0 REFERENCES

1. Baron, J., "Prediction of Plate Efficiency in the Hydrogen Deuterium-Ammonia Exchange Reaction," Supplement D.
2. Bancroft, A. R., Editor, "400 Ton per Year Water-Based Bithermal Hydrogen-Ammonia Exchange Heavy Water Plant Process Design," 1966, CRCE-1241.
3. Danckwertz, P. V., Ind. Eng. Chem., 43, 1460 (1951).
4. Gill, W. N., Chem. Eng., No. 21, 69, 189 (1962).
5. Lightfoot, E. N., Amer. Inst. Chem. Eng. J., 4, 499, (1958).
6. Lightfoot, E. N., Amer. Inst. Chem. Eng. J., 8, 710, (1962).
7. Van De Vusse, J. G., Chem. Eng. Sci., 16, 21 (1961).
8. Gao-Or B. and Resnick W., "Mass Transfer From Gas Bubbles In An Agitated Vessel With And Without Simultaneous Chemical Reaction," Chem. Eng. Sci., 19, 653-63 (1964).
9. Higbie, R., "Rate of Absorption of a Pure Gas Into a Still Liquid During Short Periods of Exposure," Trans A.I.Ch.E., 31 365-89.
10. Cholette, A., and Choutier, L., Can. J. Chem. Eng., 37, 105 (1959).

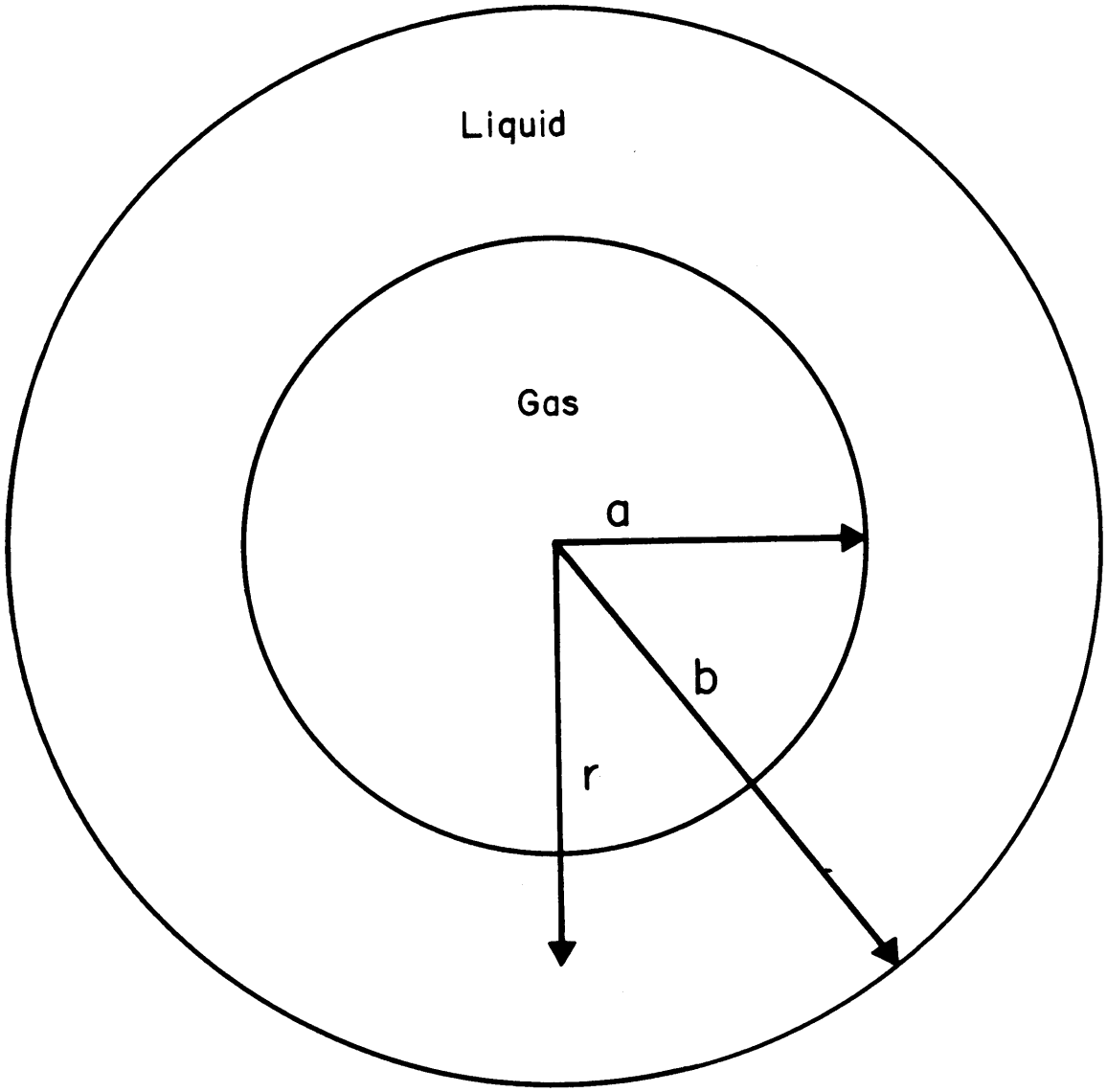

Figure 1. Spherical Gas Liquid Model

Supplement F
CHEMICALLY REFLUXED WATER-HYDROGEN SULFIDE EXCHANGE PROCESS

1.0 PROCESS DESCRIPTION

Another possible exchange process for concentration of deuterium proposed for investigation under this contract was the chemically refluxed water-hydrogen sulfide exchange process. For this process to be technically feasible it is necessary to find an element or stable chemical radical M whose oxide MO_n and sulfide MS_n take part in the reaction

$$\frac{1}{n}MO_n + H_2S \rightleftharpoons \frac{1}{n}MS_n + H_2O \qquad (1)$$

with an equilibrium constant favoring formation of the oxide at one temperature and the sulfide at another.

Figure 1 shows the principle of a process through which deuterium might be concentrated if the sulfide were stable at a low temperature and the oxide at a high temperature. Natural water is fed to a multistage gas-liquid contactor through which a liquid phase, predominantly water, is flowing down counter to a gas phase, predominantly H_2S, flowing up. In this contactor the deuterium exchange reaction

$$H_2O(\ell) + HDS(g) \rightleftharpoons HDO(\ell) + H_2S(g) \qquad (2)$$

takes place with an equilibrium constant of around 2.3 favoring concentration of deuterium in the liquid phase.

This results in progressive increase in the deuterium content of the water as it flows down through the contactor.

If sufficient amounts of water reflux at the top of the contactor and hydrogen sulfide reflux at the bottom are provided, together with a sufficient number of contacting stages, it is possible to obtain water enriched in deuterium to any desired degree at the bottom and water stripped of deuterium to any desired degree at the top. That this part of the process will work as described has been demonstrated by many years of experience in the dual-temperature water-hydrogen sulfide exchange plant of the U.S. Atomic Energy Commission at Savannah River.

The difficulty with the process depicted schematically in this figure is in finding a feasible and economic means of providing enriched hydrogen sulfide reflux at the bottom of the contactor and depleted water reflux at the top. As envisaged in this figure, hydrogen sulfide reflux at the bottom would be provided by reacting at low temperature enriched water product from the contactor with a sulfide MS_n:

$$H_2O + \frac{1}{n}MS_n \longrightarrow H_2S + \frac{1}{n}MO_n \qquad (3)$$

Depleted water reflux at the top would be provided by reacting at high temperature hydrogen sulfide leaving the top of the contactor with the oxide MO_n produced at low temperature

$$H_2S + \frac{1}{n}MO_n \longrightarrow H_2O + \frac{1}{n}MS_n \qquad (4)$$

Some of the heat required to bring reactants to the high temperature would be provided by heat exchange between water product and hydrogen sulfide reactant and by recovering heat from MS_n product and transferring it to MO_n reactant. The remainder of the heat needed to bring reactants to the high temperature and supply the heat of reaction would be provided by additional heaters.

2.0 SURVEY OF POSSIBLE METAL SULFIDE-OXIDE PAIRS

The feasibility of this method of providing reflux depends primarily on finding sulfide-oxide pair MS_n-MO_n for which the ratio of partial pressures at equilibrium

$$K \equiv P_{H_2O} \Big/ P_{H_2S} \qquad (5)$$

is much greater than unity at low temperature and much less than unity at high temperature. If favorable equilibrium constants could be found, it would then be necessary to establish that the heat input required was sufficiently low and that reaction rates were sufficiently rapid to be economically feasible.

Before undertaking a more detailed study of this process with contract funds, data on equilibrium constants for reaction (1) involving metallic oxides and sulfides were compiled in a Master's thesis investigation conducted by Mr. Jeffrey S. Bromberg (1). Values of the equilibrium

---

(1) Bromberg,Jeffrey S.: Feasibility Study for Chemical Reflux in the Water-Hydrogen Sulfide Exchange Process for Heavy Water Production, S.M. Thesis, Nuclear Engineering Dept., M.I.T., January 1969.

constant K for reaction (1) for all pairs of inorganic oxides and sulfides for which thermodynamic data could be found are given in Table 1, at 298°K and at higher temperatures where available. These equilibrium constants were calculated from free energies of formation of the pertinent oxides and sulfides.

The only element listed in this table whose equilibrium constant changes from greater than unity to less than unity over the temperature range for which data are available is molybdenum. Mr. Bromberg's correlation of these equilibrium constants with position of the elements in the periodic table disclosed no element whose equilibrium constant was likely to be more favorable for this process than molybdenum.

With molybdenum, the fact that the equilibrium constant fails to drop far below unity at any feasible operating temperature means that only part of the water entering the high-temperature reactor can be converted to H_2S, so that the unconverted water in the gases leaving this reactor must be recycled. This water must be cooled to room temperature, condensed, separated from the hydrogen sulfide, revaporized, and heated again to reaction temperature.

3.0 EVALUATION OF ENERGY REQUIREMENTS

A rough estimate was made of the minimum amount of heat which would have to be supplied to produce one

Table 1. Equilibrium Constant for Reaction

$$\frac{1}{n}MO_n + H_2S \rightleftharpoons \frac{1}{n}MS_n + H_2O$$

		Equil. Constant, $K = P_{H_2O}/P_{H_2S}$				
		Temperature, °K				
Oxide	Sulfide	298.15	1000	1400	1500	2000
Al_2O_3	Al_2S_3	0.0000				
Sb_2O_3	Sb_2S_3	8.6×10^{6}	1.4×10^{3}			
BaO	BaS	7.6×10^{15}	3.3×10^{5}		2.0×10^{4}	
BeO	BeS	0.0000				
Bi_2O_3	Bi_2S_3	∞	∞			
CaO	CaS	2.1×10^{11}	1.9×10^{3}			28.0
CdO	CdS	3.3×10^{18}	1.0×10^{17}			
Ce_2O_3	Ce_2S_3	0.0000				
Cs_2O	Cs_2S	∞				
Cu_2O	Cu_2S	7.0×10^{22}	1.2×10^{8}	2.6×10^{6}		
CoO	CoS	2.5×10^{11}	4.0×10^{4}		8.4×10^{3}	
In_2O_3	In_2S_3		0.0000			
La_2O_3	La_2S_3	2.5×10^{6}				
PbO	PbS	2.9×10^{17}	4.3×10^{5}		5.6×10^{3}	
MgO	MgS	3.9×10^{-5}	0.089			0.37
HgO	HgS	∞				
MoO_2	MoS_2	1.7×10^{6}	54		3.8	0.99
NiO	NiS	4.7×10^{12}	1.1×10^{4}			
K_2O	K_2S	∞				
Rb_2O	Rb_2S	∞				
RuO_2	RuS_2	∞	∞			
Na_2O	Na_2S	∞	5.7×10^{9}	8.6×10^{6}		
SiO_2	SiS_2	0.0000				
Ag_2O	Ag_2S	∞	2.5×10^{12}			

(continued)

Table 1 (concluded)

		Equil. Constant, $K = P_{H_2O}/P_{H_2S}$				
		Temperature, °K				
Oxide	Sulfide	298.15	1000	1400	1500	2000
SrO	SrS	4.2×10^{16}	4×10^{8}			
Tl_2O	Tl_2S	1.0×10^{24}				
ThO_2	ThS_2	0.0000				
SnO	SnS	2.5×10^{2}	9.3			
TiO	TiS	0.0000				
WO_2	WS_2	1.7×10^{5}	27	6.5		
ZnO	ZnS	8.0×10^{10}	6.0×10^{3}		2.0×10^{4}	

pound mole (20 pounds) of heavy water by this process. With feed water containing 150 ppm deuterium, 6667 pound moles of feed would be needed to produce one pound mole of heavy water. As the equilibrium constant for reaction (2) is around 2.3, the minimum number of moles of hydrogen sulfide reflux needed per mole heavy water product is:

$$\frac{2.3}{(2.3-1)\ 150\times10^{-6}} = 11{,}800 \qquad (6)$$

To produce this H_2S in the reaction

$$MoS_2 + H_2O \longrightarrow MoO_2 + 2H_2S \qquad (7)$$

a minimum of 5,900 pound moles of MoS_2 must be converted to MoO_2 to make one pound mole of heavy water. As the heat of reaction (7) at 1500°K is around 32,500 BTU/lb mole,

$$32{,}500 \times 5{,}900 = 1.92 \times 10^8 \text{BTU} \qquad (8)$$

is the minimum heat of reaction per pound mole of heavy water. Rough heat balances on the remainder of the process indicate that approximately an equal amount of heat is needed to heat recycle water to reaction temperature and make up for inefficiencies in heat exchangers. The minimum over-all heat requirement of the process per pound of heavy water thus is

$$\frac{1.98 \times 10^8 \times 2}{20} \simeq 2 \times 10^7 \text{ BTU/lb} \qquad (9)$$

The Savannah River dual temperature water-hydrogen sulfide exchange plant consumes 5600 pounds of 900 psi steam per pound of heavy water (2), equivalent to 6.4×10^6 BTU/lb of heat. The heat requirement for the chemically-refluxed process is about three times as great as for the dual temperature process, and it must be supplied at a higher temperature.

Because of the lack of a sulfide-oxide pair with equilibrium constants much greater than unity at one temperature and much less than unity at another, and because of the relatively high heat input for the most favorable sulfide-oxide pair found, it was decided not to investigate the chemically refluxed water-hydrogen sulfide process under this contract.

---

(2) Bebbington and Thayer: Chem.Eng.Progress 55(9), 70 (1959).

Figure I. Chemically Refluxed Water - Hydrogen Sulfide Exchange Process